ABSTRACT

Title of Dissertation: PALLADIUM-CATALYZED ALLYLIC-ARYLATION: MECHANISTIC STUDIES AND APPLICATION TO THE TOTAL SYNTHESIS OF (±)-7-DEOXYPANCRATISTATIN DERIVATIVES

Krupa H. Shukla, Doctor of Philosophy, 2009

Directed By: Professor Philip DeShong
Department of Chemistry and Biochemistry

Palladium-catalyzed carbon-carbon bond formation is one of the most widely used reactions for the synthesis of biologically active substances. The DeShong group has demonstrated that hypervalent silicates can be employed for allyl-aryl carbon-carbon bond couplings in the presence of a Pd(0) catalyst. The goals of this dissertation are (1) to demonstrate application of palladium-catalyzed allylic-arylation coupling to the total synthesis of (±)-7-deoxypancratistatin and its analogues, and (2) to study the mechanism of allyl-aryl cross coupling reactions.

In spite of the potent antitumor and antiviral activity of (+)-7-deoxypancratistatin, the use of this compound is limited in clinical applications because of its low natural abundance and lack of a practical scalable synthetic route. In order to test the feasibility of siloxane-based coupling in the synthesis of 7-deoxypancratistatin, a simplified analogue of (±)-7-deoxypancratistatin was synthesized. The key reaction in the synthesis

involved stereoselective construction of a carbon-carbon bond between A and C rings *via* coupling of an aryl siloxane with an allylic carbonate.

While siloxane methodology was successfully applied to the synthesis of a (±)-7-deoxypancratistatin analogue, application of this methodology to the natural product (±)-7-deoxypancratistatin proved to be a significant challenge. To understand the causes of the failure of the coupling reaction, a detailed mechanistic study was undertaken. Hammett analysis of the allyl-aryl coupling reaction demonstrated that the rate of the coupling reaction was enhanced by electron-withdrawing groups on the aryl siloxane. The positive slope of the Hammett plot indicated a charged transition state in which negative charge on the aryl ring was stabilized inductively. Furthermore, this study provided useful information regarding the nature of ligands on the palladium. Based on this study, a new family of Pd(0) olefin catalysts was developed. These catalysts were found to be highly efficient and formed carbon-carbon bond even at ambient temperature.

Novel Pd(0) olefin complexes were successfully employed in the synthesis of (±)-7-deoxypancratistatin. The key coupling reaction of allylic carbonate with aryl siloxane produced Hudlicky's intermediate, thus constituting formal total synthesis of the actual product. Though the reaction required higher catalytic loading and proceeded in moderate yields, the ability of the reaction to work at ambient temperature is advantageous for practical synthesis of the natural product. Future studies shall aim at optimization of the key coupling reaction and application of this methodology to the synthesis of pancratistatin and related derivatives.

PALLADIUM-CATALYZED ALLYLIC-ARYLATION: MECHANISTIC STUDIES AND APPLICATION TO THE TOTAL SYNTHESIS OF (±)-7-DEOXYPANCRATISTATIN DERIVATIVES

By

Krupa H. Shukla

Dissertation submitted to the Faculty of the Graduate School of the
University of Maryland, College Park, in partial fulfillment
of the requirements for the degree of
Doctor of Philosophy
2009

Advisory Committee:
Professor Philip DeShong, Chair
Professor Jeffery Davis
Professor Daniel Falvey
Professor Richard Payne
Assistant Professor Barbara Gerratana

If we knew what it was we were doing, it would not be called research, would it?

— Albert Einstein

DEDICATION

~ To My Loving Parents ~

ACKNOWLEDGMENTS

I extend my gratitude to my advisor, Professor Philip DeShong for guiding me throughout this project. Without his encouragement and guidance it would have been impossible for me to accomplish what I have. This research experience has been one of the most rewarding and challenging experiences of my life and I am indebted to him.

The entire DeShong group has been very supportive. I am grateful to all the former and current members. Special acknowledgements go to Debra Boehmler, Bridget Duvall, William McElroy, and Ju-Hee Park who have been very generous assisting and teaching me important lab skills and techniques.

I thank Yiu-Fai Lam, Yinde Wang, Noel Whittaker and Yue Li for their assistance obtaining spectral data. I also thank Professor Christian Wolf and his student Hanhui Xu at Georgetown University for their help with microwave experiments.

Many thanks to Yomi Okunola, An-Ni Chang and Julia Khusnutdinova, my friends at the University of Maryland. Special thanks to Julia for suggestions that improved this manuscript. I also thank Vasudha and Richa, my high school friends who inspired me to stay focused. I am grateful to my TA Carmen (2003-2004), who encouraged me to do undergraduate research and enthused me to pursue doctoral degree.

Finally, I express my heartfelt gratitude to my lovely family who has always been supportive and motivating. I thank my grandparents for their blessings and my parents for their endless sacrifices and providing me with the best of everything. I am greatly thankful to my sweet brother who has always stood by me and has helped me to the best of his abilities. I warmly appreciate my husband for his abundant love, encouragement and understanding. Last, but not least, I thank God for turning my dream into reality.

TABLE OF CONTENTS

LIST OF TABLES

CHAPTER 2

CHAPTER 4

LIST OF FIGURES

LIST OF SCHEMES

CHAPTER 1

CHAPTER 2

CHAPTER 4

LIST OF ABBREVIATIONS

Ac	acetyl
acac	acetylacetonate
aq.	aqueous
Ar	aryl
Bn	benzyl
BQ	1,4-benzoquinone
Bu	butyl
Bz	benzoyl
calcd	calculated
COD	1,5-cyclooctadiene
COSY	correlation spectroscopy
Cy	cyclohexyl
CBz	carboxybenzyl
dba	dibenzylideneacetone
DBU	1,8-diazabicyclo[5.4.0]undec-7-ene
DQ	duroquinone
DCN	1,4-dicyanonaphthalene
DIPHOS	1,2-bis(diphenylphosphino)ethane
DMAP	4-dimethylaminopyridine
DMF	*N*,*N*-dimethylformamide
DMSO	dimethyl sulfoxide
E	ester
EDG	electron-donating group
ee	enantiomeric excess
EI	electron ionization
equiv.	equivalent(s)
Et	ethyl
Et_2O	diethyl ether
ESI	electrospray ionization
EWG	electron-withdrawing group
FAB	fast atom bombardment
FT	fourier transform
Fu	furyl
GC	gas chromatography

h	hour(s)
HMPA	hexamethylphosphoramide
HPLC	high performance liquid chromatography
HRMS	high resolution mass spectrometry
HSQC	heteronuclear single quantum coherence
Hz	Hertz
i-Pr	isopropyl
IR	infrared
J	coupling constant
L	ligand
LRMS	low resolution mass spectrometry
m	*meta*
M^+	molecular ion
m/z	mass-to-charge ratio
MAH	maleic anhydride
m-CPBA	*meta*-chloroperoxybenzoic acid
Me	methyl
MeCN	acetonitrile
MHz	Megahertz
min	minute
MOM	methoxymethyl
mp	melting point
MS	mass spectrometry
NBD	norbornadiene
NBE	norbornene
NMO	N-methylmorpholine-N-oxide
NMP	N-methyl-2-pyrrolidone
NMR	nuclear magnetic resonance
NQ	1,4-naphthoquinone
Nu	nucleophile
o	*ortho*
OAc	acetate
OBz	benzoate
p	*para*
PEG	poly(ethylene glycol)
Ph	phenyl
PMB	*p*-methoxybenzyl

R_f	retention factor
SAR	structure activity relationship
satd	saturated
rt	room temperature
t-Bu	tertiary butyl
TBAF	tetrabutylammonium fluoride
TBAB	tetrabutylammonium bromide
TBAT	tetrabutylammonium triphenyldifluorosilicate
TBS	*t*-butyldimethylsilyl
TCNE	tetracyanoethylene
Tf	trifluoromethanesulfonyl
TFA	trifluoroacetic acid
TFP	tri-2-furylphosphine
THF	tetrahydrofuran
TLC	thin layer chromatography
TIPS	triisopropylsilyl
TMS	trimethylsilyl
Ts	tosyl
UV	ultra violet

CHAPTER 1
PALLADIUM-CATALYZED ALLYLIC-ARYLATION

INTRODUCTION

Palladium-catalyzed carbon-carbon bond formation is one of the most synthetically important and versatile reactions in the chemist's repertoire.[1,2] The two most commonly used metal derivatives used in coupling include boron (Suzuki coupling)[3] and tin (Stille coupling)[4] (Scheme 1.1). The limitations associated with boron reagents include synthesis of the boronic acid derivatives, homocoupling and incompatibility with Lewis basic functions. While Stille coupling offers functional group tolerance, it is limited in pharmaceutical applications due to the toxicity of tin reagents and the removal of the trace tin byproducts.

Scheme 1.1

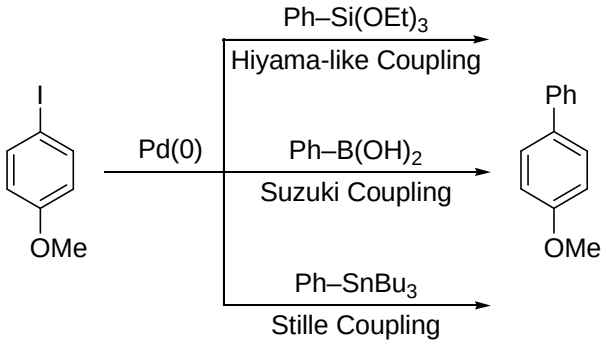

In contrast, silicon-based coupling (Hiyama coupling)[5-9] offers a viable alternative to other coupling technologies because of the low cost, low toxicity and chemical stability of silicon-derived compounds.[10,11] Hiyama demonstrated that the coupling of aryl fluorosilanes with aryl iodides and bromides proceeded in moderate to good yields.

Recently, the DeShong group developed siloxane methodology, which utilizes hypervalent siloxane derivatives in the presence of a palladium catalyst to form an aryl-aryl carbon bond.[12-16] Subsequently, an efficient cross-coupling of aryl bromides and chlorides with aryl siloxanes using the palladium/imidazolium catalytic system was reported by Lee.[17] Aryl siloxanes have also been used in aqueous systems by Wolf.[18] More recently, Clarke reported the first microwave accelerated Hiyama-like coupling of aryl siloxanes with aryl halides.[19] Not only are siloxanes less toxic than Stille reagents, they are also quite stable, easily prepared and purified.[20,21] Recently, the use of aryl silanols and aryl silanolates as efficient coupling partners has emerged as reported by Denmark.[22-25]

ALLYLIC-ARYLATION

In addition to aryl-aryl cross-coupling reaction, organometallic reagents of silicon, boron and tin can be used to construct the allyl-aryl bond (Scheme 1.2). In most cases, allyl halides or allyl carboxylates, prepared from the corresponding alcohols, are used as allylating agents.

Scheme 1.2

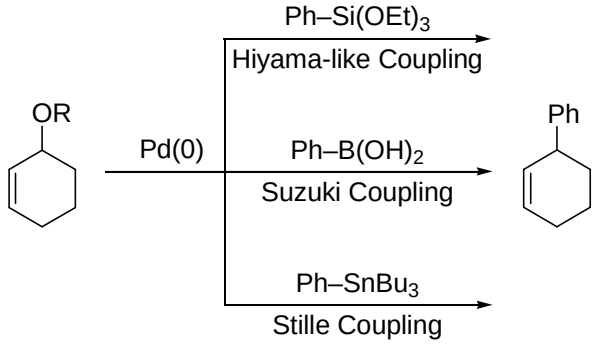

Organometallic reagents are unstabilized nucleophiles (pK_a > 25) and follow the general mechanism outlined in the Scheme 1.3.[26] Allyl benzoate **1** reacts with Pd(0) to give the π-allyl Pd intermediate **2**, with inversion of configuration. Next, the aryl group is transferred from the organometallic species **3** onto the Pd *via* transmetalation to form the Pd(II) intermediate **4**. Subsequent reductive elimination from the same face as the palladium generates **5** with overall inversion at the reaction center. Note that the π-allyl Pd intermediate **4** is a meso compound. Therefore, reductive elimination could also result in formation of *ent*-**5**.

Scheme 1.3

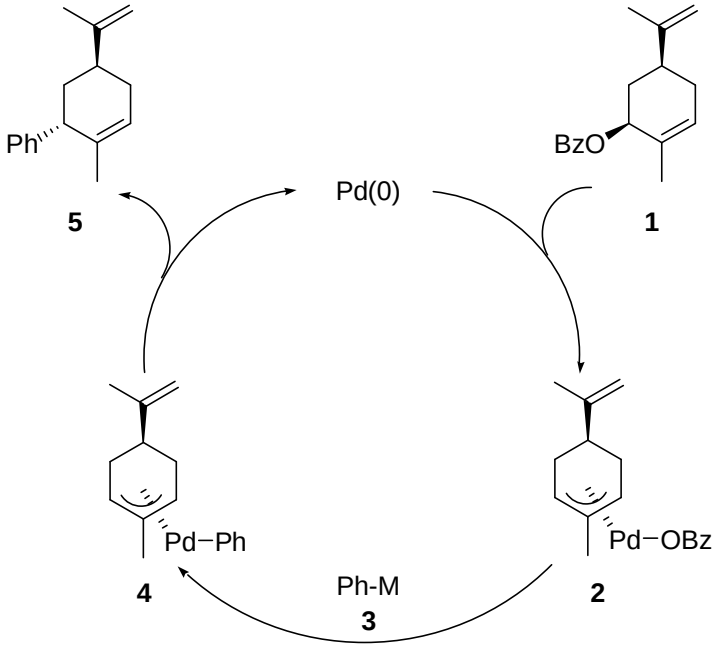

Hiyama-like Coupling

Palladium-catalyzed coupling of allylic carbonate with aryl and vinyl fluorosilanes was reported by Hiyama and Hatanaka (Scheme 1.4).[27] This reaction proceeded without fluoride ion activation; however the reaction suffered from poor

yields. Moreover, the synthesis of fluorosilanes involves multiple steps and fluorosilanes are hydrolytically unstable. Subsequently, Hiyama examined the coupling reaction of allylic and benzylic carbonate with an organo[2-(hydroxymethyl)phenyl]dimethylsilane in the absence of any activator (Scheme 1.5).[28] Upon treatment with a mild base (K_2CO_3), the proximal hydroxyl group gets converted to an alkoxide and coordinates to the nearby silicon atom to produce a five-membered penta-coordinated silicate species. In comparison to fluorosilanes, this tetraorganosilicon reagent is highly stable.

Scheme 1.4

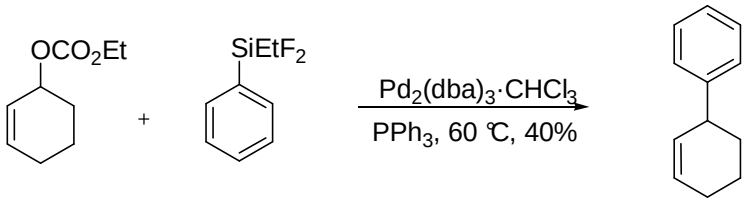

Scheme 1.5

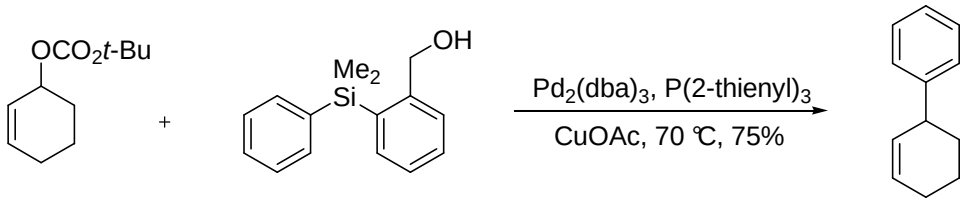

In an effort to extend the viability of silicon-based coupling, the DeShong group developed the palladium-catalyzed allylic-arylation methodology as depicted in the Scheme 1.6.[29-34] Phenyltriethoxysilane **6** when treated with tetrabutylammonium fluoride (TBAF), generated *in situ* hypervalent species **7**. This hypervalent reagent **7** reacted with allylic benzoate **8** to give cyclohexene **9**. This methodology has been shown to efficiently transfer a wide variety of aryl groups to allylic esters in excellent yields (70-95%).[32]

In more complex systems such as allylic benzoate **10**, there are regiochemical as well as a stereochemical issues (Scheme 1.6). The reaction of aryl siloxane **6** with allylic carbonate **10** forms two regioisomers **11** and **12** with an overall inversion of stereochemistry. The origin of regioselectivity and stereoselectivity can be understood from the mechanism shown in the Scheme 1.7.

When allylic benzoate **10** reacts with palladium, the benzoate group is displaced by palladium from the opposite face (inversion) to form π-allyl intermediate **13**. Next, the aryl group is transferred from the hypervalent silicate species **7** onto Pd *via* transmetalation to give π-allyl intermediate **14**. The resulting π-allyl intermediate **14** is "unsymmetrical" since palladium is pushed away from the methyl group to minimize steric interactions. Reductive elimination therefore occurs predominantly on C1 from the same face (retention) as palladium to obtain **11** as the major product with a net inversion of configuration at the allylic carbon.

Scheme 1.6

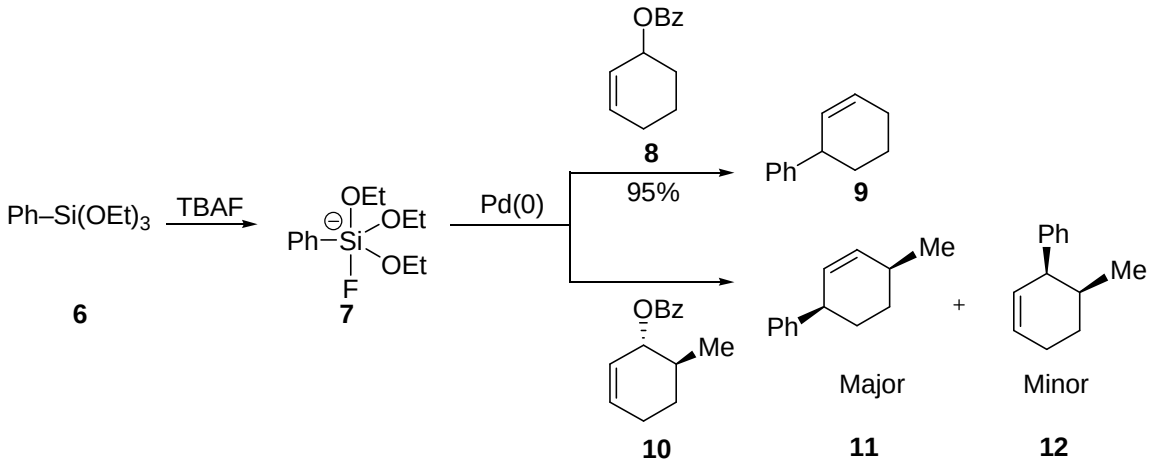

Scheme 1.7

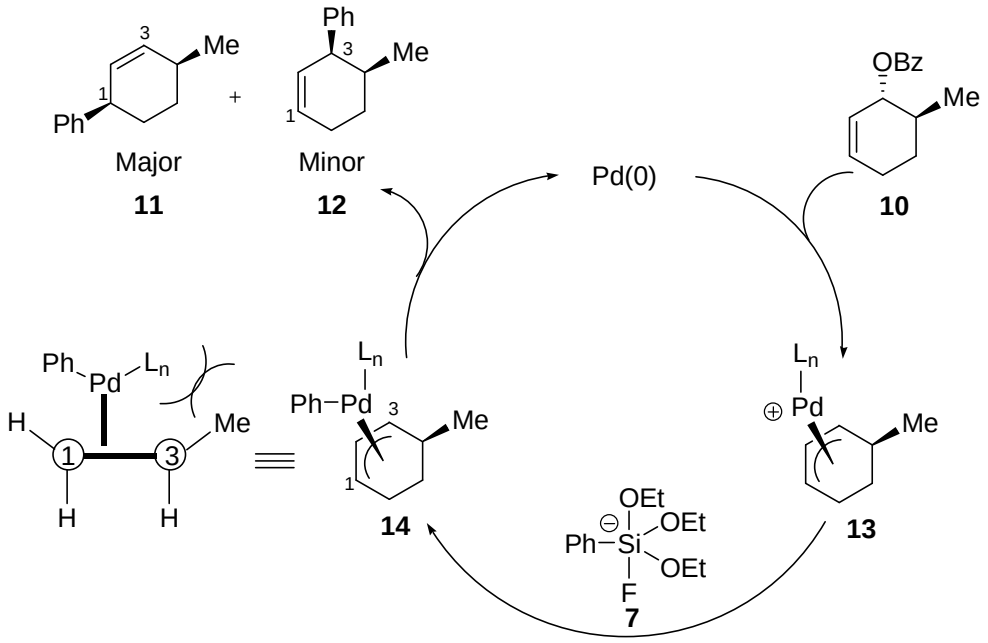

Recently, Pd(0) nanoparticle (generated *in situ*) catalyzed cross-coupling of allyl acetates and aryl and vinyl siloxane has been reported (Scheme 1.8).[35] It is postulated that Pd(II) is reduced to Pd(0) by allyl acetate and TBAB (tetrabutylammonium bromide) stabilizes Pd(0) nanoparticles. The reaction is applicable to a variety of unactivated and activated allyl acetates (Baylis-Hillman acetate adducts) and organosiloxanes. This reaction is highly regioselective providing straight chain olefins through coupling from the less substituted carbon. Moreover, the nanoparticles can be recovered after reaction and remain appreciably active through three catalytic cycles. However, this reaction has not been applied to cyclic allylic substrates.

Activated allyl acetates (Baylis-Hillman acetate adducts derived from methyl acrylate, acrylonitrile, acyclic and cyclic α,β-unsaturated ketones) have also shown to couple with aryl siloxane in poly(ethylene glycol) (PEG) by Kabalka.[36]

Scheme 1.8

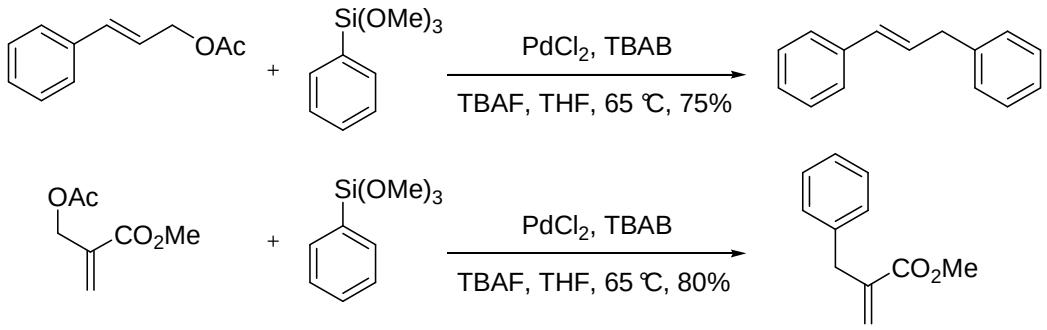

Suzuki Coupling

The coupling of sodium tetraphenylborate with allylic acetate (Scheme 1.9) was demonstrated by Fiaud and Legros.[37] However, the reaction was limited to the transfer of phenyl groups.

Scheme 1.9

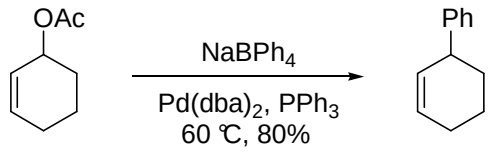

A breakthrough in this field of boron-based coupling was achieved by Moreno-Mañas who reported coupling of aryl boronic acids with allyl bromides in refluxing benzene using $Pd(dba)_2$ as catalyst (58-91% yield)[38] and by Hayashi who coupled aryl boronic acids with allyl acetates using a resin-supported palladium catalyst under basic conditions in water (45-99% yield).[39]

A practical and stereoselective synthesis of *C*-arylglycosides by coupling of arylboronic acid and peracetylated glycols in the presence of catalytic $Pd(OAc)_2$ was reported by Maddaford (Scheme 1.10).[40] In this case, the regioselectivity is governed by

the electronic effect of the oxygen functionality and is limited to this specific substrate apparently since the galacto analogue did not undergo coupling.

Scheme 1.10

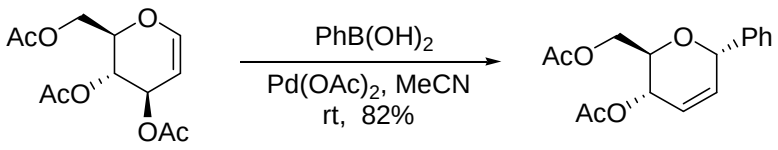

Balme and co-workers have developed a novel catalytic system [$PdCl_2(TFP)_2$] (TFP ≡ *tri*-2-furylphosphine) of allyl acetates with a variety of aryl boronic acids in the presence of fluoride (Scheme 1.11).[41] The reaction displays excellent regioselectivity and stereoselectivity as evident by the formation of a single coupling product with *E*-geometry. The reaction also works well with cyclic allyl acetates. [$PdCl_2(TFP)_2$] has been shown to also couple pinacol aryl and vinyl boronates to allyl acetates in moderate to good yields by Ortar (Scheme 1.12).[42]

Scheme 1.11

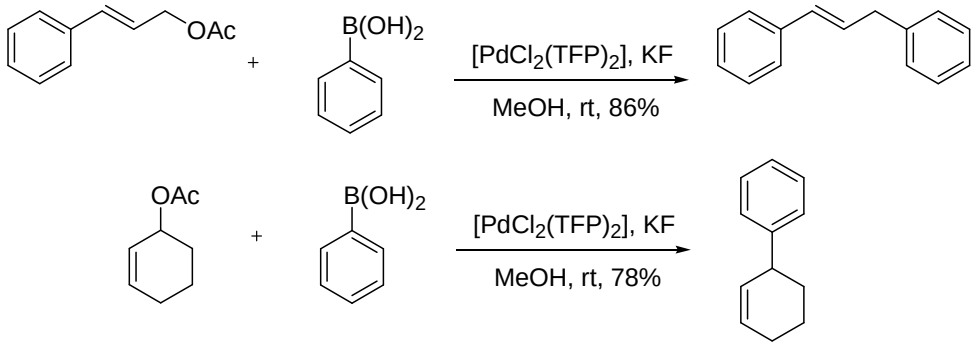

Scheme 1.12

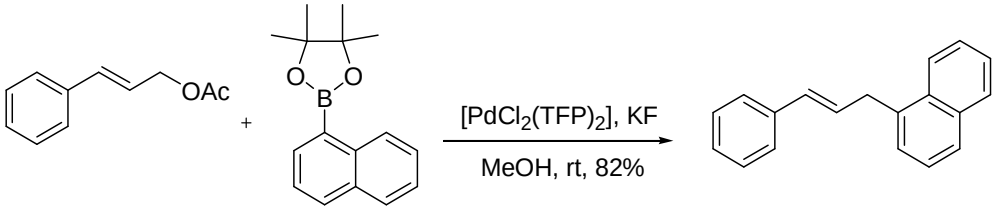

Mino and co-workers reported palladium-catalyzed coupling of allylic acetates with boronic acids at room temperature in the presence of $Pd(OAc)_2$ and phosphine-free hydrazone ligand to produce allyl benzene derivatives in good yields (Scheme 1.13).[43]

Scheme 1.13

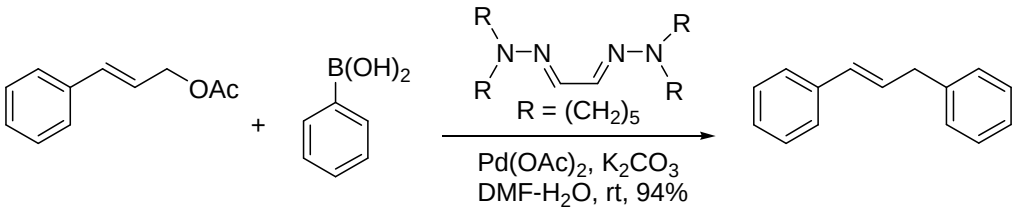

Scheme 1.14

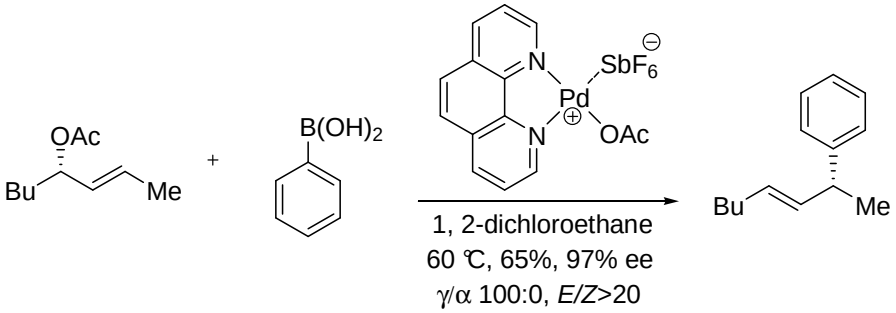

Air-tolerable allyl-aryl coupling reaction in the presence of palladium catalyst was reported by Sawamura recently.[44] The reaction of optically active allyl acetates with phenylboronic acid in the presence of $Pd(OAc)_2$, 1,10-phenanthroline and $AgSbF_6$ gave

coupling product in good yields. The reaction takes place with excellent α to γ chirality transfer and *syn*-selectivity (Scheme 1.14).

Some of the other catalysts developed for coupling of allylic substrates with arylboron derivatives are shown in Figure 1.1.[45-47] N-Heterocyclic carbene palladium complex **I** is able to catalyze reaction of activated allyl chlorides with arylboronic acid at room temperature.[45] Despite the presence of β-hydrogens in the allylic substrate, the coupling of allylic substrates proceeded to give excellent yields of coupling products. Nájera introduced a thermally stable catalyst, di(2-pyridyl)methylamine-based Pd(II) complex **II** which can function in aqueous conditions.[46] The coupling reaction of allylic substrates (allylic chlorides, allylic acetates, allylic carbonates) with arylboronic acids occurred in refluxing water or at room temperature in aqueous acetone to provide coupling products in good yields. Recently, Nájera and co-workers cross-coupled allyl chlorides with potassium aryltrifluoroborates using an oxime-derived palladacycle **III** in aqueous acetone at room temperature or 50 °C.[47] In comparison to toxic and pyrophoric phosphines, the coupling protocol employed by these catalysts (Figure 1.1) is user-friendly and environmentally benign.

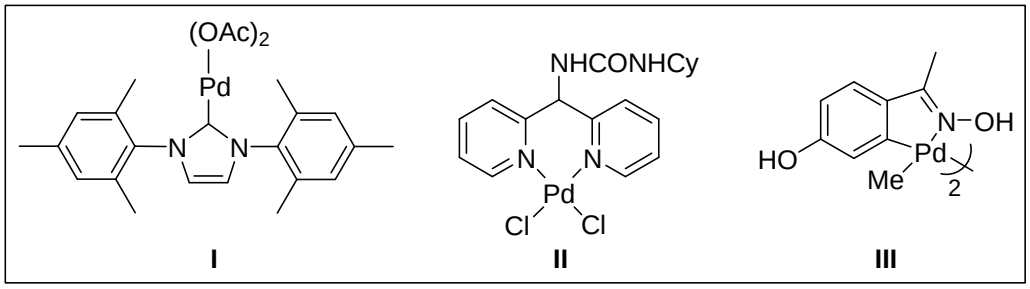

Figure 1.1: Catalysts for coupling of allylic substrates with aryl boronic acid derivatives

Recently, cross-coupling of allylic alcohol with aryl and vinyl boronic acids in organic as well as aqueous solvents have emerged.[48-51] Also, microwave assisted

allylic-arylations have been reported.[52,53] Apart from palladium-catalyzed allylic-arylation using boron reagents, nickel-catalyzed[54,55] and rhodium-catalyzed[56] coupling reactions are also known in the literature.

Stille Coupling

Stille performed palladium-catalyzed reaction of allylic acetates with aryl and vinyl stannanes (Scheme 1.15).[57] However, the reaction gave poor yields when used for cyclic allyl acetates. Later, Echavarren reported palladium-catalyzed cross-coupling reaction of allylic carbonates with organostannanes.[58]

Scheme 1.15

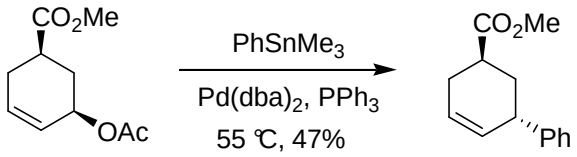

In an effort to improve the yield of these couplings, the effect of polarity of the solvent on stereoselective coupling reaction of allyl chlorides and aryl stannane was reported by Kurosawa (Scheme 1.16).[59] In the presence of weakly coordinating solvents such as benzene, acetone, CH_2Cl_2 or THF retention of configuration **15** was observed. However, nearly complete inversion **16** was observed in coordinating solvents such as DMSO or MeCN indicating a change of mechanism in the presence of strongly donor ligands on the metal.

Fairlamb has reported a new bromosuccinimido-Pd catalyst **17** synthesized from $Pd_2(dba)_3 \cdot CHCl_3$ for the coupling of allylic and benzylic bromides with vinyl stannanes (Scheme 1.17).[60]

Scheme 1.16

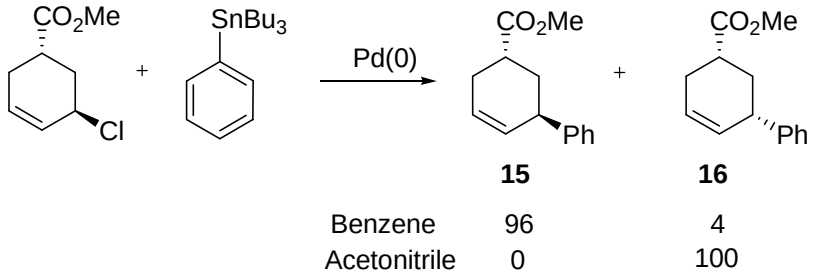

Scheme 1.17

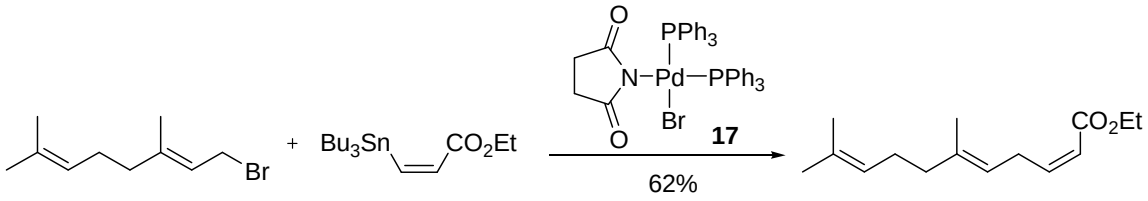

Due to high tolerance towards most functional groups, allyl-aryl Stille coupling reaction has been employed in the construction of a variety of ring systems in highly functionalized molecules.[61,62] Although the Stille coupling is tolerated by many functional groups, the reaction suffers from several limitations. The tin (IV) derivatives are toxic, the removal of tin byproducts is difficult and the coupling exhibits moderate stereoselectivities.[29] For example, the coupling of allylic benzoate **18** with hypervalent silicate (TBAT) resulted in the stereoselective formation of regioisomers **19** and **20**. Moreover, high regioselectivity was observed, evident by the formation of the major

regioisomer **19**. However, coupling of allylic benzoate **18** using Stille reaction conditions gave mixture of several products (Scheme 1.18).

Scheme 1.18

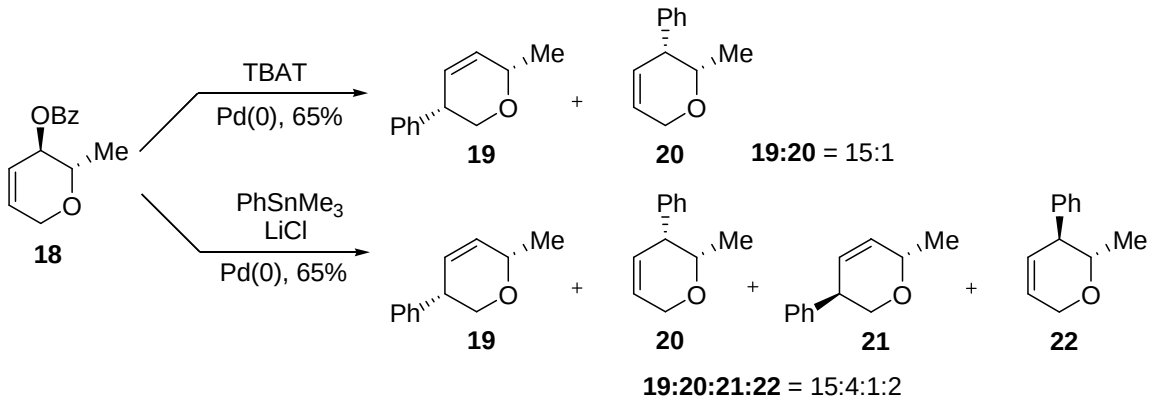

CONCLUSION

Palladium-catalyzed cross-couplings utilizing hypervalent silicate anions have several advantages compared to Stille and Suzuki coupling reactions. These include mild reaction conditions, stability, low toxicity and ease of preparation of silicon reagents. Moreover, allyl-aryl cross-coupling reaction involving siloxane methodology results in stereospecific arylation with net inversion of configuration. The succeeding chapters will demonstrate how palladium-catalyzed allylic-arylation methodology involving hypervalent silicates has been applied to the synthesis of natural product 7-deoxypancratistatin and its derivatives.

CHAPTER 2
TOTAL SYNTHESIS OF (±)-7-DEOXYPANCRATISTATIN ANALOGUE

INTRODUCTION

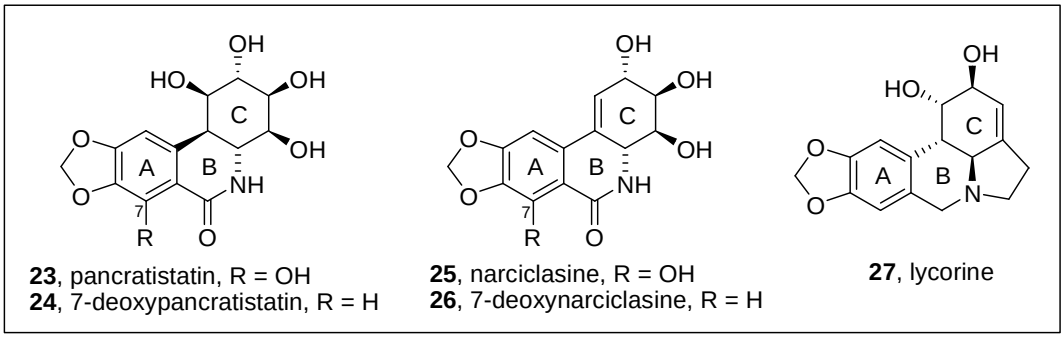

23, pancratistatin, R = OH
24, 7-deoxypancratistatin, R = H

25, narciclasine, R = OH
26, 7-deoxynarciclasine, R = H

27, lycorine

Figure 2.1: Structure of *Amaryllidaceae* alkaloids

Isolation and Biological Activity

Amaryllidaceae alkaloids (Figure 2.1) have been recognized for a long time because of their medicinal value. Among various alkaloids isolated from *Amaryllidaceae* species, (+)-pancratistatin (**23**) shows the most promising biological activity. Pancratistatin was first isolated and extracted from the Hawaiian daffodil bulb *Pancratium littorale* (also known as *Hymenocallis littorale*) in a low yield of 0.014% dry weight.[63] Since, many related analogues have been isolated including the less toxic analogue, (+)-7-deoxypancratistatin (**24**).[64] This deoxygenated analogue (**24**) was isolated from the roots of the bulbs *Haemanthus kalbreyeri* and is eight to thirty-two times less toxic[65] and about ten fold less potent than pancratistatin (**23**).[66]

The U.S. National Cancer Institute identified the potent anticancer activity of (+)-pancratistatin (**23**) in early 1980s.[67,68] Pancratistatin (**23**) was shown to inhibit growth

of numerous cell lines including leukemia and ovarian sarcoma. Recently, Pandey and co-workers have shown that pancratistatin *selectively* induces apoptosis in various types of cancer cell lines (breast, colon, prostrate, neuroblastoma, melanoma and leukemia) at micro molar concentrations.[69-71]

Apoptosis (programmed cell death) can be activated through intrinsic or extrinsic pathway (Figure 2.2).[71,72] In intrinsic pathway, disruption of mitochondrial membrane followed by release of cytochrome *c* activates caspase-3. The extrinsic pathway is initiated by receptor/ligand binding that ultimately leads to an activation of caspase-3. Caspase-3 activates deoxyribonuclease to cause DNA fragmentation and consequently apoptosis. Conventional anticancer therapies (chemotherapy and radiotherapy) trigger intrinsic pathway by inducing DNA damage. However, these treatments carry risk of DNA damage and mutations in non-cancerous cells.

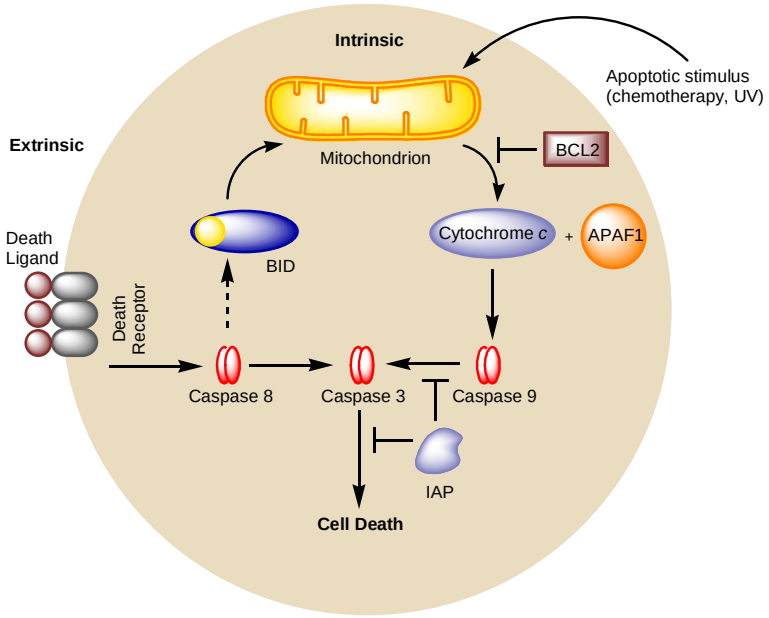

Figure 2.2: Signaling pathways to apoptosis. Redrawn from ref 72.

To understand the selectivity of (+)-pancratistatin (**23**), Pandey and co-workers studied the mechanism of the action of pancratistatin in human leukemia cell line.[71] These studies suggested a possible interaction between pancratistatin, caspase-3 and Fas receptor within the plasma membrane to induce apoptosis. It is postulated that high expression of Fas receptors or the presence of caspase-3 in the plasma membrane in leukemia cells might be responsible for the selective targeting of cancer cells. Additionally, an early increase in caspase-3 activity and intact mitochondrial membrane potential upon treatment with pancratistatin indicated involvement of an extrinsic pathway in apoptosis. Interestingly, DNA fragmentation did not occur prior to caspase-3 activation, indicating that pancratistatin's target is non-genomic.

Apart from potent antitumor activity, (+)-pancratistatin (**23**) and (+)-7-deoxypancratistatin (**24**) also possess antiviral activity.[65] Antiviral activity was observed against RNA flaviviruses (Japanese encephalitis, yellow fever and dengue) and bunya viruses (Punta Toro and Rift Valley viruses).

In spite of its interesting biological profile, (+)-pancratistatin (**23**) and (+)-7-deoxypancratistatin (**24**) have found limited clinical application because of their low natural abundance and lack of practical synthetic route. Therefore, there is a need to design a practical scalable route for the preparation of multigram quantities of antitumor alkaloids (**23**) and (**24**). Several unnatural derivatives and analogues have been subjected to SAR (structure activity relationship) to identify the pharmacore. However, none of these are as potent as natural products (+)-pancratistatin (**23**) and (+)-7-deoxypancratistatin (**24**), indicating the necessity of the entire structure.[73-76]

Synthetic Strategies

In addition to interesting biological activity, (+)-pancratistatin (**23**) and (+)-7-deoxypancratisatin (**24**) natural products have drawn considerable attention because of their structural complexity. The structure of (**23**) and (**24**) involves a highly functionalized cyclohexyl ring (C ring) with six contiguous stereocenters coupled through a carbon-carbon bond to a flat aromatic (A ring), with a *trans*-fused lactam forming the B ring of the molecule (Figure 2.1).

There are numerous reports towards the total syntheses of this compounds (Table 2.1).[73-93] The first total synthesis of racemic pancratistatin (**23**) was reported by Danishefsky in 1989[77], followed by the first asymmetric synthesis of pancratistatin by Hudlicky in 1995.[78] Moreover, Pettit has developed synthesis of (+)-pancratistatin from (+)-narciclasine because of higher natural abundance of narciclasine in plant extracts.[84] There have been attempts to synthesize simplified analogues and derivatives of pancratistatin as well.[73-75] Despite these efforts, none of these approaches are suitable for commercially viable synthesis of pancratistatin (**23**) and 7-deoxypancratistatin (**24**). The majority of the synthetic routes that have been reported to date are too long or low yielding for practical preparations of the natural product (Table 2.1). Besides a short 10-step relay synthesis of (+)-pancratistatin from (+)-narciclasine by Pettit, only three other syntheses (Hudlicky, Madsen, Li) involve less than 15 steps (a number suggested by Hudlicky for synthetic practical applications). Though the syntheses of Hudlicky (entries 2, 11 and 12) and Madsen (entry 13) are comparatively short, they are rather low yielding. The shortest synthesis so far is that reported by Li's group (entry 9). The synthesis proceeds in 13 steps with 9% overall yield, however, uses expensive (+)-pinitol

as the starting material. Based on these criteria, none of the reported strategies are efficient for practical applications.

Entry	Isocarbostyril	Year	Author	no. of steps[a]	Yield (%)
1	(±)-pancratistatin	1989	Danishefsky	27	0.16
2	(+)-pancratistatin	1995	Hudlicky	14	2
3	(+)-pancratistatin	1995	Trost[b]	19	8
4	(+)-pancratistatin	1997	Haseltine	24	0.97
5	(+)-pancratistatin	1998	Magnus	22	1.2
6	(+)-pancratistatin	2000	Rigby	23	0.35
7	(+)-pancratistatin	2001	Pettit[c]	10	3.6
8	(±)-pancratistatin	2002	Kim	21	4
9	(+)-pancratistatin	2006	Li	13	9
10	(+)-7-deoxypancratistatin	1995	Keck	22	4
11	(+)-7-deoxypancratistatin	1995	Hudlicky	12	2.6
12	(+)-7-deoxypancratistatin	1995	Hudlicky	10	3
13	(+)-7-deoxypancratistatin	1996	Chida	29	0.03
14	(+)-7-deoxypancratistatin	1998	Keck	15	12
15	(+)-7-deoxypancratistatin	2000	Plumet	21	3
16	(+)-7-deoxypancratistatin	2006	Madsen	13	1.4
17	(+)-7-deoxypancratistatin	2006	Madsen	15	4.3
18	(±)-7-deoxypancratistatin	2006	Padwa	23	3

[a] Number of steps and overall yield from commercially available starting material for the longest linear sequence. One-pot procedures are counted as one step. [b] Full procedures have not been disclosed. [c] Relay synthesis from (+)-narciclasine.

Table 2.1: Reported total syntheses of the *Amaryllidaceae* isocarbostyrils. Adapted from ref 76.

The most common strategy towards synthesis of pancratistatin (**23**) and 7-deoxypancratistatin (**24**) involve formation of a bond between aromatic ring (A ring) and more or less functionalized cyclohexane (C ring) ring. The approaches used for coupling of A and C rings include *Michael addition* (Plumet), *nucleophilic addition* (Magnus), *electrophilic aromatic substitution* (Haseltine), *S_N2/S_N2' coupling reaction*

(Hudlicky, Trost and Li), *palladium-catalyzed coupling reaction* (Chida) and *photocyclization* (Rigby). These synthetic strategies are discussed below. As mentioned earlier, these strategies are not viable for practical production of pancratistatin (**23**) and 7-deoxypancratistatin (**24**) (*vide infra*). Alternatively, there are less common approaches where the ring C is constructed after linkage of the aromatic ring to suitable precursor of ring C as reported by Danishfeky[77], Kim[85], Keck[89, 90], Madsen[92] and Padwa.[93]

(i) Michael Addition

Heathcock was the first to construct ABC network based on the coupling of aryl ring with cyclohexyl ring.[94] Aromatic anion **28** underwent 1,4-addition with nitrocyclohexene to give a mixture of the *cis* and *trans* aryl nitrocyclohexanes **29** (Scheme 2.1). The *cis*/*trans* mixture was equilibrated to obtain the *trans* isomer, which was used to generate lactam **30** in three subsequent steps.

Scheme 2.1

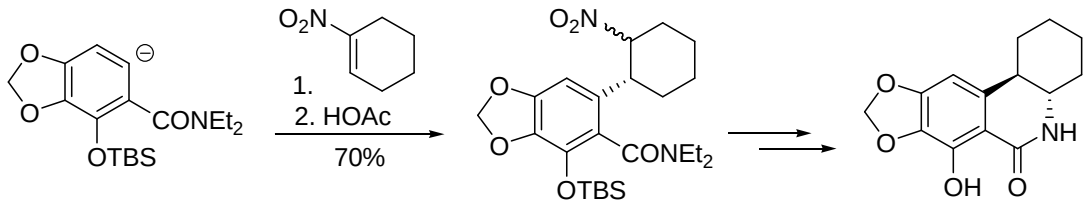

28 **29** **30**

Plumet devised synthesis of (+)-7-deoxypancratistatin (**24**) *via* ring opening of vinyl sulfone **32** (Scheme 2.2).[91] 1,4-addition of aromatic anion **31** to vinyl sulfone **32** gave cyclohexenol **33** with the correct configuration at C_{10b}. Epoxidation of cyclohexenol **33**, followed by oxirane opening with concomitant intramolecular

lactonization completed the synthesis of (+)-7-deoxypancratistatin (**24**). Plumet's synthesis is fairly long (21 steps) as well as low yielding (3%).

Scheme 2.2

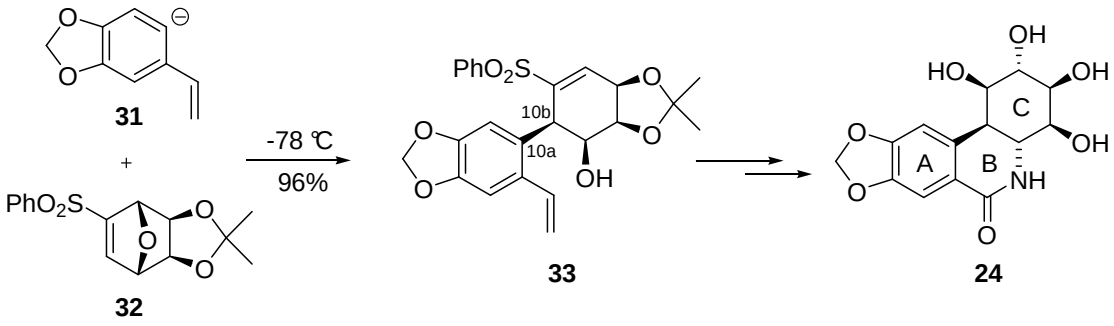

Branchaud and Friestad proposed a palladium-catalyzed intramolecular 1,4-addition of aryl iodide on an chiral enone to construct bond between A and C rings.[95,96] However, this route has not been extended to pancratistatin (**23**) and 7-deoxypancratistatin (**24**) to date.

(ii) Nucleophilic Addition

Magnus reported the total synthesis of (+)-pancratistatin (**23**) *via* intermolecular coupling of an aromatic anion **34** with the cyclohexanone derivative **35** to form 10a-10b carbon-carbon bond (Scheme 2.3).[82] Nucleophilic addition of anion **34** to the cyclohexanone **35** gave alcohol **36**. Benzylic alcohol **36** was converted to ketone **37** in three steps. The treatment of ketone **37** with the chiral amide **38** in the presence of LiCl gave asymmetric lithium enolate, which was trapped with TIPSOTf to form silyl enol ether **39**. Further manipulations completed the synthesis of (+)-pancratistatin (**23**) (22 steps) in a low yield of 1.2%.

Scheme 2.3

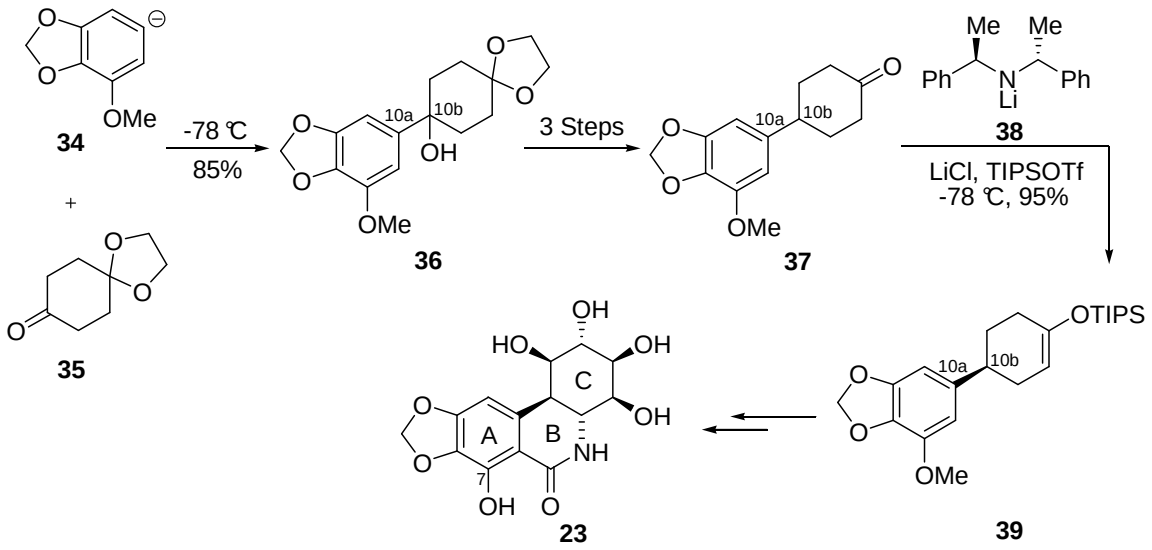

(iii) Electrophilic Aromatic Substitution

Haseltine accomplished a formal total synthesis of (+)-pancratistatin (**23**) *via* Danishfesky's intermediate **42**.[81] The key bond between A and C rings was constructed using an intramolecular electrophilic aromatic substitution (Scheme 2.4). Triflation of alcohol **40** in the presence of 2,6-lutidine gave the expected cyclized product **41**. Several protection and deprotection steps provided Danishfesky's lactone intermediate **42** constituting a formal total synthesis (24 steps, 0.97% yield). It is interesting to note that when a donor substituent (OBn) is present on the aromatic ring (on carbon 7), the desired cyclized adduct was obtained in very low yield (8%). Instead, a major regioisomer arising from an undesired rearrangement was observed. Electrophilic aromatic substitution has also been applied to construct 7-deoxynarciclasine (**26**) analogue *via epi*-selenonium ion.[97]

Scheme 2.4

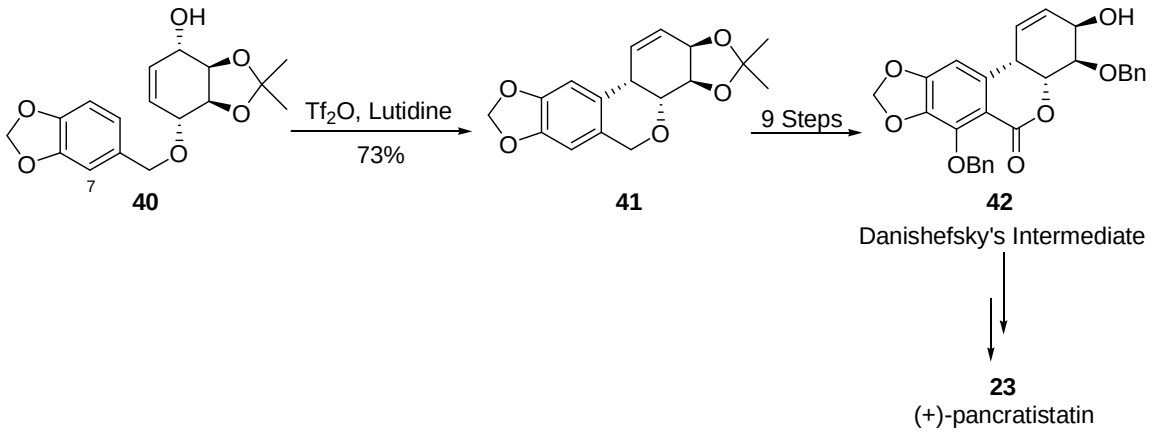

(iv) S_N2 and S_N2' Coupling

Hudlicky's Approach

The first asymmetric synthesis of (+)-pancratistatin (**23**) by Hudlicky involved opening of aziridine ring **44** by aromatic cuprate reagent **43** (Scheme 2.5).[78] The regioselective S_N2 ring opening of aziridine **44** led to inversion at C_{10b}, establishing the desired stereochemistry. Subsequent key steps included installation of *trans*-diol and the formation of lactam to complete the synthesis of (**23**). However, the presence of benzamide moiety led to lengthy manipulations to affect the lactamization and the functionalization of the double bond.

To overcome problems associated with the manipulations of benzamide, the amide was introduced in (+)-7-deoxypancratistatin (**24**) as the last step after the coupling reaction (Scheme 2.6) in the second-generation synthesis.[80,87] However, the coupling of cuprate **46** with aziridine **44** produced compound **45** in lower yield. The low yield might be due to the instability of the organolithium compound and the corresponding cuprate compared to the compound **43**.

Scheme 2.5

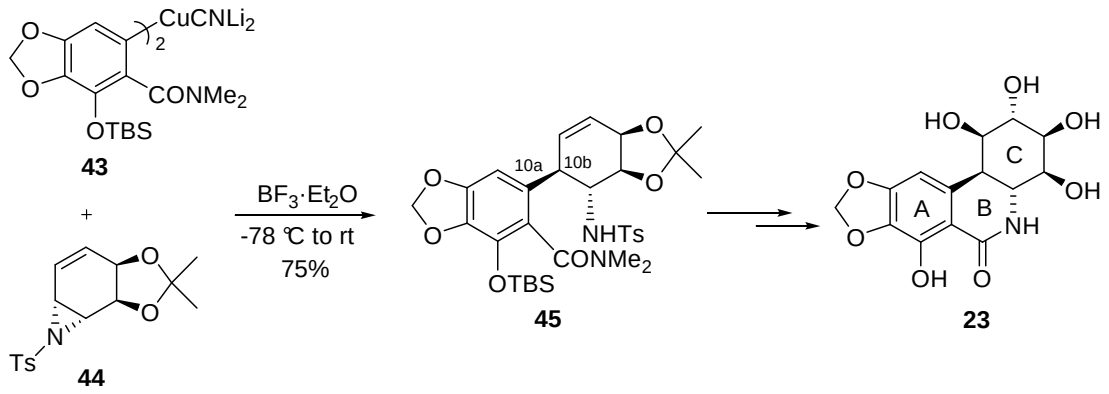

To save the number of functional group interconversion steps, aziridine **48** was prepared where the amide carbon was also used as the protecting group of aziridine (Scheme 2.6).[87] The ring opening of aziridine **48** by cuprate **46** produced carbamate **49**. Similar synthetic sequence (using enantiomer of aziridine **48**) was used to synthesize an enantiomer of 7-deoxypancratistatin.[98] Hudlicky has also made considerable efforts towards the synthesis of analogues of pancratistatin (**23**) and 7-deoxypancratistatin (**24**) using a similar approach (Scheme 2.6).[73-75]

Though short (10 steps), the synthesis by Hudlicky is rather low yielding (3%) and arduous. The key steps that reduce the yield are aziridination and aziridine ring-opening. The aziridine ring-opening requires extremely low temperature, thus making this synthesis unsuitable for practical applications. Furthermore, both coupling partners **46** and **48** are moderately unstable, entailing a difficulty in their preparation.

Scheme 2.6

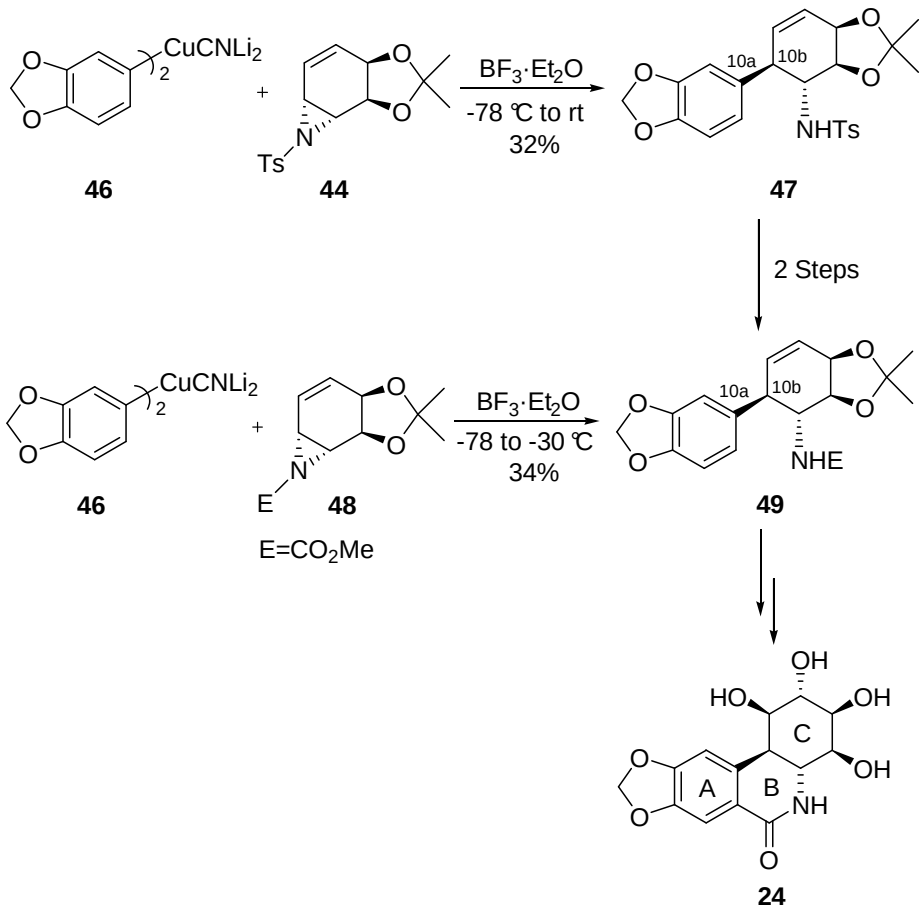

Trost's Approach

In the asymmetric synthesis of (+)-pancratistatin (**23**) by Trost, carbon-carbon bond between A and C rings was constructed by allylic substitution of the carbonate **51** *via* S_N2' chemistry (Scheme 2.7).[79] Reaction of allylic carbonate **51** with mixed cuprate **50** resulted in inversion of configuration to provide allylic-arylated system **52**. This type of mixed cuprate **50** is unstable and significant optimization was required for this step. Due to the difficulty associated with purification of the azide, azide **52** was not isolated. Additionally, full procedures have not been disclosed for this synthesis.

Scheme 2.7

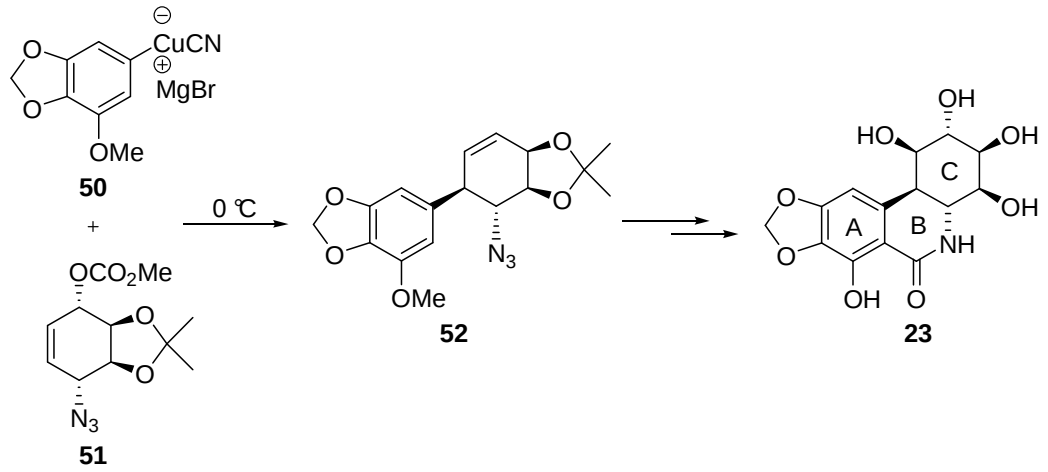

Li's Approach

Li's synthetic approach towards (+)-pancratistatin (**23**) is outlined in the Scheme 2.8. Intramolecular nucleophilic opening of cyclic sulfate **53** using aryl cerium reagent constructed the key bond to generate **54**.[86] In comparison to organomagnesium and organolithium reagents, organocerium reagents are much milder to avoid side reactions. Though the synthesis represents the shortest (13 steps) and the most high yielding (9%) route, the starting material (+)-pinitol is relatively expensive ($1,027 per 10 g).[75]

Scheme 2.8

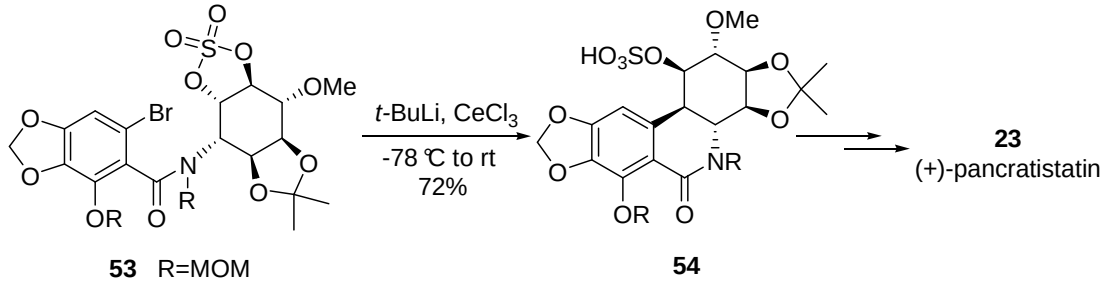

(iv) Palladium-Catalyzed Coupling

Heck Reaction

Ogawa synthesized (+)-7-deoxypancratistatin[88] from the key intermediate **56** produced in the synthesis of (+)-7-deoxynarciclasine.[99] Intramolecular Heck reaction of aryl bromide **55** generated intermediate **56** (Scheme 2.9). Interestingly this Heck reaction proceeds *via anti* elimination instead of generally observed *syn* elimination. The desired stereochemistry at C_{10b} for the synthesis of (+)-7-deoxypancratistatin (**24**) was achieved *via* hydrogenation of alkene **56**. The synthetic route towards (**24**) is the longest reported to date (29 steps) and is also extremely low yielding (0.03%).

Scheme 2.9

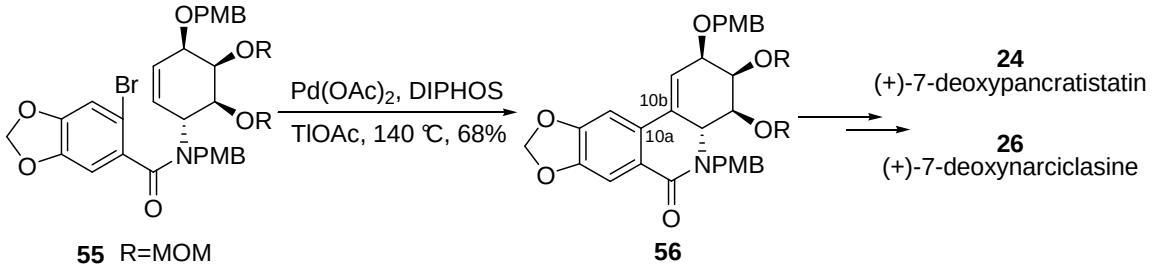

55 R=MOM **56**

Suzuki Coupling

Hudlicky employed palladium-catalyzed Suzuki coupling to construct the bond between A and C rings in narciclasine (**25**) (Scheme 2.10).[98] The reaction of arylboronic acid **57** with vinyl bromide **58** formed alkene **59**. Analogous approach has also been used by Banwell to construct an enantiomer of narciclasine (**25**).[100]

Scheme 2.10

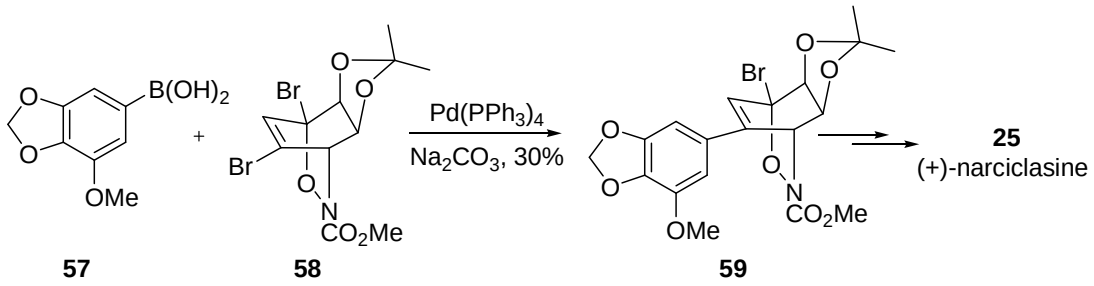

57 **58** **59**

Recently, Pandey and co-workers formed *epi*-7-deoxypancratistatin **63** *via* cross-coupling of arylboronic acid **60** with iodo enone **61** (Scheme 2.11).[101] This was followed by intramolecular aza-Michael addition to generate *cis*-fused lactam ring in **63**.

Scheme 2.11

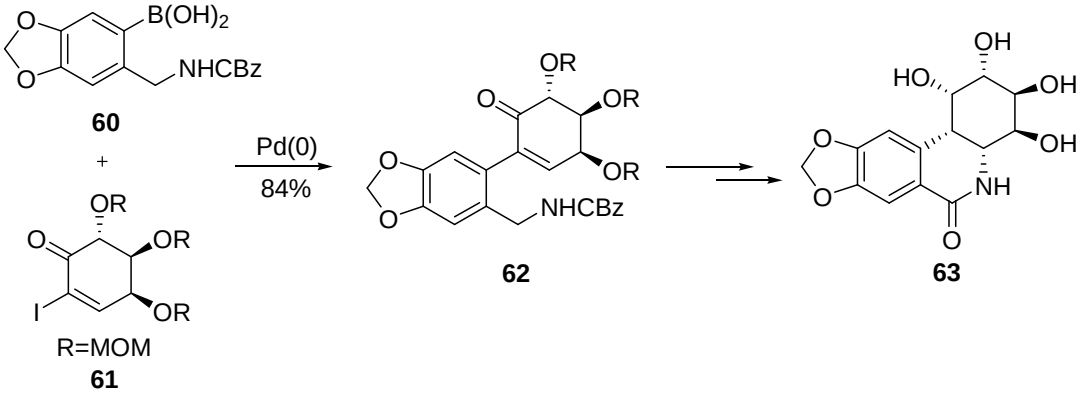

(v) Photocyclization

Rigby's synthetic approach is based on a hydrogen bond controlled aryl enamide photocyclization (Scheme 2.12).[83] Irradiation of enamide **64** at 254 nm in benzene established desired stereochemistry at C_{10b} in compound **65** in 30% yield (60% based on recovered starting material). Further functionalization of C ring completed the synthesis

of (+)-pancratistatin (**23**). This synthesis is fairly long (23 steps) and enormously low yielding (0.35%) as well.

Scheme 2.12

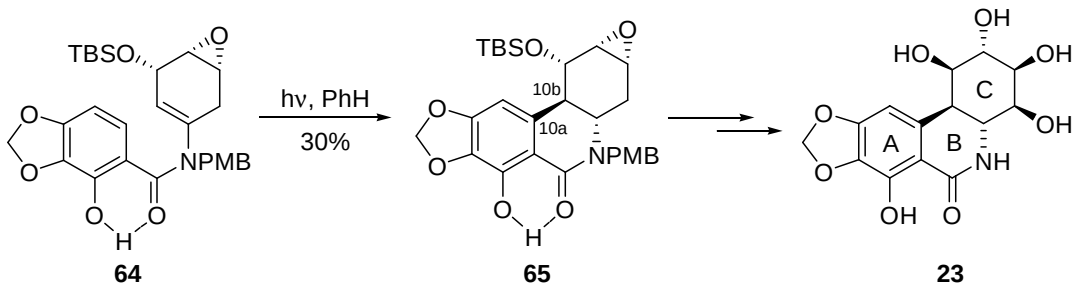

Analogous photocyclization approach was adapted in the synthesis of 7-deoxypancratistatin analogue **68** by Pandey (Scheme 2.13).[102] Irradiation of carbamate **66** at 280 nm gave the cyclized product **67** as single isomer.

Scheme 2.13

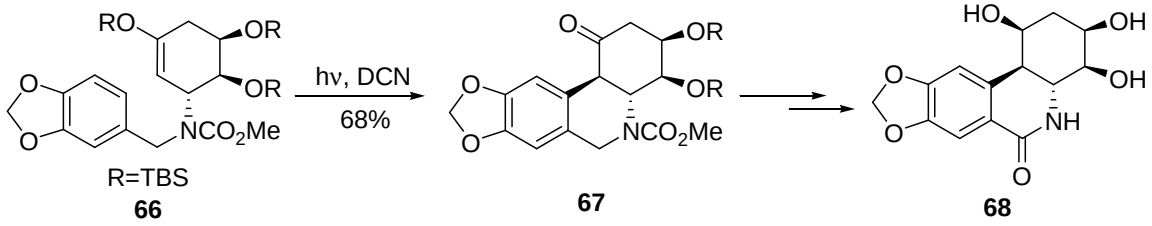

RESEARCH GOAL

The purpose of this work is to design an efficient synthetic route to antitumor alkaloids pancratistatin (**23**) and 7-deoxypancratistatin (**24**) using palladium-catalyzed allylic-arylation coupling methodology, thus providing multi-gram quantities of these compounds for clinical evaluations.

In order to test the feasibility of aryl-allyl coupling, (±)-7-deoxypancratistatin analogue **69** was first synthesized. The retrosynthetic approach to the synthesis of 7-deoxypancratistatin analogue **69** is outlined in the Scheme 2.14. The *trans* diol in **69** will be generated from the alkene **70** *via* opening of epoxide. The B ring of the alkene **70** will be obtained from the carbamate **71** by Friedel-Crafts cyclization. The allyl-aryl bond between the A and C rings in carbamate **71** will be constructed from palladium-mediated coupling of the aryl siloxane **72** and allylic carbonate **73**.

The synthetic route to aryl siloxane **72** and allyl carbonate **73** had already been established in the DeShong group.[34] Also, the synthesis of carbamate **71** had been accomplished by the coupling reaction between aryl siloxane **72** and allylic carbonate **73**. However, the subsequent steps to form the B ring and installation of *trans* diol had not been optimized. Provided with carbamate **71**, the goal of my research project was to optimize these subsequent steps and complete the synthesis of 7-deoxypancratistatin analogue **69**.

Scheme 2.14

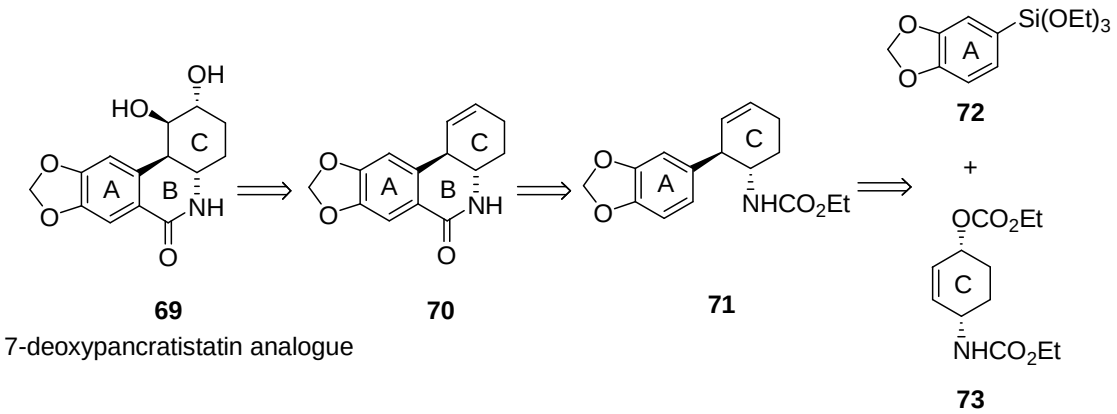

RESULTS AND DISCUSSION

Synthesis of Coupling Partners: Allylic Carbonate and Aryl Siloxane

Allylic carbonate **73** was synthesized as outlined in the Scheme 2.15. The synthesis of carbonate **73** commenced from the commercially available cyclohexadiene **74**. Diels-Alder reaction of cyclohexadiene **74** with the acyl nitroso dienophile (generated *in situ)* formed hydroxamate **75**.[103] The cleavage of N-O bond in hydroxamate **75** using molybdenum hexacarbonyl yielded allylic alcohol **76**.[104] Finally, acylation of **76** with ethyl chloroformate afforded allylic carbonate **73**.

Aryl siloxane **72** was synthesized as shown in the Scheme 2.16.[20] The commercially available aryl bromide **77** underwent a Grignard reaction to generate the organomagnesium species which was quenched by tetraethylorthosilicate ($Si(OEt)_4$) to form aryl siloxane **72**.

Scheme 2.15

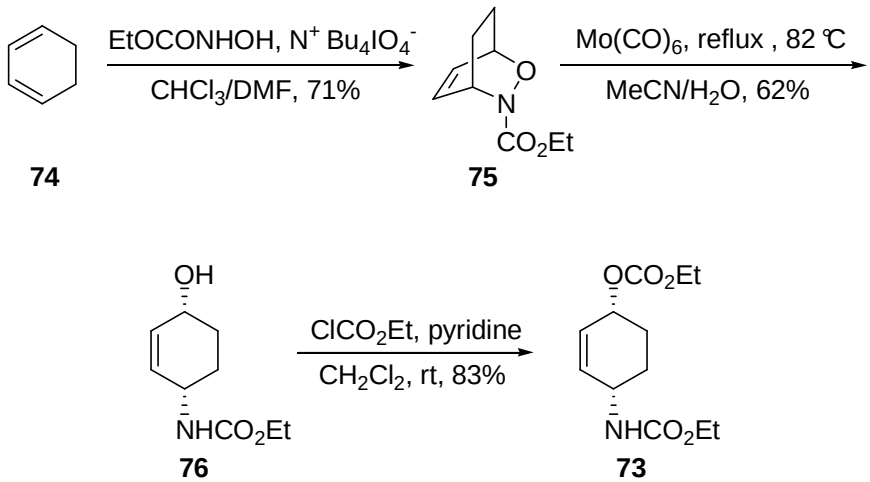

Scheme 2.16

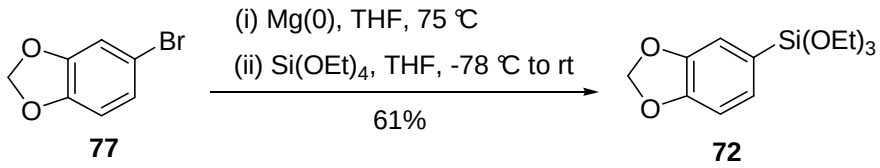

Coupling of Allylic Carbonate with Aryl Siloxane

The coupling of allylic carbonate **73** with electron-rich aryl siloxane **72** in the presence of TBAF and $Pd(dba)_2$ catalyst gave the allylic arylated coupling products **73** and **79**, respectively, as 1:1.6 ratio of diastereomers in 81% yield (Scheme 2.17).

Scheme 2.17

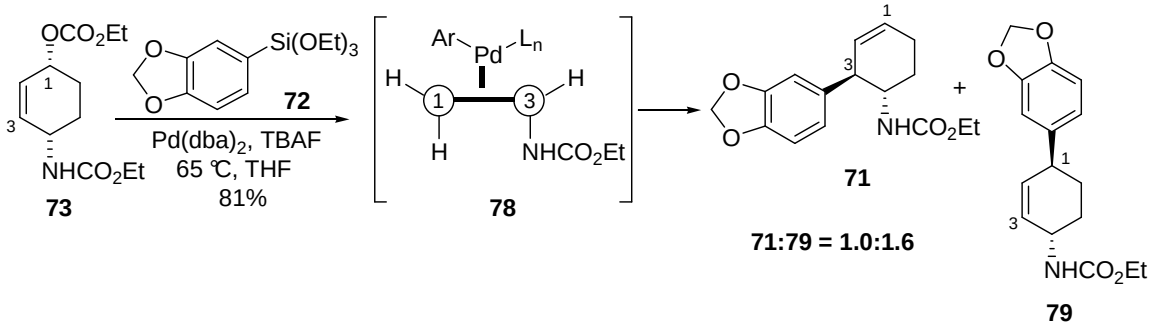

The low regioselectivity in the products is consistent with the previously proposed model for regioselectivity in cyclohexenyl systems. Using the model developed in our lab, the π-allyl Pd complex **78** derived from allylic carbonate **73** formed on the face opposite from the departing carbonate. This "symmetrical" Pd-complex **78** does not have substituents on the face of the π-complex which has Pd attached. Accordingly, subsequent reductive elimination of the aryl group from silicon is equally probable at the 1 and 3 positions and therefore, a modest regioselectivity was observed. The role of

electronic factors on the regioselectivity of the coupling reaction was unknown. However, the results from Szabó[105] indicated that the coupling reaction would favor carbamate **79**, as observed in the experiment. Surprisingly, when benzyl carbamate (CBz) analogue of **73** was used as the coupling partner with the aryl siloxane **72**, the yield of coupling products (CBz analogues of **71**/**79**) decreased (33-50%) dramatically.

Scheme 2.18

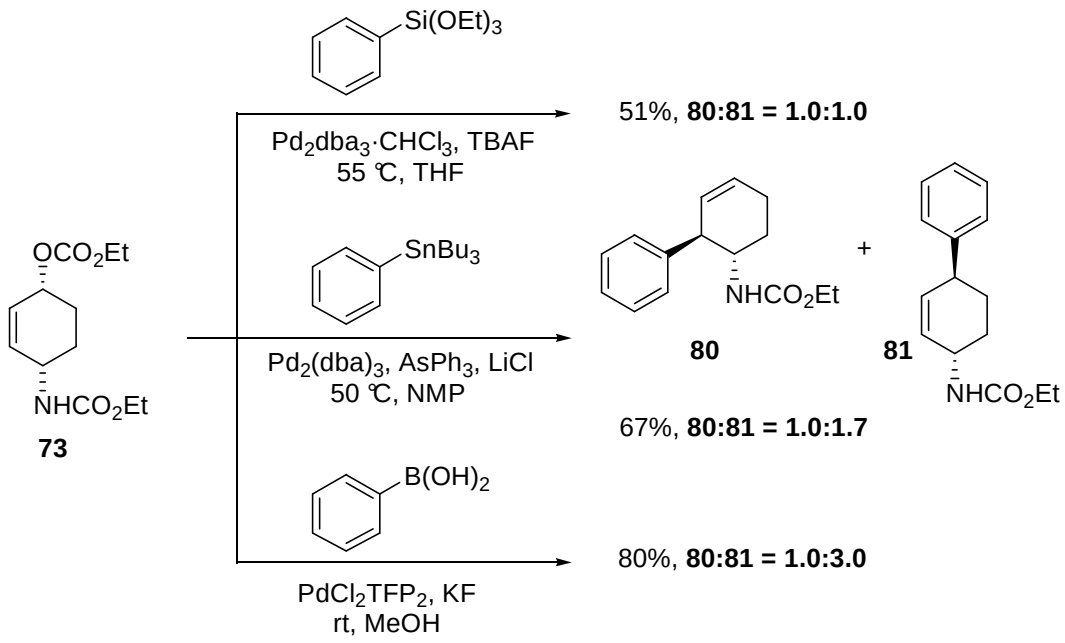

Similar allyl-aryl coupling reaction can also be accomplished *via* Stille[29] (tin) and Suzuki[41] (boron) reaction (Scheme 2.18). Both Stille and Suzuki reaction worked well to produce regioisomers **80** and **81**. However, the undesired coupling product **81** was obtained in much greater amount in the Suzuki reaction compared to Stille and Hiyama coupling reaction.

Generation of B ring and Installation of diol

With carbamate **71** in hand, the next goal was to construct the B ring *via* Friedel-Crafts acylation. When both ethyl carbamate **71** and CBz analogue of **71** were subjected to Bischler-Napieralski cyclization using DMAP/Tf_2O, the yield of lactam was very low (15-20%). Therefore, an alternative route was investigated.

The mixture of regioisomeric carbamates **71** and **79** was subjected to Friedel-Crafts acylation using P_2O_5 and $POCl_3/Me_3SiOSiMe_3$ (1:1) (Scheme 2.19).[106] The cyclization reaction was completely regioselective where only regioisomer **71** underwent cyclization to form the lactam **20** in good yield (55-65%). Attempts to optimize the reaction conditions indicated that reaction worked well as indicated in the literature. However, when mixture of CBz analogues **71**/**79** was subjected to similar reaction conditions, the lactam **70** was obtained in low yield (15%) comparable to that using Tf_2O/DMAP reagent. We decided to change the sequence of steps by forming the epoxide first and then perform the cyclization (Scheme 2.19). While the epoxidation of alkenes **71**/**79** proceeded in moderate yield to give epoxides **82**/**83**, the cyclization of **82**/**83** using $POCl_3/P_2O_5$ showed decomposition. This route was abandoned therefore.

Having optimized the yield of lactam **70**, the next goal was to install *trans* diol *via* epoxidation. Previous work in DeShong group had shown that the epoxidation of the double bond using *m*-CPBA[107] gave a mixture of diastereomeric epoxides **84** in low yield (15-30%) (Scheme 2.20). Attempts to improve the yield of epoxides using more reactive epoxidation reagents led to extensive decomposition of the alkene. The subsequent step of epoxide opening of **84** gave poor yield of diol **69** as well.

Scheme 2.19

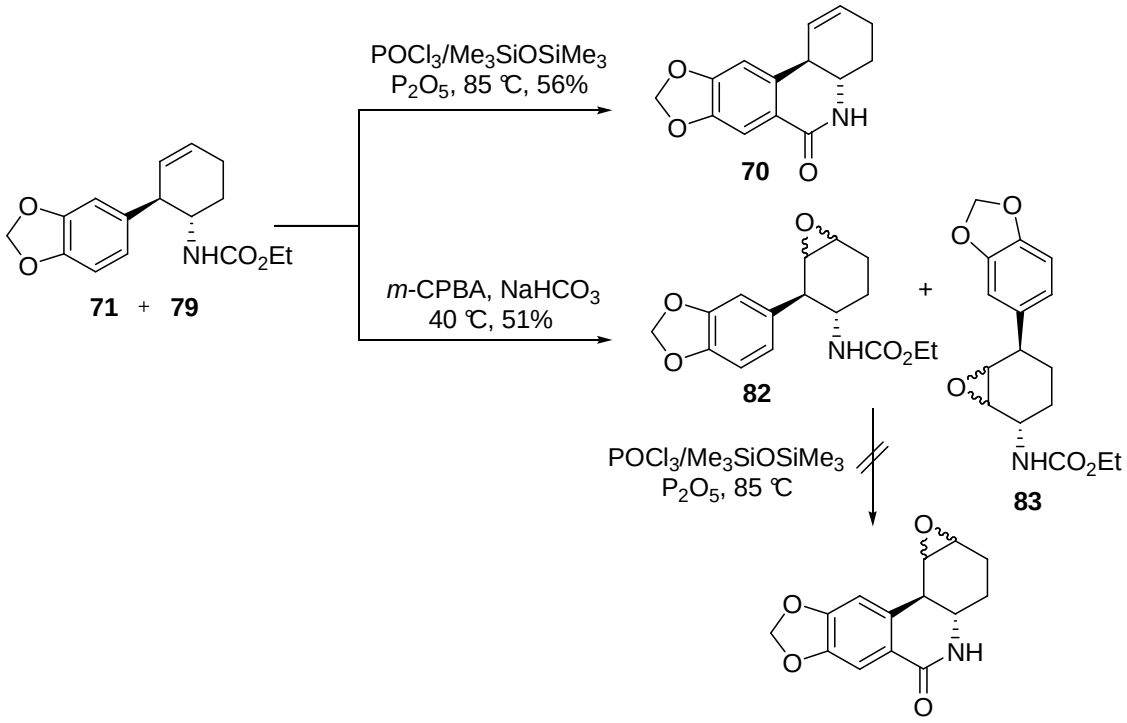

Scheme 2.20

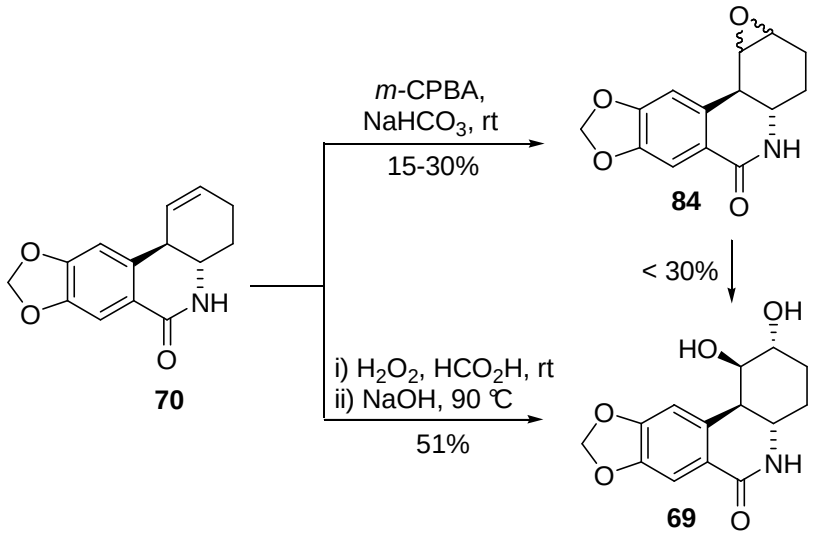

A more direct method of introducing the *trans* diol functionality was used for the synthesis of diol **69** (Scheme 2.20). According to this one-pot *trans*-dihydroxylation, the

reaction of alkene **70** with hydrogen peroxide in formic acid generates diastereomeric epoxides **84a/84b** (Scheme 2.21).[108] Under acidic conditions (formic acid), the epoxides are protonated and then opened by formic acid to generate a mixture of alcohol formates **85a/85b**. Because of *trans*-diaxial opening of epoxide to avoid intermediate boat conformation, only the desired *trans* relationship will be installed. Therefore, hydrolysis of mono-formates provides the desired diol **69** with a single stereoconfiguration. In principle, the stereoselectivity in the epoxidation reaction was of no consequence since the diaxial opening of each epoxide should be regiospecific and give only *trans*-diol **69**.

Scheme 2.21

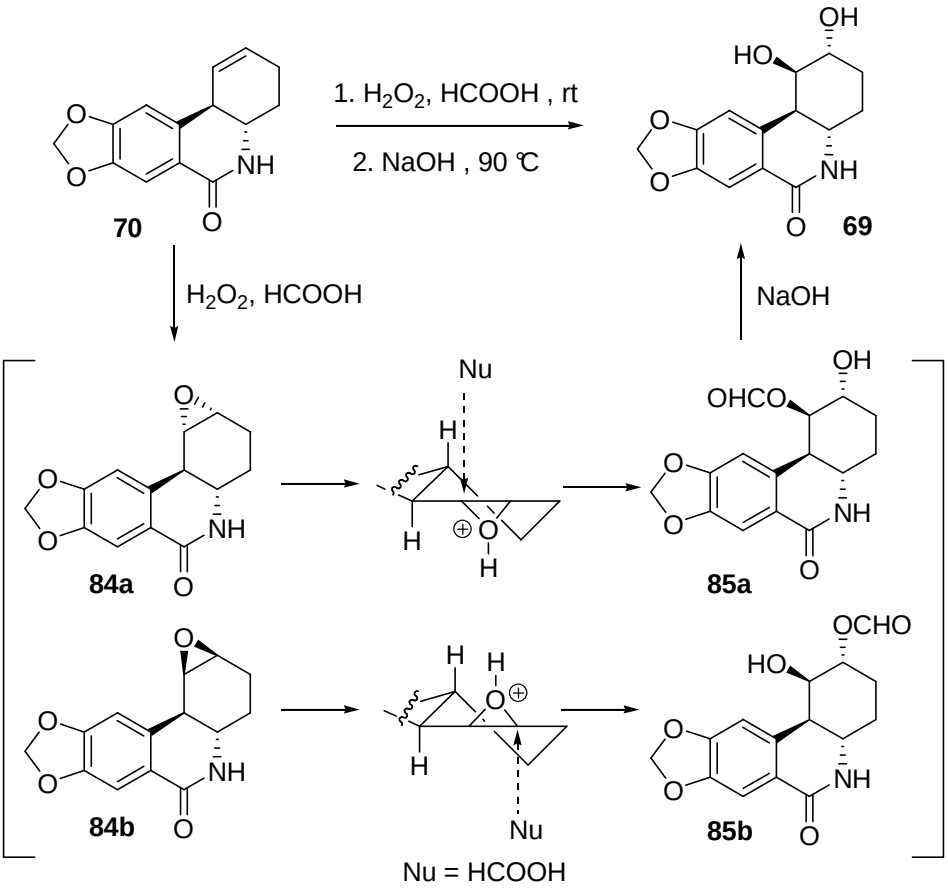

Much optimization was required for the isolation of diol **69** because of difficulty while working with such a polar compound, which is poorly soluble in most organic solvents (ethyl acetate, acetone, methanol). A variety of normal or reverse-phase methods led to an extensive loss of product. The most efficient purification method ultimately involved an extraction-precipitation regime, which gave *trans* diol in 51% yield (Scheme 2.20). Attempts to acylate hydroxyl groups to improve the solubilty of diol **69** in organic solvents failed, presumably because of sterical interference caused by *peri* hydrogen on C_{10} of aromatic A ring (Figure 2.1).

The relative stereochemistry of diol **69** was confirmed by the COSY experiment and by correlation to the published ^{1}H NMR data of the benzoate of the 7-deoxypancratistatin derivative **86** (Figure 2.3).[109] The coupling constant of 2 Hz between H_1 and H_{10b} of **69** is diagnostic of a *cis* relationship between the two protons. Protons H_{4a} and H_{10b} of **69** exhibit a 13 Hz coupling constant which is indicative of a *trans* diaxial relationship. These coupling constant values are in accord with the coupling observed (J = 2 Hz) for protons H_1 and H_{10b} and (J = 13 Hz) for protons H_{4a} and H_{10b} respectively in **86**.

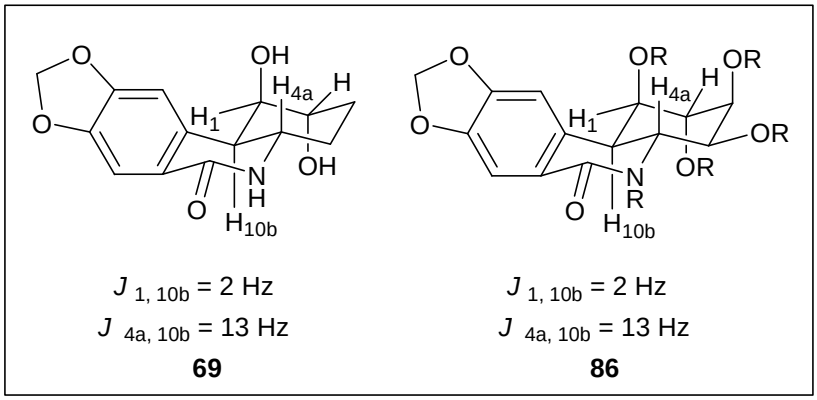

Figure 2.3: Relative stereochemistry confirmed from correlation with ^{1}H NMR coupling constants

CONCLUSION

The synthesis of (±)-7-deoxypancratistatin analogue has been accomplished *via* palladium-catalyzed allylic-arylation. The key reaction in the synthesis involves the stereoselective formation of a carbon-carbon bond between the A and C rings by coupling of aryl siloxane with allylic carbonate. Subsequent steps include generation of B ring by Friedel-Crafts acylation and installation of the *trans* diol. The key coupling reaction is advantageous compared to Stille reaction because it avoids the use of toxic tin reagents. Additionally, the coupling is superior to the Suzuki reaction which results in formation of undesired regioisomer predominantly (Scheme 2.18). Our palladium-catalyzed allylic-arylation coupling methodology is also superior to allyl-aryl coupling by Hudlicky and Trost because of the ease of preparation of coupling partners, aryl siloxane and allyl carbonate as well as trouble-free coupling reaction.

EXPERIMENTAL DETAILS

General Methods

All reactions were run under an atmosphere of argon unless otherwise noted. Glassware used in the reactions was dried for a minimum of 12 h in an oven at 120 °C or flame dried prior to use. Tetrahydrofuran was distilled from sodium/benzophenone ketyl, while methylene chloride, pyridine, methanol and N-methyl-2-pyrrolidone were distilled from calcium hydride. Phosphorous oxychloride was distilled from P_2O_5.

Thin-layer chromatography (TLC) was performed on 0.25 mm silica gel coated plates treated with a UV-active binder with compounds being identified by one or more of the following methods: UV (254 nm), vanillin/sulfuric acid charring, or $KMnO_4$ charring. Flash chromatography was performed using glass columns and medium pressure silica gel (Sorbent Technologies, 45-70 μ).

Infrared spectra were recorded on a Nicolet 560 FT-IR spectrophotometer. Samples used for obtaining infrared spectra were either dissolved in carbon tetrachloride or taken neat. IR band positions are reported in reciprocal centimeters (cm^{-1}) and relative intensities are listed as br (broad), s (strong), m (medium), or w (weak). Nuclear magnetic resonance (^1H, ^{13}C NMR) spectra were recorded on a 400 MHz spectrometer. Chemical shifts are reported in parts per million (δ) and coupling (*J* values) are reported in hertz (Hz). Spin multiplicities are indicated by the following symbols: s (singlet), d (doublet), t (triplet), q (quartet), m (multiplet), br s (broad singlet), br d (broad doublet). Low resolution mass spectrometry (LRMS) and high resolution mass spectrometry (HRMS) were obtained on a JEOL SX-02A instrument.

Aryl Siloxane 72

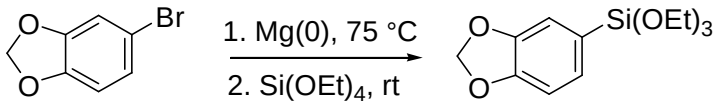

77 61% **72**

To 811 mg (33.8 mmol, 2.00 equiv.) of washed magnesium turnings was added 10.0 mL of anhydrous THF. After heating the reaction mixture at 75 °C, 2.00 mL (16.9 mmol, 1.00 equiv.) of the aryl bromide **77** was added dropwise under argon and reaction was allowed to stir for 45 min. This was followed by addition of 10.0 mL of anhydrous THF to the reaction mixture. After 4 h, the Grignard mixture was cannulated into 9.55 mL (42.3 mmol, 2.50 equiv.) of $Si(OEt)_4$ in 20.0 mL anhydrous THF. The reaction was allowed to stir for 3 h under argon at room temperature. The black solution was extracted with 3 × 200 mL Et_2O and the organic layers were washed with 200 mL H_2O. The combined organic extracts were dried over $MgSO_4$, filtered and concentrated *in vacuo* to give a brown oil. Purification by column chromatography (2% EtOAc/98% hexane, R_f = 0.26) yielded 2.94 g (61%) of aryl siloxane **72** as a colorless oil: IR (CCl_4) 2970 (s), 2926 (m), 2885 (m), 2780 (w), 2739 (w), 1611 (w), 1479 (s), 1234 (s), 1169 (s), 1095 (s) cm^{-1}; ^1H NMR (400 MHz, $CDCl_3$) δ 7.16 (dd, *J* = 1, 8 Hz, 1H), 7.09 (d, *J* = 1 Hz, 1H), 6.84 (d, *J* = 8 Hz, 1H), 5.93 (s, 2H), 3.83 (q, *J* = 7 Hz, 6H), 1.20 (t, *J* = 7 Hz, 9H); ^{13}C NMR (100 MHz, $CDCl_3$) δ 149.3, 147.3, 129.2, 123.6, 113.8, 108.5, 100.5, 58.6, 18.1; LRMS (FAB) 284.4 (M^+, 100), 283.4 (42), 239 (80), 161 (65); HRMS (FAB) calcd 284.1080 (M^+), found 284.1080.

Hydroxamate 75

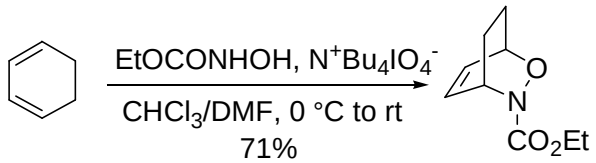

74 **75**

To 6.29 g (14.5 mmol, 1.40 equiv.) of $NBu_4^+IO_4^-$ (tetrabutylammonium periodate) under argon was added chloroform (12.0 mL) and DMF (4.00 mL). The reaction mixture was cooled to 0 °C and then 0.990 mL (104 mmol, 1.00 equiv.) of cyclohexadiene **74** was added. Finally, 1.09 g (104 mmol, 1.00 equiv.) of hydroxamic acid (EtOCONHOH) dissolved in chloroform (6.00 mL) and DMF (2.00 mL) was added *via* addition funnel. The reaction mixture was stirred at 0 °C to room temperature for 17 h. The product was extracted with Et_2O (4 × 100 mL), washed with H_2O (100 mL), dried over $MgSO_4$, concentrated *in vacuo* to give the crude hydroxamate **75** as a brown oil. Flash column chromatography on silica gel (50% EtOAc/50% hexane, R_f = 0.49) gave 1.36 g (71%) of hydroxamate **75** as a light orange oil: IR (CCl_4) 3062 (w), 2984 (m), 2936 (m), 2862 (w), 1706 (s), 1380 (s), 1268 (s), 1081 (s) cm^{-1}; ^1H NMR (400 MHz, $CDCl_3$) δ 6.55-6.46 (m, 2H) , 4.76 (m, 1H), 4.70 (m, 1H), 4.18-4.07 (m, 2H), 2.17-2.04 (m, 2H), 1.45 (qt, *J* = 2, 12 Hz, 1H), 1.33 (t, *J* = 12 Hz, 1H), 1.20 (dt, *J* = 2, 7 Hz, 3H); ^{13}C NMR (100 MHz, $CDCl_3$) δ 158.3, 132.0, 131.6, 71.0, 62.2, 49.9, 23.4, 20.6, 14.5; EI mass spectrum, *m/z* (relative intensity) 183 (M^+, 98), 105 (72), 79 (92), 77 (80), 67 (65), 29 (76), 27 (65); HRMS (ESI) calcd for $C_9H_{14}NO_3$ $(M+H)^+$ 184.0974, found 184.0974.

Alcohol-Carbamate 76

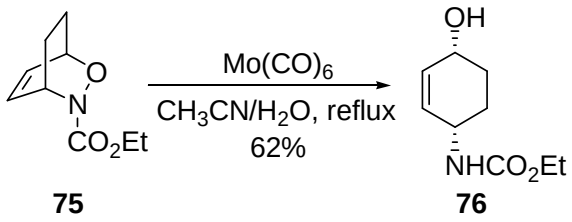

75 **76**

To 7.71 g (42.1 mmol, 1.00 equiv.) of the hydroxamate **75** dissolved in 240 mL acetonitrile and 15 mL distilled water was added 12.2 g (46.3 mmol, 1.10 equiv.) of molybdenum hexacarbonyl ($Mo(CO)_6$). The reaction mixture was refluxed at 82 °C for 66 h. The black-brown reaction mixture was vacuum filtered through Celite and the filtrate was concentrated *in vacuo* to give crude alcohol-carbamate **76** as a yellow oil. Flash column chromatography on silica gel (75% EtOAc/25% hexane, R_f = 0.33) gave 4.81 g (62%) of carbamate **76** as a yellow oil: IR (CCl_4) 3619 (m), 3450-3100 (br s), 3028 (m), 2981 (s), 2940 (s), 1713 (s), 1502 (s), 1316 (s), 1231 (s), 1067 (s) cm^{-1}; ^1H NMR (400 MHz, $CDCl_3$) δ 5.86 (d, *J* = 10 Hz, 1H), 5.73 (dd, *J* = 2, 10 Hz, 1H), 4.67 (br s, 1H), 4.16-4.07 (m, 4H), 1.88-1.80 (m, 2H), 1.72-1.63 (m, 2H), 1.53 (br s, 1H), 1.22 (t, *J* = 7 Hz, 3H); ^{13}C NMR (100 MHz, $CDCl_3$) δ 156.0, 132.5, 130.9, 64.5, 60.8, 46.2, 28.9, 25.6, 14.6; EI mass spectrum, *m/z* (relative intensity) 185 (M^+, 4), 157 (100), 141 (92), 96 (76), 68 (87), 55 (99), 39.5 (99.5); HRMS calcd for $C_9H_{15}NO_3$ (M^+) 185.1053, found 185.1052.

Carbonate-Carbamate 73

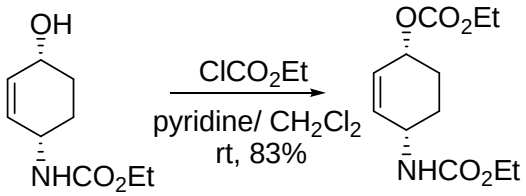

76 **73**

To 2.84 g (15.4 mmol, 1.00 equiv.) of alcohol-carbamate **76** in 35.0 mL anhydrous CH_2Cl_2 and 1.85 mL (23.0 mmol, 1.50 equiv.) anhydrous pyridine was added 2.28 mL (23.0 mmol, 1.50 equiv.) of ethyl chloroformate dropwise *via* syringe under argon. The reaction was allowed to stir at room temperature for 5 days. The reaction mixture was extracted with CH_2Cl_2 (3 × 50 mL), washed with H_2O (50 mL), dried over $MgSO_4$ and concentrated *in vacuo*. Flash chromatography on silica gel (30% EtOAc/70% hexane, R_f = 0.43 afforded 3.28 g (83%) of the carbonate-carbamate **73** as a yellow oil: IR (CCl_4) 3450 (m), 3042 (w), 2987 (w), 1747 (s), 1727 (s), 1502 (s), 1265 (s) cm^{-1}; ^1H NMR (400 MHz, $CDCl_3$) δ 5.86 (m, 2H), 5.03 (m, 1H), 4.64 (br s, 1H), 4.19-4.14 (m, 3H), 4.08 (q, *J* = 7 Hz, 2H), 1.88 (br s, 3H), 1.67-1.63 (m, 1H), 1.28 (t, *J* = 7 Hz, 3H), 1.21 (t, *J* = 7 Hz, 3H); ^{13}C NMR (100 MHz, $CDCl_3$) δ 156.2, 155.0, 134.4, 128.3, 127.7, 70.3, 64.2, 61.2, 46.6, 26.2, 25.6, 14.9, 14.5; FAB mass spectrum, *m/z* (relative intensity) 258 ($(M+H)^+$, 2), 168 (100), 90 (40), 62 (46); HRMS (FAB) calcd for $C_{12}H_{19}O_5N$ $(M+H)^+$ 258.1332, found 258.1342.

Carbamates 80 and 81

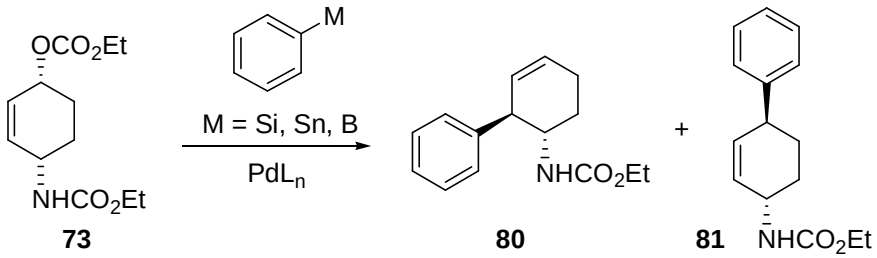

73 **80** **81**

Hiyama-like Coupling

The coupling reaction of carbonate **73** with $PhSi(OEt)_3$ had been performed previously by Bogaczyk in the DeShong group.[31] To a solution of 100 mg (0.389 mmol) of allyl carbonate **73** and 20 mg (0.020 mmol) $Pd_2(dba)_3 \cdot CHCl_3$ in 10 mL dry THF was added 190 μL (0.778 mmol) $PhSi(OEt)_3$, followed by 778 μL (0.778 mmol, 1.0 M solution in THF) TBAF. The solution was degassed *via* a single freeze-pump-thaw cycle and then heated to 55 °C. The reaction mixture was quenched after 48 h with 40 mL H_2O. The layers were separated and the aqueous phase was extracted with 3×40 mL Et_2O. The combined organic layers were dried over Na_2SO_4 and concentrated *in vacuo*. Purification of the residue by flash chromatography (20 mm, 20 cm, 5% EtOAc/95% hexane) gave 48 mg (51%) of carbamates **80:81** as a white solid. The ratio of carbamates **80** to **81** was 1.0:1.0. The pure regioisomers were separated using preparative HPLC (3:1 hexane:EtOAc). **Carbamate 80:** TLC R_f = 0.35 (3:1 hexane:EtOAc); IR (CCl_4) 3447 (w), 3029 (w), 2933 (w), 1729 (s), 1552 (s) cm^{-1}; ^1H NMR ($CDCl_3$) δ 7.21-7.29 (m, 5H), 5.89 (ddd, *J* = 2, 4, 10 Hz, 1H), 5.62 (ddd, *J* = 2, 4, 10 Hz, 1H), 4.80 (br s, 1H), 4.01 (q, *J* = 7 Hz, 2H), 3.78-3.83 (m, 1H), 3.29-3.33 (m, 1H), 2.14-2.24 (m, 2H), 1.87-1.92 (m, 1H), 1.58-1.62 (m, 1H), 1.16 (t, *J* = 7 Hz, 3H); ^{13}C NMR ($CDCl_3$) δ 156.0, 142.6, 128.4

(2C), 128.3, 127.9, 126.7, 60.6, 52.6, 48.0, 25.5, 23.0, 14.5; FAB mass spectrum *m*/*z* (relative intensity) 246 ((M + H), 17), 102 (100), 91 (25); HRMS (FAB) calcd for $C_{15}H_{20}O_2N$ (M+H) 246.1494, found 246.1491. **Carbamate 81**: TLC R_f = 0.35 (3:1 hexane:EtOAc); IR (CCl_4) 3454 (w), 3026 (w), 2943 (w), 1728 (s), 1500 (s) cm^{-1}; ^1H NMR ($CDCl_3$) δ 7.16-7.31 (m, 5H), 5.82 (d, *J* = 10 Hz, 1H), 5.77 (d, *J* = 10 Hz, 1H), 4.63 (br s, 1H), 4.32-4.34 (m, 1H), 4.12 (q, *J* = 7 Hz, 2H), 3.36-3.38 (m, 1H), 2.07-2.09 (m, 2H), 1.58-1.63 (m, 1H), 1.47-1.52 (m, 1H), 1.25 (t, *J* = 7 Hz, 3H); ^{13}C NMR ($CDCl_3$) δ 156.0, 145.2, 133.1, 129.6, 128.4, 127.5, 126.3, 60.7, 47.0, 41.8, 31.0, 29.6, 14.6; FAB mass spectrum *m*/*z* (relative intensity) 246 ((M + H), 17), 157 (66), 91 (100); HRMS (FAB) calcd for $C_{15}H_{20}O_2N$ (M+H) 246.1494, found 246.1491.

Suzuki Coupling

To 60.2 mg (0.234 mmol, 1.00 equiv.) of allyl carbonate **73** under argon was added 13.6 mg (0.0234 mmol, 0.100 equiv.) $PdCl_2TFP_2$. This was followed by addition of 57.1 mg (0.468 mmol, 2.00 equiv.) $PhB(OH)_2$, 57.4 mg (0.936 mmol, 4.00 equiv.) KF and 4.00 mL dry MeOH. The reaction mixture was stirred at room temperature for 24 h. The product was extracted with Et_2O (5 × 20 mL), washed with H_2O (20 mL), dried over $MgSO_4$, concentrated *in vacuo* to give the crude as a yellow oil. Flash column chromatography on silica gel (10% EtOAc/90% hexane, R_f = 0.14) gave 46.0 mg (80%) of carbamates **80** and **81**, respectively, in a 1.0:3.0 ratio as a yellow solid.

Stille Coupling

To 70.4 mg (0.274 mmol, 1.00 equiv.) carbonate **73** and 201 mg (0.548 mmol, 2.00 equiv.) $PhSnBu_3$ in 10 mL dry NMP was added 25.2 mg (0.0822 mmol, 3.00 equiv.) $AsPh_3$, 75.3 mg (0.0822 mmol, 3.00 equiv.) $Pd_2(dba)_3$ and 69.7 mg (1.64 mmol, 6.00

equiv.) LiCl. The reaction mixture was stirred at 50 °C for 24 h. The product was extracted with Et_2O (5 × 20 mL), washed with H_2O (20 mL), dried over $MgSO_4$, concentrated *in vacuo* to give the crude as a yellow oil. Flash column chromatography on silica gel (20% EtOAc/80% hexane, R_f = 0.33) gave 45.0 mg (67%) of carbamates **80** and **81**, respectively, in a 1.0:1.7 ratio as a yellow solid.

Carbamates 71 and 79

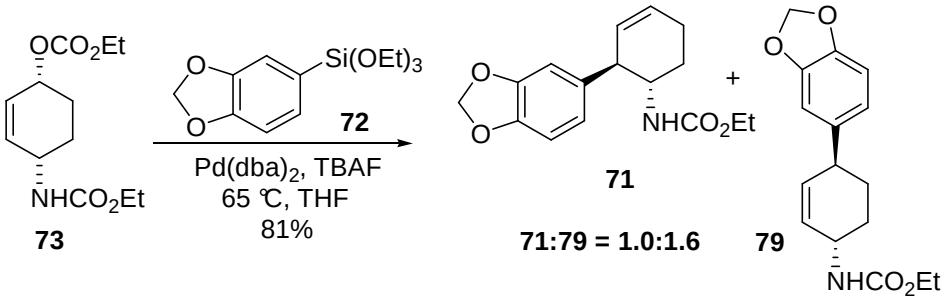

To 338 mg (1.19 mmol, 2.00 equiv.) of aryl siloxane **72** nd 153 mg (0.595 mmol, 1.00 equiv.) of carbonate-carbamate **73** dissolved in 15.0 mL anhydrous THF was added 1.19 mL (1.19 mmol, 2.00 equiv.) TBAF under argon. This was followed by addition of 68.4 mg (0.119 mmol, 0.100 equiv.) $Pd(dba)_2$. The reaction mixture was subjected to one freeze pump thaw cycle and then heated at 65 °C for 24 h. The reaction was then quenched by addition of 30 mL H_2O. The product was extracted with 3 × 25 and washed with H_2O. The combined organic extracts were dried over $MgSO_4$, filtered and concentrated *in vacuo* to give a brown oil. Flash column chromatography on silica gel (15% EtOAc/85% hexane, R_f = 0.20) gave 140 mg (81%) of carbamates **71** and **79**, respectively, in a 1.0:1.6 ratio as a yellow solid. The two regioisomers were inseparable using column chromatography and were thus carried as mixture through the next step.

The regioisomers however, are separable by HPLC.[34] A small amount of the mixture was separated on preparative HPLC (25% EtOAc/75% hexane) for spectral analysis. **Carbamate 71:** mp 111-113 °C; IR (CCl_4) 3443 (w), 2930 (w), 2858 (w), 1727 (m), 1550 (s), 1502 (m), 1485 (m), 1251 (m) cm^{-1}; ^1H NMR (400 MHz, $CDCl_3$ δ 6.73-6.67 (m, 3H), 5.90 (s, 2H), 5.87 (dd, *J* = 2, 10 Hz, 1H), 5.58 (dd, *J* = 2, 10 Hz, 1H) 4.72 (br s, 1H), 4.03 (q, *J* = 7 Hz, 2H), 3.72 (br s, 1H), 3.22 (s, 1H), 2.25-2.10 (m, 2H), 1.91-1.88 (m, 1H), 1.58 (sextet, *J* = 7 Hz, 1H) 1.18 (t, *J* = 7 Hz, 3H); ^{13}C NMR (100 MHz, $CDCl_3$) δ 156.0, 147.6, 146.2, 136.5, 128.0, 127.9, 121.5, 108.7, 108.0, 100.9, 60.6, 52.7, 47.6, 25.5, 22.9, 14.5; FAB mass spectrum *m/z* (relative intensity) 290 ($(M+H)^+$, 21), 201 (100), 174 (31), 135 (81), 73 (90); HRMS (FAB) calcd for $C_{16}H_{20}O_4N$ $(M+H)^+$ 290.1392, found 290.1379. **Carbamate 79:** mp 90-92 °C; IR (CCl_4) 3446 (w), 3028 (w), 2943(w), 1727 (s), 1547 (s), 1489 (s) cm^{-1}; ^1H NMR (400 MHz, $CDCl_3$) δ 6.72 (d, *J* = 8 Hz, 1H), 6.64-6.59 (m, 2H), 5.90 (m, 2H), 5.75 (m, 2H), 4.63 (br s, 1H), 4.29 (br s, 1H), 4.10 (q, *J* = 7 Hz, 2H), 3.29-3.28 (m, 1H), 2.07-2.01 (m, 2H), 1.54-1.41 (m, 2H), 1.23 (t, *J* = 7 Hz, 3H); ^{13}C NMR (100 MHz, $CDCl_3$) δ 156.1, 147.6, 146.0, 139.2, 133.2, 129.6, 120.4, 108.1, 108.0, 100.8, 60.7, 46.9, 41.4, 31.1, 29.5, 14.6; FAB mass spectrum *m/z* (relative intensity) 290 ($(M+H)^+$, 46), 201 (100), 174 (24), 135 (60), 73 (48); HRMS (FAB) calcd for $C_{16}H_{20}O_4N$ $(M+H)^+$ 290.1392, found 290.1390.

Lactam 70

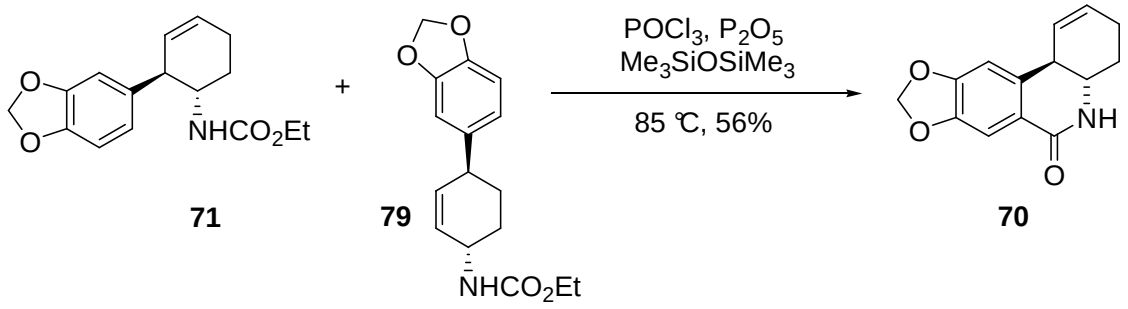

To 294 mg (1.02 mmol, 1.00 equiv.) of coupling product mixture **71**/**79** was added P_2O_5 (3.13 g, 21.6 equiv.) and then 5.00 mL (23.0 equiv.) hexamethyldisiloxane under argon. This was followed by dropwise addition of $POCl_3$ (5.00 mL) *via* syringe. The reaction mixture was stirred at 85 °C for 19 h. The purple reaction mixture was quenched with 100 mL ice water and was stirred for 5.5 h at room temperature. The product was extracted with EtOAc (7 × 75 mL), dried over $MgSO_4$, concentrated *in vacuo* to give crude as a yellow solid. Flash column chromatography on silica gel (75% EtOAc/25% hexane, R_f = 0.23) gave 48 mg (56%, based on the amount of carbamate **71** in the original mixture) of alkene **70** as a white solid: mp >300 °C; IR (Neat) 3185 (w), 2920 (m), 1665 (s), 1612 (m), 1451 (s), 1254 (s), 1036 (w) cm^{-1}; ^1H NMR (400 MHz, $CDCl_3$) δ 7.55 (s, 1H), 6.85 (s, 1H), 6.09-6.07 (m, 2H 1H), 6.00 (s, 2H), 5.88-5.86 (m, 1H), 3.46-3.44 (m, 1H), 2.26 (m, 2 H), 1.94-1.93 (m, 1H), 1.86-1.82 (m, 1H); ^{13}C NMR (100 MHz, $CDCl_3$) δ 166.0, 151.2, 146.4, 136.6, 128.8, 123.7, 122.7, 108.7, 103.6, 101.6, 53.5, 41.1, 28.1, 24.5; HRMS (FAB) calcd for $C_{14}H_{13}NO_3$ 244.0973, found 244.0974.

Epoxides 82 and 83

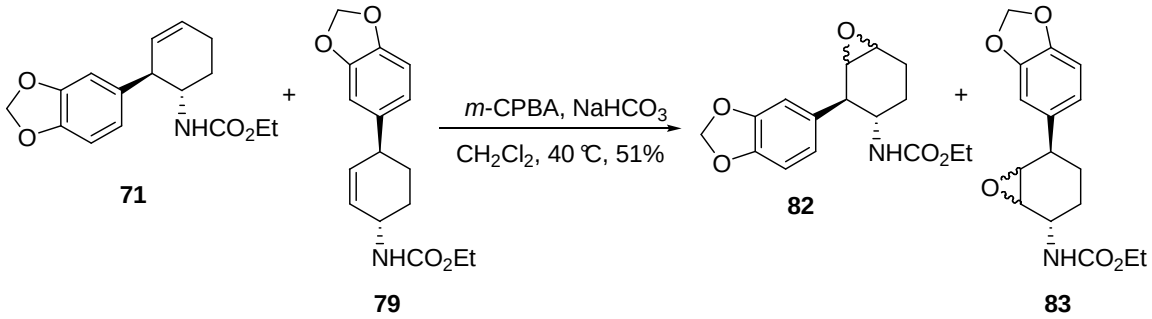

To 209 mg (0.723 mmol, 1.00 equiv.) of mixture of coupling products **71** and **79** dissolved in anhydrous CH_2Cl_2 was added 243 mg (2.89 mmol, 4.00 equiv.) of sodium bicarbonate ($NaHCO_3$), followed by addition of 375 mg (2.17 mmol, 3.00 equiv.) of *m*-CPBA. The reaction mixture was stirred at 40 °C for 25 h and was quenched with 25.0 mL of saturated $NaHCO_3$ and 25 mL of saturated $Na_2S_2O_3$ (sodium thiosulfate) solution. The product was extracted with 4 × 50 mL EtOAc and washed with 50 mL water. The combine organic layers were dried over $MgSO_4$ and concentrated *in vacuo* to give crude as a yellow solid. Flash chromatography on silica gel (30% EtOAc/70% hexane) yielded 41 mg of epoxide **82** (R_f = 0.25) and 72 mg of epoxide **83** (R_f = 0.34) as white solids (51% combined yield): **Epoxide 82:** mp 178-181 °C; IR (Neat) 3314 (m), 2979 (w), 2921 (w), 2845 (w), 1684 (s), 1540 (s), 1473 (s), 1282 (m), 1238 (s), 1051 (s) cm^{-1}; ^1H NMR (400 MHz, $CDCl_3$) δ 6.77-6.69 (m, 3H), 5.93 (s, 2H), 4.87 (br s, 1H), 3.99 (q, *J* = 7 Hz, 2H), 3.60 (br s, 1H), 3.31 (m, 1H), 3.17 (d, *J* = 4 Hz, 1H), 2.96 (d, *J* = 7 Hz, 1H), 2.21-2.16 (m, 1H), 2.06-2.00 (m, 1H), 1.69-1.65 (m, 1H), 1.46-1.38 (m, 1H) , 1.15 (t, *J* = 7 Hz, 3H); ^{13}C NMR (100 MHz, $CDCl_3$) δ 155.7, 147.9, 146.6, 134.3, 121.4, 108.5, 108.4, 101.0, 60.6, 56.0, 52.4, 51.9, 46.8, 22.6, 22.4, 14.5. HRMS (ESI) calcd for $C_{16}H_{20}O_5N$ $(M+H)^+$ 306.1342, found 306.1310. **Epoxide 83:** mp 157-160 °C; IR (Neat) 3295 (m),

2988 (w), 2936 (w), 2859 (w), 1675 (s), 1531 (s), 1488 (s), 1440 (m), 1243 (s), 1042 (s) cm^{-1}; ^1H NMR (400 MHz, $CDCl_3$) δ 6.76-6.65 (m, 3H), 5.93 (s, 2H), 4.91 (d, *J* = 8 Hz, 1H), 4.15-4.10 (m, 3H), 3.36 (m, 1H), 3.25 (d, *J* = 4 Hz, 1H), 2.97 (dd, *J* = 6, 4 Hz, 1H), 1.87-1.81 (m, 1H), 1.72-1.67 (m, 1H), 1.37-1.31 (m, 2H), 1.24 (t, *J* = 7 Hz, 3H); ^{13}C NMR (100 MHz, $CDCl_3$) δ 156.1, 147.8, 146.2, 137.1, 120.6, 108.4, 108.1, 101.0, 60.9, 59.1, 55.0, 48.0, 40.2, 30.0, 24.6, 14.6. HRMS (ESI) calcd for $C_{16}H_{20}O_5N$ $(M+H)^+$ 306.1342, found 306.1310.

Epoxides 84a, 84b

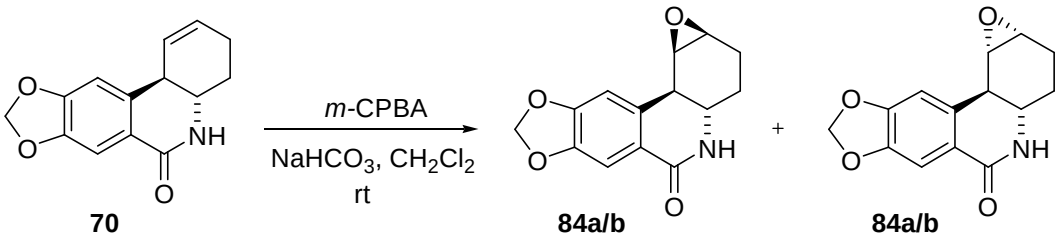

To a solution of the lactam **70** (59 mg, 0.24 mmol, 1.0 equiv.) in dichloromethane (2.0 mL), was added sodium bicarbonate (41 mg, 0.48 mmol, 2.0 equiv.), followed by purified *m*-CPBA (63 mg, 0.36 mmol, 1.5 equiv.). The two phase reaction mixture was vigorously stirred for 24 h at room temperature, before diluting with water (2.0 mL) and stirring for another 30 min. The two phases were separated, and then extracted with dichloromethane (3 × 5 mL). The combined organics were washed with satd. aq. sodium bicarbonate (2 × 3 mL), dried over $MgSO_4$ and concentrated *in vacuo*. Flash chromatography on silica gel (gradient elution 75%-100% EtOAc/hexane) gave faster eluting **84** (3 mg, 5%) and slower eluting **84** (6 mg, 9%), both as white solids. Faster eluting **84**: TLC R_f = 0.37 (80% EtOAc/20% hexane); mp >300 °C; IR (CCl_4) 2957 (w), 2930 (s), 2851 (m), 1720

(s), 1360 (w), 1217 (w), 909 (m) cm^{-1}; ^1H NMR (400 MHz, $CDCl_3$) δ 7.56 (s, 1H), 7.00 (s, 1H), 6.03 (s, 2H), 3.54 (d, *J* = 4 Hz, 1H), 3.44 (br s, 1H), 3.29 (dd, *J* = 2, 2 Hz, 1H), 3.23 (dd, *J* = 4, 12 Hz, 1H), 3.00 (d, *J* = 12 Hz, 1H), 1.95-1.90 (m, 1H), 1.65-1.59 (m, 3H); HRMS (FAB) calcd for $C_{14}H_{13}NO_4$ 260.0924 (M+H), found 260.0923. Slower eluting **84**: TLC R_f = 0.21 (80% EtOAc/20% hexane); mp >300 °C; ^1H NMR (400 MHz, $CDCl_3$) δ 7.51 (s, 1H), 6.97 (s, 1H), 6.02 (s, 2H), 5.97 (br s, 1H), 3.72 (s, 1H), 3.51 (dt, *J* = 3, 12 Hz, 1H), 3.36 (t, *J* = 3 Hz, 1H), 3.11 (d, *J* = 12 Hz, 1H), 2.20-2.16 (m, 1H), 2.07-2.02 (m, 1H), 1.69-1.59 (m, 2H).

Diol 69

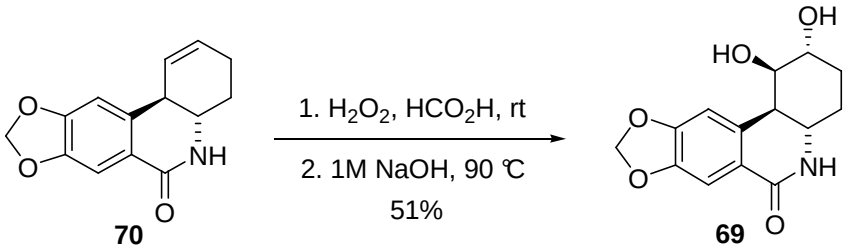

To a solution of alkene **70** (68 mg, 0.28 mmol, 1.0 equiv.) in formic acid (1.7 mL) was added 0.15 mL of 30% aqueous hydrogen peroxide. This yellow solution was stirred for 14 h at room temperature and then volatile material was removed on rotary evaporator to obtain 90 mg white solid. Aqueous sodium hydroxide (1 M, 0.35 mL, pH = 9) and 2.0 mL MeOH was then added and reaction mixture was heated at 90 °C for 3 h. The reaction mixture was cooled and solvents were evaporated to obtain a light brown solid. Washing the crude product with copious amount of hot ethyl acetate (30 × 30 mL) gave 60 mg light yellow solid. An attempt to recrystallize the crude solid using acetone/methanol failed because of poor solubility of the product in most organic solvents as well as water.

Instead, white solid precipitated when the acetone/methanol solution was cooled at 0 °C for a week. The solution was vacuum filtered to obtain product as a white solid. The filtrate was cooled at 0 °C and the process was repeated two additional times to obtain 40 mg (51%) of diol **69** as a white solid: mp 232-234 °C; IR (Neat) 3356-3199 (br s), 2938 (w), 2892 (w), 1629 (s), 1601 (s), 1469 (s), 1261 (s), 1040 (s) cm^{-1}; ^{1}H NMR (400 MHz, DMSO) δ 7.64 (s, 1H), 7.28 (s, 1H), 6.89 (s, 1H), 6.05 (d, *J* = 2 Hz, 2H), 4.86 (d, *J* = 5 Hz, 1H), 4.81 (d, *J* = 4 Hz, 1H), 4.21 (m, 1H), 3.76 (m, 1H), 3.48 (ddd, *J* = 8, 8, 12 Hz, 1H), 2.85 (dd, *J* = 2, 13 Hz, 1H), 1.79-1.74 (m, 1H), 1.65-1.60 (m, 1H), 1.53 (dd, J = 2, 13 Hz, 1H); ^{13}C NMR (100 MHz, DMSO) δ 163.8, 150.2, 145.6, 136.1, 124.3, 106.7, 104.9, 101.3, 68.2, 67.3, 49.0, 40.6, 25.5, 25.3; HRMS (FAB) calcd for $C_{14}H_{15}NO_5$ $(M+H)^+$ 278.1029, found 278.1028.

CHAPTER 3
FORMAL TOTAL SYNTHESIS OF (±)-7-DEOXYPANCRATISTATIN

INTRODUCTION

We have successfully applied palladium-catalyzed allylic-arylation to the synthesis of (±)-7-deoxypancratistatin analogue (**69**) (see Chapter 2) by coupling an aryl siloxane **72** with allylic carbonate **73** (Scheme 3.1).[110] The reaction proceeds *via* formation of a "symmetrical" π-allyl palladium complex **78** (Scheme 3.2). In this instance, reductive elimination from complex **78** is equally probable onto either carbon 1 and 3, resulting in formation of two regioisomers **71** and **79**.

Scheme 3.1

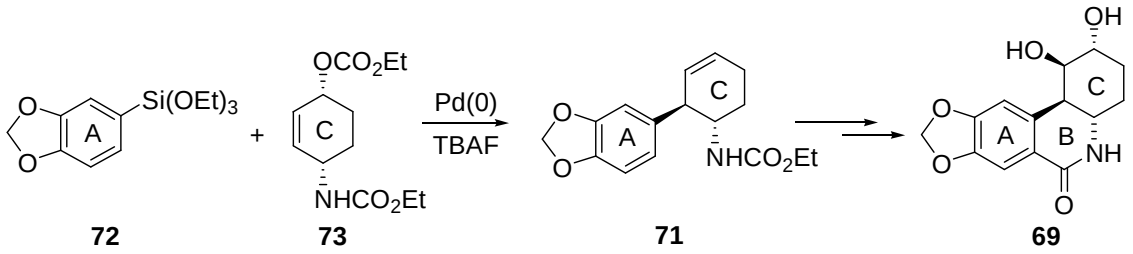

72 **73** **71** **69**

Scheme 3.2

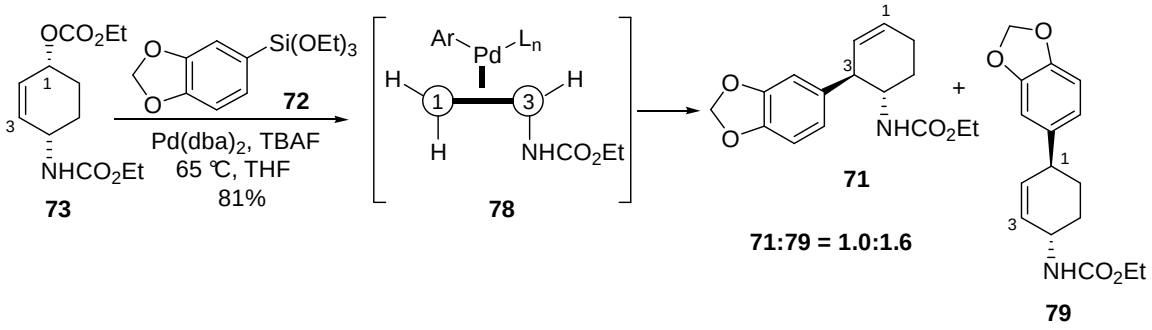

73 **78** **71** **79**

Having demonstrated that this coupling reaction would occur, the next goal was to extend siloxane methodology to the synthesis of (±)-7-deoxypancratistatin (**24**). As shown in the retrosynthesis presented in Scheme 3.3, the coupling of aryl siloxane **72** with allylic carbonate **87** would form the desired bond between A and C rings to produce carbamate **49**. In comparison to allyl carbonate **73** (Scheme 3.1), allyl carbonate **87** has large isopropylidene protected diol portion. We anticipate the coupling of allylic carbonate **87** will result in formation of "unsymmetrical" π-allyl palladium complex **88** (Scheme 3.4). Due to steric bulk provided by isopropylidene group, palladium would predominantly reside toward carbon 3 in complex **88**. Subsequently, reductive elimination would preferentially result in formation of carbamate **49**, the desired regioisomer required for the synthesis of (**24**).

Scheme 3.3

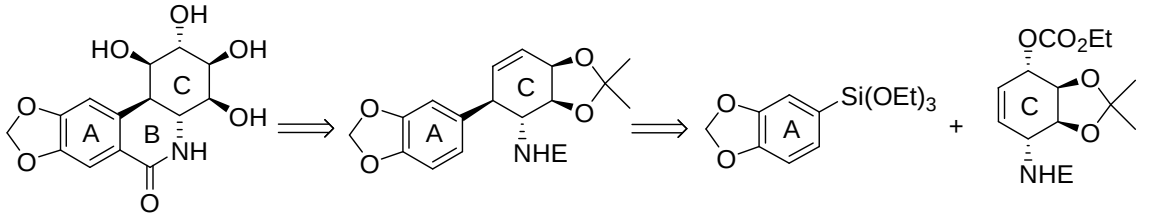

24 **49** **72** **87** E = Ester

Scheme 3.4

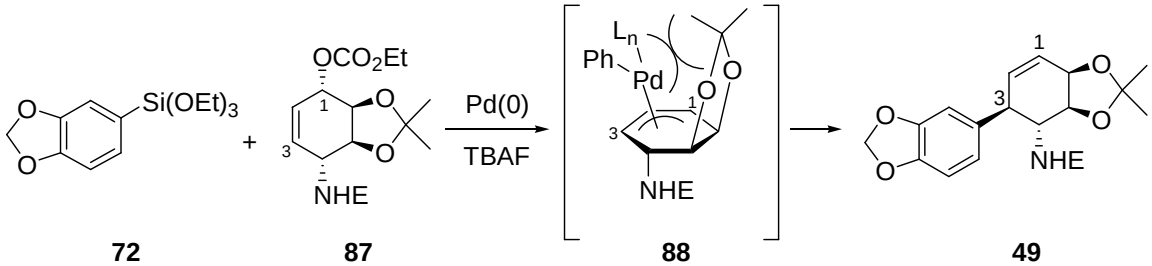

72 **87** **88** **49**

RESULTS AND DISCUSSION

Synthesis of Coupling Partners: Allylic Carbonate and Aryl Siloxane

Allylic carbonate **87** was synthesized using strategy similar to that used for carbonate **73** (see Chapter 2) from 1,4-cyclohexadiene. Diene **93** was synthesized from commercially available 1,4-cyclohexadiene (**89**) using Yang's procedure (Scheme 3.5).[111] Dibromination of diene **89** at low temperature afforded dibromoalkene **90**, which was dihydroxylated to obtain *cis*-diol **91**. Protection of diol **91** with 2,2-dimethoxypropane gave acetonide **92**. Subsequent dehydrobromination of **92** with DBU provided diene **93**.

Scheme 3.5

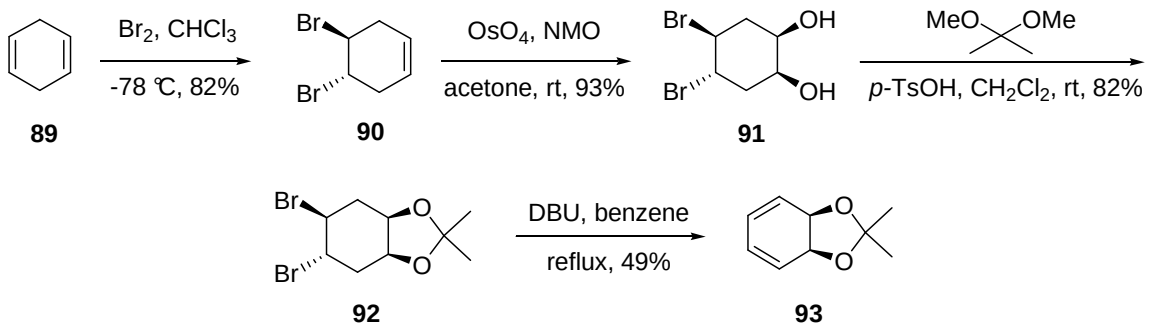

89 **90** **91** **92** **93**

Diene **93** was used to prepare allyl carbonate **87** (Scheme 3.6) using the methodology developed for the model system (see Chapter 2). Diels-Alder reaction of diene **93** with acyl nitroso dienophile (generated *in situ*) provided racemic hydroxamate **94**.[103] Reduction of N-O bond to generated allylic alcohol **95**[104] and subsequent protection of alcohol with chloroformate provided allylic carbonate **87**.

Scheme 3.6

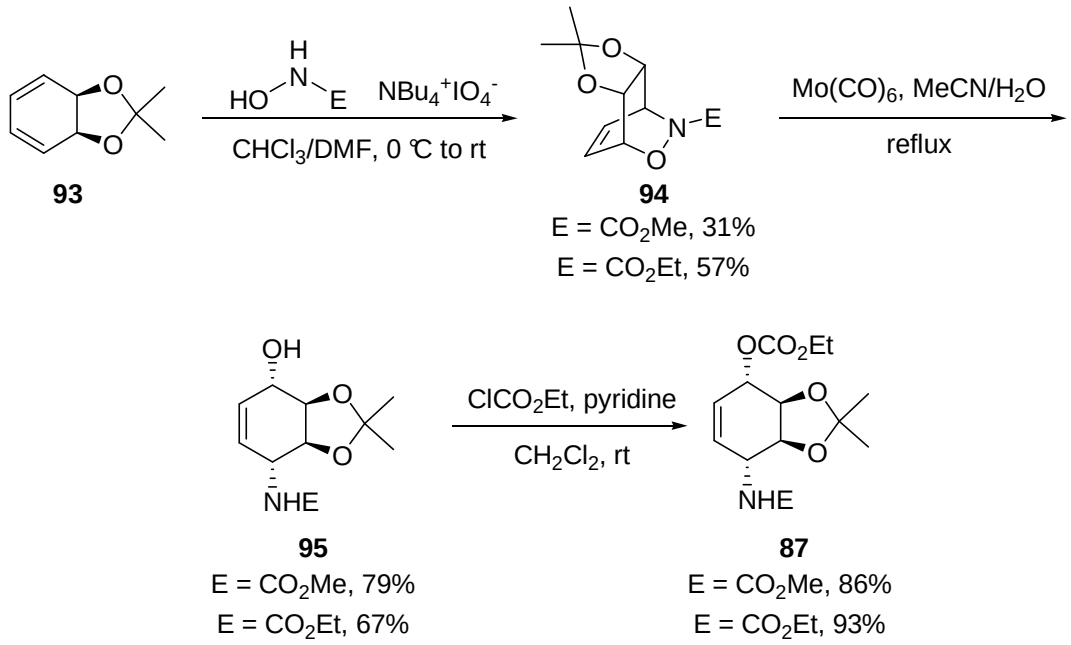

93

94

E = CO_2Me, 31%

E = CO_2Et, 57%

95

E = CO_2Me, 79%

E = CO_2Et, 67%

87

E = CO_2Me, 86%

E = CO_2Et, 93%

Aryl siloxane **72** was synthesized as shown in the Scheme 3.7.[20] The commercially available aryl bromide **77** underwent a Grignard reaction to generate the organomagnesium species which was quenched by tetraethylorthosilicate ($Si(OEt)_4$) to form aryl siloxane **72**.

Scheme 3.7

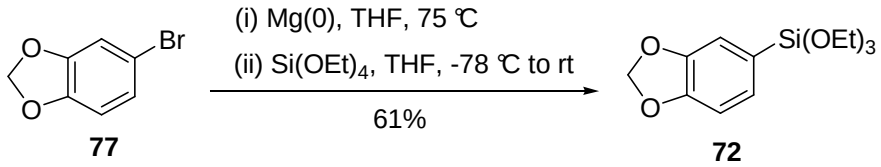

77

72

Coupling of Allylic Carbonate with Aryl Siloxane

Preliminary Attempts

It was anticipated that palladium-catalyzed coupling of allylic carbonate **87** with aryl siloxane **72** would yield the coupling product **49** with high regioselectivity based on the formation of "unsymmetrical" π-allyl palladium complex **88** (Scheme 3.8). However, repeated attempts to couple allylic carbonate **87** and aryl siloxane **72** were unsuccessful and no traces of carbamate **49** were detected. The use of a more active catalyst such as π-allyl palladium chloride dimer did not form carbamate **49**, but interestingly gave arene ether **96**.[34]

Scheme 3.8

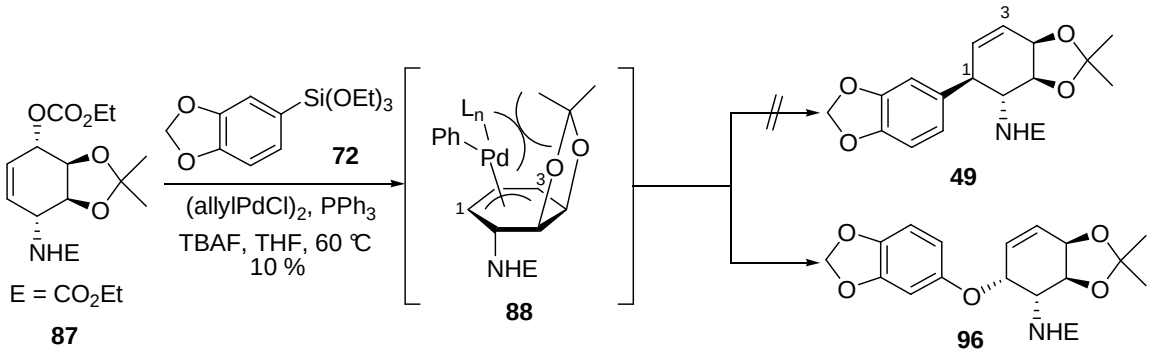

The plausible mechanism for the formation of arene ether **96** is outlined in the Scheme 3.9. Upon reaction of palladium with allylic carbonate **87**, the carbonate rearranged to form carbonate **97**, which underwent hydrolysis under the coupling conditions to give allylic alcohol **98**. Alcohol **98** reacted with aryl siloxane **72** in the presence of palladium to generate arene ether **96**. This mechanism is supported by the isolation of allylic alcohol **98** (18-32%) under various reaction conditions. The highly

regioselective formation of ether **96** is in accordance with our proposed model in Scheme 3.4. The regiochemistry of compound **96** was confirmed using ^{1}H-^{1}H COSY experiment. The crystal structure of arene ether **96** further verified regiochemistry, stereochemistry as well as ether functionality.[34]

Since the coupling of siloxane **72** and carbonate **87** failed under all conditions, it was decided that the coupling of carbonate **87** using arylboronic acid (Suzuki coupling) and aryl stannane (Stille coupling) would be investigated. While traces of coupled product (7% yield) were detected in the Stille coupling, no coupling was seen in the Suzuki reaction. The coupling of carbonate with aryl siloxane in the presence of $Pd(dba)_2$ was unsuccessful under microwave irradiation as well.

Scheme 3.9

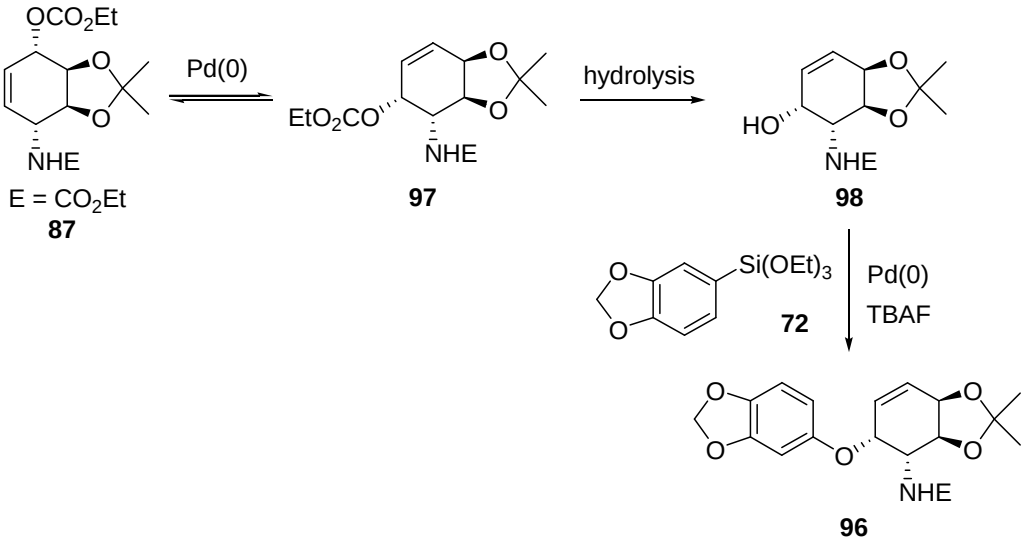

Investigation of Problems

The failure of allylic carbonate **87** to undergo allylic-arylation reaction can be attributed to the steric bulk of isopropylidene group that blocks the β face of the alkene,

the face on which the palladium metal must reside (Scheme 3.8). We wanted to know if the steric bulk is blocking the formation of π-allyl intermediate **99** or if it is blocking the subsequent transmetalation step (Scheme 3.10). To test if the π-allyl intermediate **99** was formed, we decided to couple malonate anion (a soft nucleophile) with allylic carbonate **87**. Since the Tsuji-Trost coupling[26] of malonate anion with allylic carbonate **87** will occur *via* the same π-allyl intermediate **99**, the success of this coupling reaction will infer that formation of π-allyl intermediate **99** is possible.

Scheme 3.10

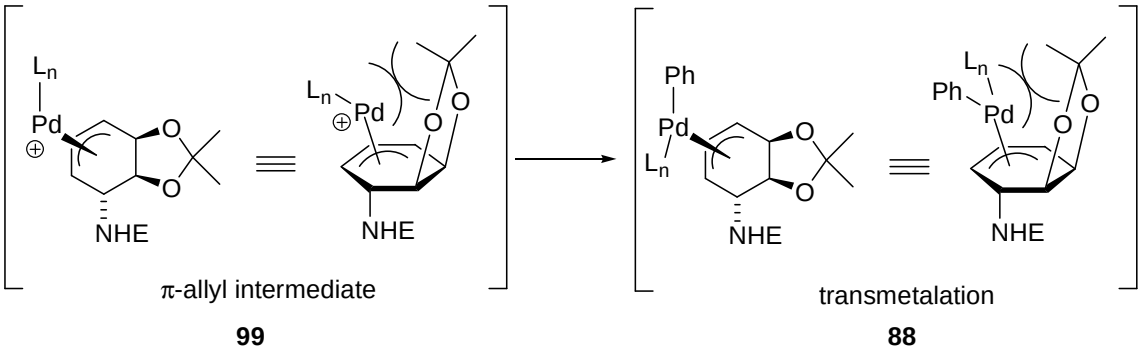

Coupling of malonate anion **100** was first attempted with the model allylic carbonate **73** (Scheme 3.11). Unfortunately, $Pd(dba)_2$ and $Pd_2(dba)_3{\cdot}CHCl_3$ catalysts which were used for the coupling of carbonate **73** with aryl siloxane **72** were ineffective (see Chapter 2), and showed predominance of starting material **73** even with stoichiometric catalyst loading. However, the $Pd(OAc)_2/PPh_3$ system gave diester **101** in 56% yield. The success of this coupling reaction was not surprising. Since we had already demonstrated that coupling of aryl siloxane **72** with allylic carbonate **73** proceeds *via* π-allyl intermediate **102** to form carbamates **71**/**79** (Scheme 3.11), it was expected that

coupling of carbonate **73** with malonate anion **100** would proceed through the same π-allyl intermediate **102** and generate diester **101** with equal feasibility.

The observance of single regioisomer (**101**) in the coupling was consistent with the model developed in our group (Scheme 3.12). After the formation of π-allyl adduct **102**, the malonate anion **100** attacked from the face opposite to the palladium (the same face as the leaving group) to retain the stereochemistry. However, because the carbamate moiety (NHE) is on the same face of attacking malonate anion **100**, the nucleophile attacks at C_1, further away from the carbamate moiety: resulting in the formation of regioisomer **101** with an overall retention of stereochemistry.

Scheme 3.11

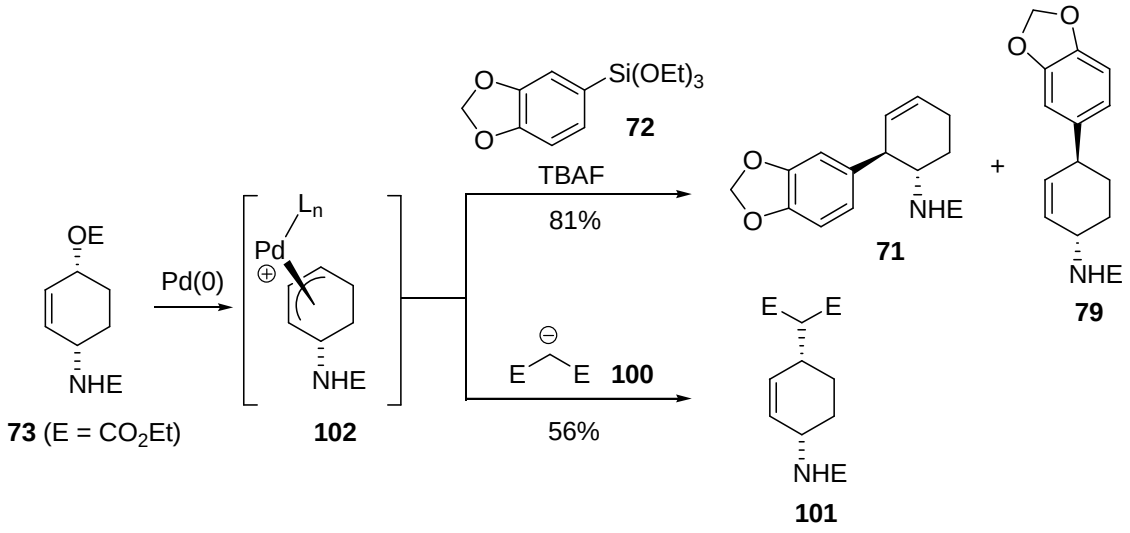

Having accomplished the coupling of malonate anion **100** with model allylic carbonate **73** (Scheme 3.11), we investigated whether the π-allyl intermediate **99** (Scheme 3.10) is formed in the coupling of more complex allylic carbonate **87** with malonate system. The coupling of allylic carbonate **87** with malonate anion **100**

proceeded in a good yield to give regioisomeric diesters **102** and **103** in 4.8:1.0 ratio (Scheme 3.13). The ratio of two regioisomers was determined from the integration of methyl groups of isopropylidene moiety. The major regioisomer was identified as diester **102** using a ^{1}H-^{1}H COSY experiment (see Experimental Section for details of the COSY analysis).

Scheme 3.12

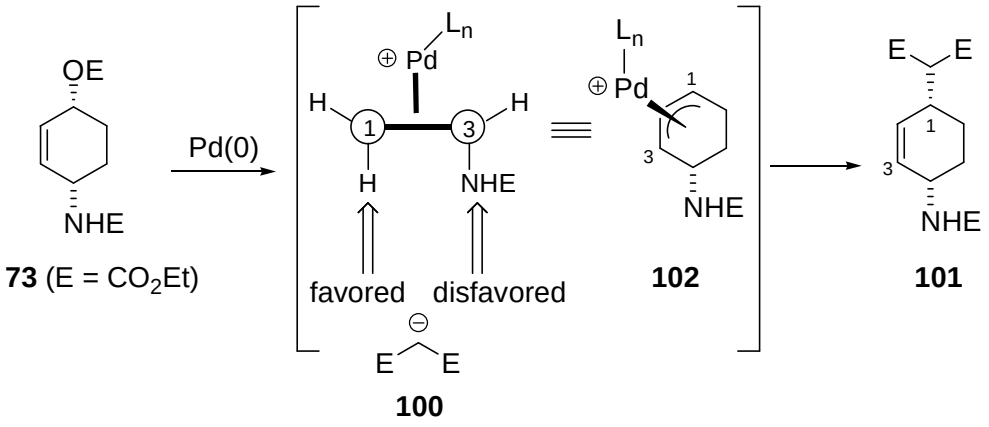

73 (E = CO_2Et) **100** **102** **101**

Scheme 3.13

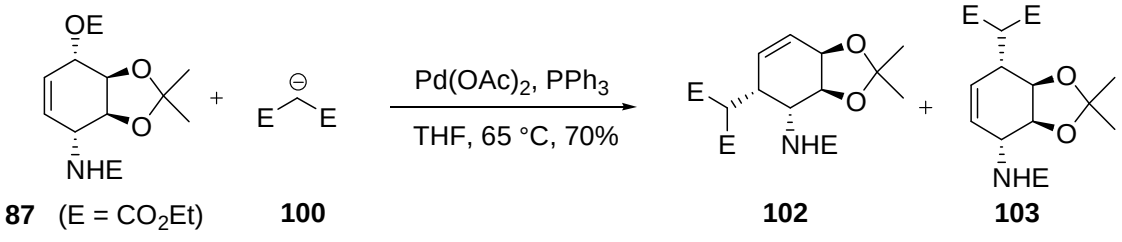

87 (E = CO_2Et) **100** **102** **103**

102:103 = 4.8:1.0

The regioselectivity of the malonate coupling reaction with allyl carbonate **102** is rationalized in Scheme 3.14. It was anticipated that the reaction of carbonate **87** will result in formation of "unsymmetrical" π-allyl palladium complex **99** as previously discussed. Since palladium resides more towards C_1 due to steric compression with the

isopropylidene group, malonate anion **100** was expected to attack at C_3 to produce diester **103** as the major regioisomer. Furthermore, since the nucleophile attacks from the bottom face, attack further away from the carbamate moiety (NHE) would be preferred. However, diester **102** was observed as the predominant regioisomer. The formation of diester **102** suggests preferential attack of malonate anion **100** at C_1 termini. This is attributed to possible palladium-oxygen coordination with the isopropylidene moiety which pushes palladium away from C_1, preferring attack of nucleophile at C_1.

Scheme 3.14

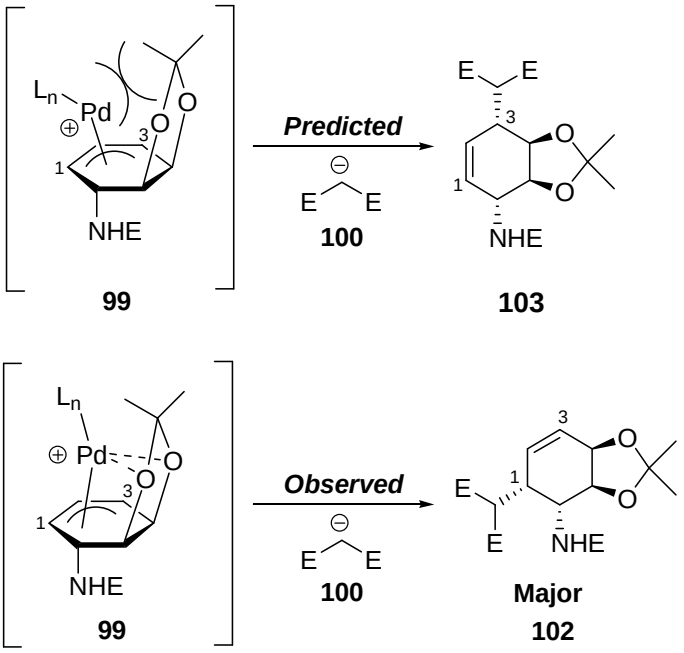

*The success of this coupling reaction proves that the π-allyl palladium intermediate **99** from the allylic carbonate **87** is formed during the Tsuji-Trost coupling.* However, when the same reaction is conducted with aryl siloxane **72**, the undesired arene ether **96** as well as rearrangement product **98** was obtained (Scheme 3.9). This suggests either transmetalation or subsequent reductive elimination must be the cause for the

failure of coupling reaction between aryl siloxane **72** and allylic carbonate **87** (Scheme 3.8). However, since reductive elimination of aryl systems is known to be fast (ary-aryl > alkyl-aryl > alkyl-alkyl)[4], it was more likely that transmetalation was the root of the problem.

In order to understand the failure of allyl-aryl coupling in the 7-deoxypancratistatin (**24**) synthesis (Scheme 3.8) mechanistic study on the siloxane reaction was performed. The details of this study are reported in Chapter 4. This study had indicated that the best catalyst system for allyl-aryl cross-coupling reaction would consist of palladium bonded to sterically demanding, but weakly σ-bonding ligands. This set of ligand requirements is not found in most Pd(0) catalysts since Pd(0) is stabilized typically by strong σ-donating ligand systems (phosphines). However, some Pd(0) catalysts have been prepared that have these characteristics (**IV**[112] and **V**[113,114], Figure 3.1)

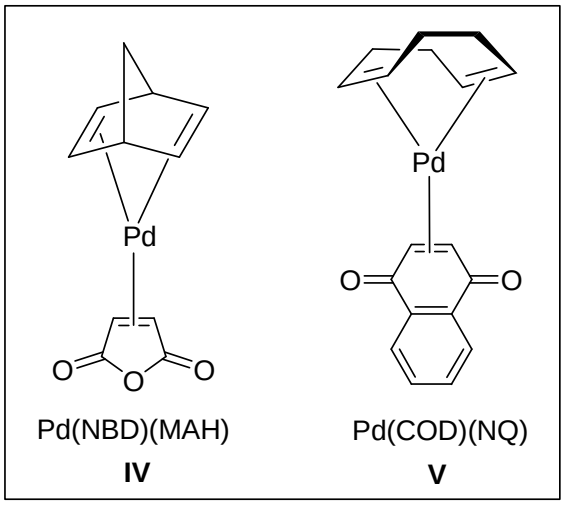

Figure 3.1: Pd(NBD)(MAH) and Pd(COD)(NQ) complexes

Successful Coupling

Pd(NBD)(MAH) **IV** and Pd(COD)(NQ) **V** were employed in the coupling reaction of complex allyl carbonate **87** and aryl siloxanes **72** and **6** (Scheme 3.15). The coupling reaction catalyzed by Pd(NBD)(MAH) **IV** resulted in lower yield of carbamate **104**. However, the reaction in the presence of Pd(COD)(NQ) **V** worked reasonably well, even at ambient temperatures to give coupled products **49** and **104** in 30-40% yield. As anticipated the coupling reaction exclusively produced regioisomers **49** and **104**, respectively. Carbamate **49** is the much desired regioisomer for the synthesis of natural product 7-deoxypancratistatin (**24**).

Scheme 3.15

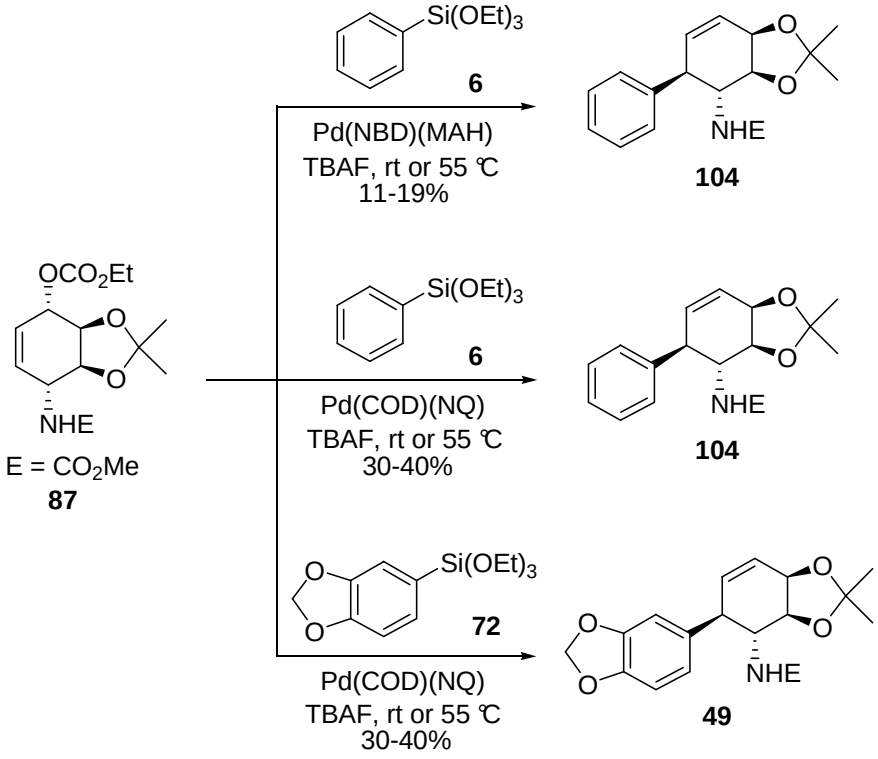

Scheme 3.16

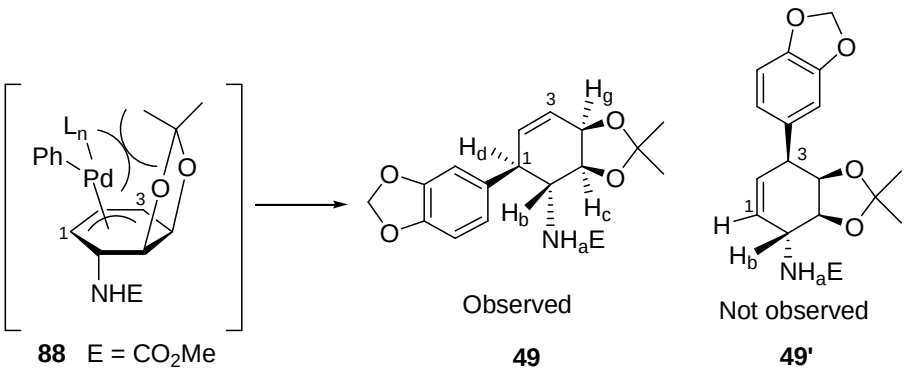

88 E = CO_2Me Observed **49** Not observed **49'**

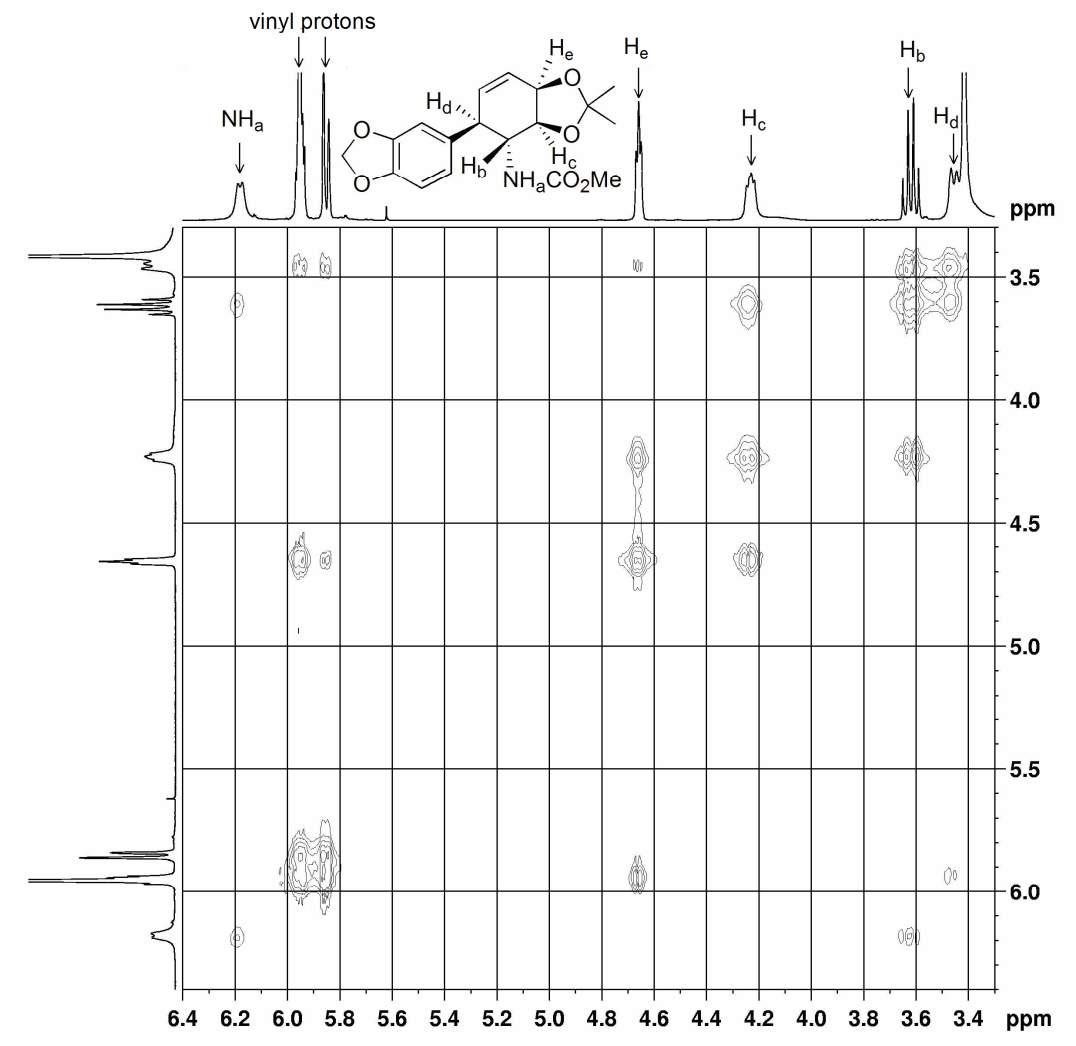

Figure 3.2: ^1H-^1H COSY of carbamate **49** (Hudlicky's intermediate)

The observed regiochemistry is consistent with the model proposed by DeShong (Scheme 3.16). Due to steric bulk arising from the acetonide moiety, an "unsymmetrical" palladium complex is formed where palladium resides farther from the acetonide group. The regioselectivity of carbamate **49** was established using ^{1}H-^{1}H COSY (Figure 3.2). Having identified the NH_a proton at δ 6.18 using HSQC spectroscopy, it was possible to locate H_b proton adjacent to the NH_a. Since H_b proton is not coupled to adjacent olefinic proton, the regioisomer was determined to be **49**. If product **49'** (Scheme 3.16) had formed, H_b proton would show correlation with the neighboring olefinic proton.

The formation of carbamate **49** *via* palladium-catalyzed allylic-arylation constitutes the formal total synthesis of 7-deoxypancratistatin (**24**). Carbamate **49** is an intermediate reported in Hudlicky's synthesis of 7-deoxypancratistatin. The spectra of **49** were identical to those reported by Hudlicky.[80]

Allylic-arylation using Hudlicky's approach (Scheme 3.17) involves coupling of aziridine **48** with cuprate **46** *via* S_N2 process.[80,87] The yield of the key reaction is comparable to our palladium-catalyzed allylic-arylation using siloxane methodology. However, the use of extremely low temperature (-78 to -30 °C) in Hudlicky's procedure, limits its application for large-scale synthesis. On other hand, our allyl-aryl coupling reaction can be performed at ambient temperature (Scheme 3.15), and is suitable for large-scale industrial production.

Allylic-arylation approach has also been used by Trost to synthesize (+)-pancratistatin (**23**) (Scheme 3.18).[79] Reaction of allylic carbonate **51** with mixed cuprate **50** provide allylic-arylated system **52** *via* S_N2' reaction. However, Trost's synthesis used complex reaction conditions and was limited to small quantities of

material. Moreover, preparation of mixed cuprate is arduous due to its instability, thus making this synthesis unsuitable for practical applications.

Scheme 3.17

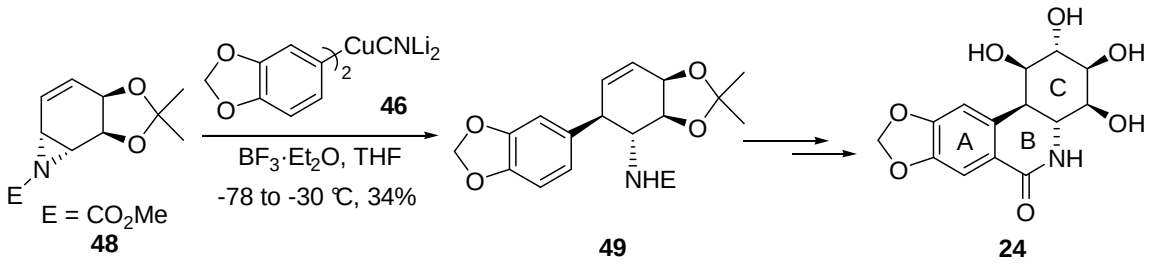

Scheme 3.18

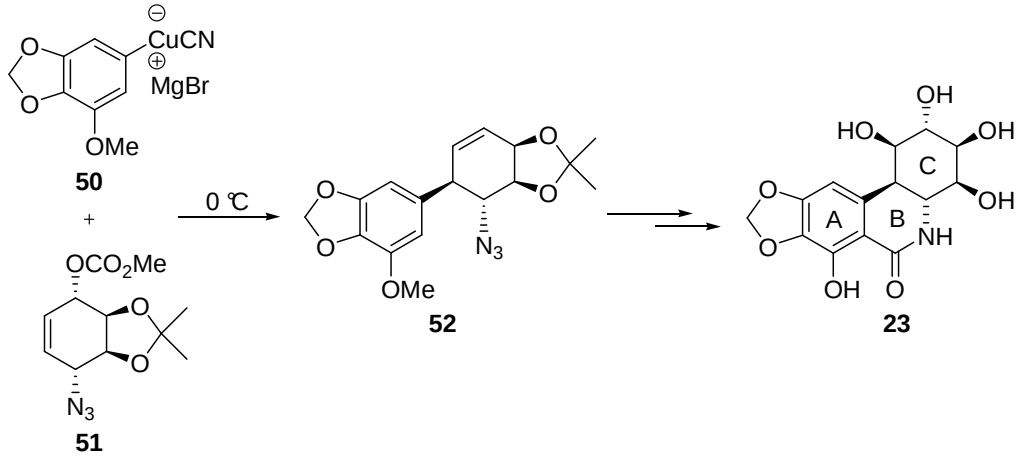

According to Hudlicky's procedure, the key steps after the formation of carbamate include installation of *trans*-diol *via* allylic-alcohol **52** directed epoxidation and Friedel-Crafts acylation to generate B ring (Scheme 3.19). Following Hudlicky's procedure, carbamate **49** was deprotected to generate allylic alcohol **105** (not isolated). The subsequent step of epoxidation of allyl alcohol **105** was performed in benzene as reported by Hudlicky. However, the poor solubility of diol **105** in benzene led to longer reaction times and in consequence extensive decomposition. Switching to acetonitrile as solvent

improved solubility of the diol **105** and NMR analysis of the crude product indicated formation of epoxide **106**. However, the yield of **106** has not been optimized. Nonetheless, the formation of carbamate **49** by siloxane methodology constitutes formal total synthesis of (±)-7-deoxypacratistatin (**24**). In future, this allylic-arylation approach shall be extended to the synthesis of pancratistatin (**23**) (Scheme 3.20).

Scheme 3.19

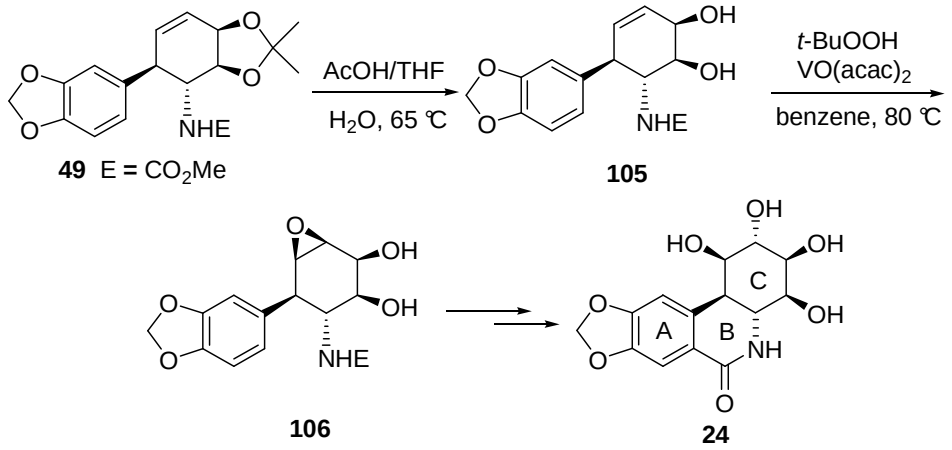

49 E = CO_2Me **105** **106** **24**

Scheme 3.20

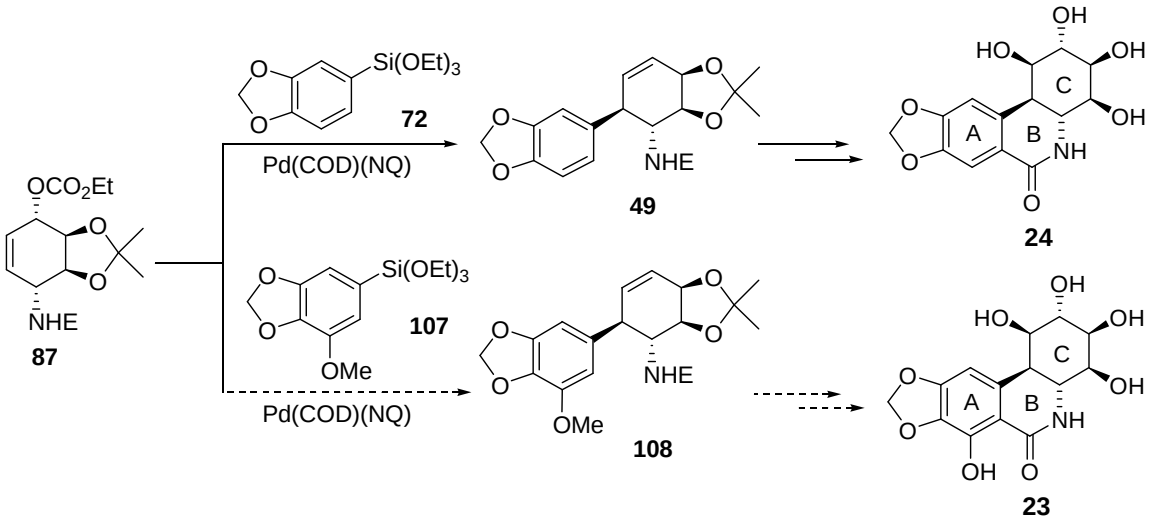

87 **72** **49** **24** **107** **108** **23**

CONCLUSION

Palladium-catalyzed allylic-arylation involving coupling of allylic carbonate and aryl siloxane has been applied to produce (±)-7-deoxypancratistatin (**24**) *via* Hudlicky's intermediate. The key reaction involves the use of a novel Pd(0) olefin complex (Pd(COD)(NQ)) and results in stereospecific arylation to form single regioisomer. This is a first example of application of palladium-catalyzed allylic arylation to the synthesis of 7-deoxypancratistatin (**24**). Though the yield for the key reaction is moderate, the ability of the coupling to work at ambient temperature is an advantage compared to allylic-arylation methodology by Hudlicky and Trost. Also, due to the ease of preparation of coupling partners, aryl siloxane and allyl carbonate compared to unstable aryl cuprate and aziridine, the siloxane coupling methodology is particularly well-suited for the synthesis of these materials. We believe our synthetic approach is short as well as efficient and thus has potential of getting commercialized. Future goals aim at development of olefin based palladium catalysts to optimize the key reaction with the goal of obtaining multigram quantities of (**24**) and application of this methodology to the synthesis of pancratistatin (**23**) derivatives.

EXPERIMENTAL DETAILS

General Methods

All reactions were run under an atmosphere of argon unless otherwise noted. Glassware used in the reactions was dried for a minimum of 12 h in an oven at 120 °C or flame dried prior to use. Tetrahydrofuran was distilled from sodium/benzophenone ketyl, while methylene chloride and pyridine were distilled from calcium hydride.

Thin-layer chromatography (TLC) was performed on 0.25 mm silica gel coated plates treated with a UV-active binder with compounds being identified by one or more of the following methods: UV (254 nm), vanillin/sulfuric acid charring, or $KMnO_4$ charring. Flash chromatography was performed using glass columns and medium pressure silica gel (Sorbent Technologies, 45-70 μ).

Infrared spectra were recorded on a Nicolet 560 FT-IR spectrophotometer. Samples used for obtaining infrared spectra were either dissolved in carbon tetrachloride or taken neat. IR band positions are reported in reciprocal centimeters (cm^{-1}) and relative intensities are listed as br (broad), s (strong), m (medium), or w (weak). Nuclear magnetic resonance (^1H, ^{13}C NMR) spectra were recorded on a 400 or 500 MHz spectrometer. Chemical shifts are reported in parts per million (δ) and coupling (*J* values) are reported in hertz (Hz). Spin multiplicities are indicated by the following symbols: s (singlet), d (doublet), t (triplet), q (quartet), m (multiplet), br s (broad singlet), br d (broad doublet). Low resolution mass spectrometry (LRMS) and high resolution mass spectrometry (HRMS) were obtained on a JEOL SX-02A instrument.

Dibromoalkene 90

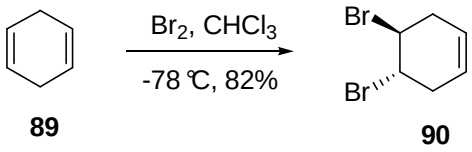

The dibromoalkene **90** was prepared from 1,4-cyclohexadiene **89** according to Yang's procedure.[111] To 15.0 mL (159 mmol, 1.00 equiv.) of 1,4-cylcohexadiene **89** dissolved in 35.0 mL of $CHCl_3$ at -78 °C was added 8.15 mL (159 mmol, 1.00 equiv.) of Br_2 dropwise over 2 h. The reaction mixture was stirred for additional 2 h, and then quenched by the addition of 75.0 mL 0.1 M aqueous sodium thiosulfate ($Na_2S_2O_3$) solution. The product was extracted with 5 × 100 mL CH_2Cl_2 and washed with 100 mL of $Na_2S_2O_3$ solution. The combined organic layers were dried over $MgSO_4$, filtered and concentrated *in vacuo* to afford 31.0 g (82%) of dibromoalkene **90** as a white solid, mp 33-37 °C (lit.[111] 34-37 °C) which was used without further purification. IR (CCl_4) 3037 (w), 2937 (w), 2882 (w), 2819 (w), 1660 (w), 1421 (s), 1325 (m), 1211 (s), 1187 (m), 1159 (m) cm^{-1}; ^1H NMR (400 MHz, $CDCl_3$) δ 5.65 (s, 2H), 4.50 (s, 2H), 3.17 (d, *J* = 19 Hz, 2H), 2.59 (d, *J* = 19 Hz, 2H); ^{13}C NMR (100 MHz, $CDCl_3$) δ 122.3, 48.7, 31.2; LRMS (EI^+) *m/z* 240 (M^+ 25), 161 (23), 159 (25), 79 (100), 77 (38). The spectral data was identical to the literature.[111]

Dibromodiol 91

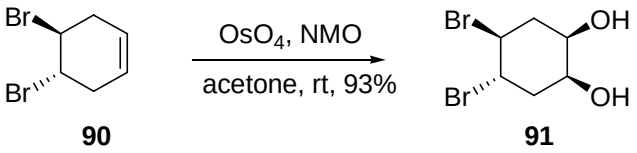

To 16.0 g (66.9 mmol, 1.00 equiv.) of dibromoalkene **90** dissolved in 170 mL of acetone and 25.0 mL of H_2O was added 11.8 g (100 mmol, 1.50 equiv.) of NMO under argon. This was followed by addition of 100 mg of OsO_4. The reaction was allowed to stir for 3 days at room temperature and was then quenched by the addition of 28.5 g of (150 mmol, 2.24 equiv.) sodium metabisulfite. The product was extracted with 5 × 200 mL CH_2Cl_2 and washed with 200 mL H_2O. The combined organic extracts were dried over $MgSO_4$, filtered and concentrated *in vacuo* to give 17.0 g (93%) of dibromodiol **91** as a creamy solid, mp 103-104 °C (lit.[111] 103-105 °C), which was used without further purification. IR (CCl_4) 3491-2953 (br s), 2951 (w), 2889 (w), 1685 (w) cm^{-1}; ^1H NMR (400 MHz, pyridine - d_5) δ 6.11 (br s, 2H), 4.86 (ddd, *J* = 12, 11, 4 Hz, 1H), 4.40 (ddd, *J* = 12, 11, 4 Hz, 1H), 4.26 (m, 1H), 3.98 (ddd, *J* = 12, 4, 3 Hz, 1H), 2.94 (ddd, *J* = 12, 12, 11 Hz, 1H), 2.84 (ddd, *J* = 15, 4, 3 Hz, 1H), 2.71 (dddd, *J* = 12, 4, 4, 1 Hz, 1H), 2.15 (ddd, *J* = 15, 12, 2 Hz, 1H); ^{13}C NMR (100 MHz, pyridine - d_5) δ 71.5, 70.9, 56.5, 55.6, 43.7, 42.1; LRMS (EI^+) *m/z* 274 (M^+, 5), 195 (90), 193 (95), 177 (78), 175 (98), 113 (28), 95 (100), 67 (94), 55 (51). The spectral data was identical to the literature.[111]

Acetonide 92

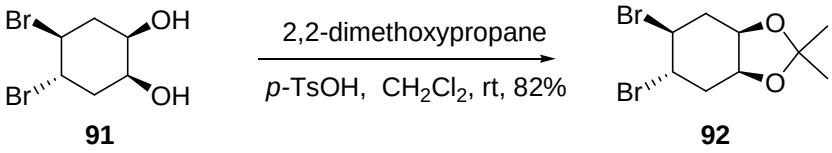

91 **92**

To 17.0 g (62.1 mmol, 1.00 equiv.) of dibromodiol **91** in 400 mL CH_2Cl_2 was added 87.7 mL (621 mmol, 10.0 equiv.) of 2,2-dimethoxypropane, followed by the addition of 2.10 g (11.0 mmol, 0.177 equiv.) *p*-TsOH. The reaction was allowed to stir for 64 h. The

reaction mixture was extracted with 3 × 300 mL CH_2Cl_2 and washed with 300 mL H_2O. The combined organic layers were dried over $MgSO_4$, filtered and concentrated *in vacuo* to obtain 15.9 g (82%) of acetonide **92** as a yellow oil, which was used without further purification. IR (CCl_4) 2990 (m), 2932 (m), 2877 (m), 2827 (w), 1720 (w), 1456 (m) cm^{-1}; ^1H NMR (400 MHz, $CDCl_3$) δ 4.39-4.44 (dt, *J* = 4, 8, Hz, 1H), 4.28 (q, *J* = 5 Hz, 1H), 4.14-4.22 (m, 2H), 2.70-2.77 (m, 2H), 2.32-2.40 (m, 1H), 2.17-2.25 (m, 1H), 1.51 (s, 3H), 1.32 (s, 3H); ^{13}C NMR (100 MHz, $CDCl_3$) δ 109.4, 73.0, 72.6, 51.6, 49.4, 36.5, 35.0, 28.7, 26.5. The spectral data was identical to the literature.[111]

Diene 93

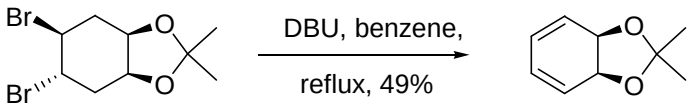

92 **93**

To 16.3 g (52.0 mmol, 1.00 equiv.) of acetonide **92** in 58.0 mL benzene was added 18.7 mL (187 mmol, 3.6 equiv.) of DBU dropwise *via* an addition funnel. The reaction mixture was heated at reflux (80 °C) for 24 h. The HBr was removed by vacuum filtration and the filtrate was extracted with 3 × 500 mL pentane and washed with 500 mL H_2O. The combined organic extracts were dried over $MgSO_4$, filtered and concentrated *in vacuo* to afford a yellow oil. Purification by column chromatography (60% CH_2Cl_2/pentane; R_f = 0.22) rendered 3.87 g (49%) of diene **93** as a yellow oil. IR (CCl_4) 3049 (m), 2986 (m), 2928 (m), 2862 (m), 2792 (w), 1961 (w), 1472 (w), 1441 (m), 1383 (m), 1351 (m), 1243 (m), 1216 (m) cm^{-1}; ^1H NMR (400 MHz, $CDCl_3$) δ 5.96-5.99 (m, 2H), 5.85-5.89 (m, 2H), 4.63 (s, 2H), 1.40 (s, 3H), 1.38 (s, 3H); ^{13}C NMR (100 MHz,

$CDCl_3$) δ 126.7, 123.7, 104.5, 70.2, 27.8, 25.2. The spectral data was identical to the literature.[111]

Hydroxamate 94

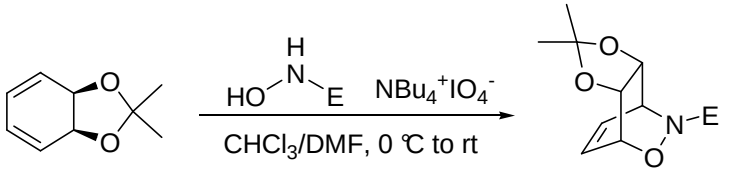

93 **94**

E = CO_2Me, 31%

E = CO_2Et, 57%

Hydroxamate (E = CO_2Et): To 23.6 g (54.6 mmol, 1.40 equiv.) of $NBu_4^+IO_4^-$ (tetrabutylammonium periodate) under argon was added chloroform (80.0 mL) and DMF (26.0 mL). The reaction mixture was cooled to 0 °C and then 5.93 g (39.0 mmol, 1.00 equiv.) of diene **93** was added. Finally, 4.10 g (39.0 mmol, 1.00 equiv.) of hydroxamic acid ($HONHCO_2Et$) dissolved in chloroform (40.0 mL) and DMF (13.0 mL) was added *via* addition funnel. The reaction mixture was stirred at 0 °C to room temperature for 50 h. The product was extracted with Et_2O (5 × 100 mL), washed with H_2O (100 mL), dried over $MgSO_4$, concentrated *in vacuo* to give the crude hydroxamate **94** as a brown oil. Flash column chromatography on silica gel (30% EtOAc/70% hexane, R_f = 0.26) gave 5.72 g (57%) of hydroxamate **94** as a creamy solid, mp 126-128 °C; IR (CCl_4) 2994 (m), 2933 (m), 1717 (s), 1373 (s), 1254 (s), 1210 (s), 1081 (s) cm^{-1}; ^1H NMR (400 MHz, $CDCl_3$) δ 6.47-6.38 (m, 2H), 5.06-5.03 (m, 1H), 4.90-4.87 (m, 1H), 4.55-4.49 (m, 2H), 4.25-4.12 (m, 2H), 1.30-1.25 (m, 9H); ^{13}C NMR (100 MHz, $CDCl_3$) δ 158.1, 130.6, 129.5, 111.0, 73.1, 72.6, 71.3, 62.8, 52.9, 25.6, 25.4, 14.4; EI mass spectrum, *m/z*

(relative intensity) 255 (M^+, 37), 240 (100), 95 (78), 85 (50), 29 (47); HRMS (EI) calcd for $C_{12}H_{17}NO_5$ $(M)^+$ 255.1107, found 255.1112.

Hydroxamate (E = CO_2Me): light yellow solid. mp 146-148 °C; IR (CCl_4) 3087 (w), 2999 (m), 2985 (m), 2935 (m), 1719 (s), 1440 (s), 1379 (s), 1336 (s), 1250 (s), 1215 (s) cm^{-1}; ^{1}H NMR (400 MHz, $CDCl_3$) δ 6.45-6.35 (m, 2H), 5.03-5.00 (m, 1H), 4.87-4.84 (m, 1H), 4.53-4.46 (m, 2H), 3.72 (s, 3H), 1.27 (s, 3H), 1.26 (s, 3H); ^{13}C NMR (100 MHz, $CDCl_3$) δ 158.4, 130.6, 129.4, 110.9, 73.0, 72.5, 71.3, 53.6, 52.8, 25.5, 25.3; HRMS (ESI) calcd for $C_{11}H_{16}O_5N$ $(M+H)^+$ 242.1029, found 242.1016.

Alcohol-Carbamate 95

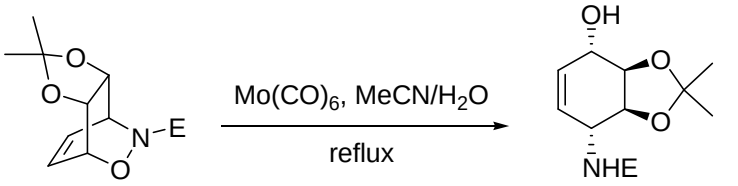

94
E = CO_2Me, 31%
E = CO_2Et, 57%

95
E = CO_2Me, 79%
E = CO_2Et, 67%

Alcohol-Carbamate (E = CO_2Et): To 5.72 g (22.4 mmol, 1.00 equiv.) of the hydroxamate **94** dissolved in 240 mL acetonitrile and 12.0 mL distilled water was added 7.10 g (26.9 mmol, 1.20 equiv.) of molybdenum hexacarbonyl ($Mo(CO)_6$). The reaction mixture was refluxed at 82 °C for 15 h. The black-brown reaction mixture was vacuum filtered through celite and the filtrate was concentrated *in vacuo* to give crude alcohol-arbamate **95** as a black solid. Flash column chromatography on silica gel (50% EtOAc/50% hexane, R_f = 0.44) gave 3.85 g (67%) of carbamate **95** as a white solid, mp 124-127 °C; IR (CCl_4) 3617 (w), 3451 (w), 2988 (w), 2902 (w), 1735 (s), 1545 (m), 1210

(m) cm^{-1}. ^1H NMR (400 MHz, $CDCl_3$) δ 5.94-5.90 (m, 1H), 5.81-5.78 (m, 1H), 5.12 (br s, 1H), 4.24-4.18 (m, 3H), 4.14-4.09 (m, 3H), 2.42 (br s, 1H), 1.43 (s, 3H), 1.33 (s, 3H), 1.23 (t, *J* = 7 Hz, 3H); ^{13}C NMR (100 MHz, d_6- DMSO) δ 155.9, 132.6, 129.5, 107.9, 79.8, 75.9, 69.2, 59.7, 51.5, 27.2, 25.0, 14.6; LRMS (FAB) *m/z* 258 ($M+1^+$, 42), 240 (66), 182 (70), 154 (63), 110 (100); HRMS calcd 258.1342, found 258.1341.

Alcohol-Carbamate (E = CO_2Me): white solid. mp 86-88 °C; IR (CCl_4) 3617 (m), 3449 (m), 3414 (w), 3049 (w), 2995 (m), 2942 (m), 2909 (m), 1730 (s), 1551 (m) cm^{-1}. ^1H NMR (400 MHz, $CDCl_3$) δ 5.91-5.88 (m, 1H), 5.78-5.74 (m, 1H), 5.35 (br d, *J* = 8Hz, 1H), 4.21-4.18 (m, 3H), 4.08-4.06 (m, 1H), 3.65 (s, 3H), 3.12 (br s, 1H), 1.41 (s, 3H), 1.31 (s, 3H); ^{13}C NMR (100 MHz, $CDCl_3$) δ 156.6, 131.1, 129.7, 109.1, 79.2, 76.8, 68.9, 52.2, 51.1, 26.9, 24.6; HRMS (ESI) calcd for $C_{11}H_{18}O_5N$ $(M+H)^+$ 244.1185, found 244.1180.

Carbonate-Carbamate 87

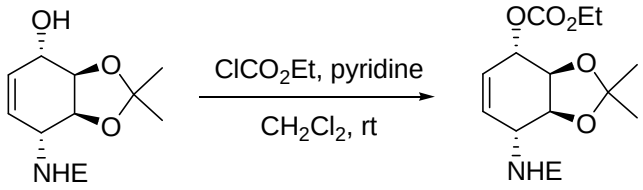

95
E = CO_2Me, 79%
E = CO_2Et, 67%

87
E = CO_2Me, 86%
E = CO_2Et, 93%

Carbonate-Carbamate (E = CO_2Et): To 1.11 g (4.32 mmol, 1.00 equiv.) of alcohol-carbamate **95** in 15 mL anhydrous CH_2Cl_2 and 0.522 mL (6.48 mmol, 1.50 equiv.) anhydrous pyridine was added 0.642 mL (6.48 mmol, 1.50 equiv.) of ethyl chloroformate dropwise *via* syringe under argon. The reaction was allowed to stir at room temperature

for 5 days. The reaction mixture was extracted with CH_2Cl_2 (5 × 25 mL), washed with H_2O (25 mL), dried over $MgSO_4$ and concentrated *in vacuo*. Flash chromatography on silica gel (75% EtOAc/25% hexane, R_f = 0.75 afforded 1.32 g (93%) of the carbonate-carbamate **87** as a white solid, mp 82-84 °C; IR (CCl_4) 3446 (m), 2984 (m), 2933 (m), 2912 (m), 1754 (s), 1730 (s), 1506 (s), 1370 (s), 1254 (s), 1224 (s), 1064 (s), 1040 (s) cm^{-1}; ^1H NMR (400 MHz, $CDCl_3$) δ 5.93-5.86 (m, 2H), 5.11 (br s, 1H), 4.93 (br s, 1H), 4.36-4.33 (m, 1H), 4.21 (q, *J* = 7 Hz, 4H), 4.12 (q, *J* = 7 Hz, 2H), 1.44 (s, 3H), 1.33-1.29 (m, 6H), 1.24 (t, *J* = 7 Hz, 3H); ^{13}C NMR (100 MHz, $CDCl_3$) δ 156.0, 154.3, 131.5, 127.1, 109.3, 76.1, 75.9, 73.9, 64.4, 61.1, 50.2, 26.9, 24.9, 14.6, 14.2; LRMS (FAB) *m/z* 330 ($M+1^+$, 6), 154 (38), 136 (40), 73 (48); HRMS (FAB) calcd $(M + 1)^+$ 330.1553, found 330.1553.

Carbonate-Carbamate (E = CO_2Me): creamy solid. mp 63-65 °C. IR (CCl_4) 3442 (m), 2992 (m), 2956 (m), 2906 (m), 1751 (s), 1733 (s), 1554 (m), 1508 (s) cm^{-1}; ^1H NMR (400 MHz, $CDCl_3$) δ 5.86-5.80 (m, 2H), 5.21 (br s, 1H), 5.1 (s, 1H), 4.30-4.27 (m, 1H), 4.19-4.14 (q, *J* = 8 Hz 4H), 1.40 (s, 3H), 1.28-1.24 (m, 6H); ^{13}C NMR (100 MHz, $CDCl_3$) δ 156.4, 154.2, 131.3, 127.0, 109.2, 75.9, 75.8, 73.9, 64.3, 52.1, 50.3, 26.8, 24.7, 14.1; HRMS (ESI) calcd for $C_{14}H_{22}O_7N$ $(M+H)^+$ 316.1396, found 316.1383.

Arene Ether 96

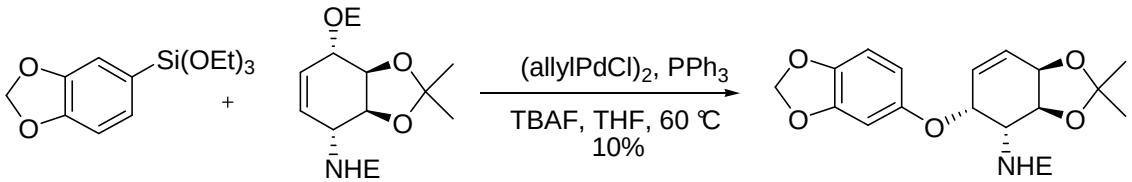

72 **87** E = CO_2Et **96**

To a solution of 245 mg (0.900 mmol, 2.00 equiv.) of siloxane **72** in anhydrous THF (10.0 mL) was added 154 mg (0.468 mmol, 1.00 equiv.) of carbonate **87**, 8 mg (0.021 mmol, 5 mol %) of $(allylPdCl)_2$, 16.0 mg (0.063 mmol, 15 mol %) of PPh_3 and 0.900 mL (0.900 mmol, 1 M in THF, 2.00 equiv.) of TBAF. The reaction mixture was heated to 60 °C and after 10 min, the color changed from yellow to amber. After 18 h, the reaction mixture was quenched by addition of brine (30 mL), extracted with ether (3 × 30 mL), dried over $MgSO_4$ and concentrated *in vacuo*. Flash chromatography on silica gel (10% EtOAc/90% hexane) gave 18 mg (10%) of arene ether **96** as a white solid: recrystallized from CH_2Cl_2/hexane, mp 126-127 °C; TLC R_f = 0.27 (25% EtOAc/75% hexane); IR (CCl_4) 3444 (m), 2963 (m), 2928 (m), 1724 (s), 1558 (m) cm^{-1}; ^1H NMR (400 MHz, $CDCl_3$) δ 6.69 (d, *J* = 8 Hz, 1H), 6.49 (d, *J* = 2 Hz, 1H), 6.34 (dd, *J* = 2, 8 Hz, 1H), 6.08 (dd, *J* = 4, 10 Hz, 1H), 6.01 (dd, *J* = 4, 10 Hz, 1H), 5.95 (s, 2H), 5.01 (d, *J* = 6 Hz, 1H), 4.72-4.70 (m, 1H), 4.66-4.64 (m, 1H), 4.45-4.42 (m, 1H), 4.22-4.19 (m, 1H), 4.10 (q, *J* = 7 Hz, 2H), 1.48 (s, 3H), 1.38 (s, 3H), 1.27 (t, *J* = 7 Hz, 3H); ^{13}C NMR (400 MHz, $CDCl_3$) δ 156.9, 154.1, 148.8, 143.0, 129.2, 128.7, 108.6, 108.4, 101.8, 100.3, 76.1, 75.3, 73.0, 71.7, 52.7, 28.4, 26.2, 14.5. FAB mass spectrum *m/z* (relative intensity) 378, 320, 240, 180, 119, 85. X-ray crystal confirmed regiochemistry, stereochemistry as well as ether functionality.[34]

Diester 101

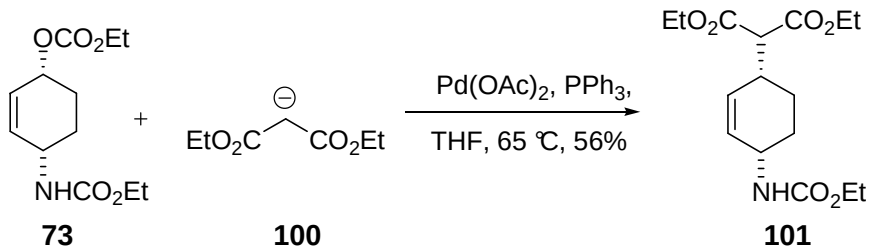

73 **100** **101**

Sodium hydride (33 mg of 60% dispersion in oil, 0.83 mmol, 3.0 equiv.) was washed with 3 × 2 mL of hexane and 2 × 3 mL of anhydrous THF. To a suspension of the oil-free sodium hydride in 2 mL THF was added 0.13 mL (0.88 mmol, 3.2 equiv.) of diethyl malonate and stirred for 10 minutes. The diethyl malonate anion **100** was then added to a solution of 71 mg (0.28 mmol, 1.0 equiv.) of allyl carbonate **73** dissolved in 1 mL anhydrous THF. This was followed by addition of 36 mg (0.14 mmol, 0.50 equiv.) triphenyl phosphine and 6.2 mg (0.028 mmol, 0.10 equiv.) of palladium acetate. The reaction mixture was allowed to stir at 65 °C for 22 h. The solution was filtered through Celite and the filtrate was extracted with 5 × 25 mL Et_2O and washed with 25 mL H_2O. The combined organic layers were dried over $MgSO_4$, concentrated in vacuo to give crude diester **101** as a brown oil. Flash column chromatography on silica gel (20% EtOAc/80% hexane, R_f = 0.15) gave 50 mg (56%) of diester **101** as a colorless oil; IR (CCl_4) 3450 (w), 2987 (m), 2936 (m), 2872 (w), 1730 (s) 1502 (m), 1214 (m) cm^{-1}; ^1H NMR (400 MHz, $CDCl_3$) δ 5.71 (s, 2H), 4.74 (d, *J* = 8 Hz, 1H), 4.21-4.11 (m, 5H), 4.06 (q, *J* = 7 Hz, 2H), 3.26 (d, *J* = 8 Hz, 1H), 2.83-2.79 (m, 1H), 1.74-1.67 (m, 3H), 1.50-1.44 (m, 1H), 1.25-1.17 (m, 9H); ^{13}C NMR (100 MHz, $CDCl_3$) δ 168.2, 168.1, 155.7, 131.5, 128.8, 61.4, 60.7, 56.1, 44.7, 35.0, 27.7, 22.2, 14.6, 14.0; FAB mass spectrum *m/z* (relative intensity) 328 ((M+H), 9), 239 (28), 161 (100), 79 (38); HRMS (FAB) calcd for $C_{16}H_{26}O_6N$ $(M+H)^+$ 328.1760, found 328.1773.

The regiochemistry of carbamate **101** was established using ^1H-^1H COSY (400 MHz, $CDCl_3$) (see page 79). NH_a proton identified using HSQC spectroscopy is coupled only to H_b proton. Since, H_b proton is coupled to vinyl proton; the regioisomer was determined to be **101**. (If **101'** had formed, H_b would not couple to vinyl proton.)

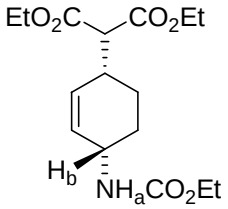

101

Only Observed

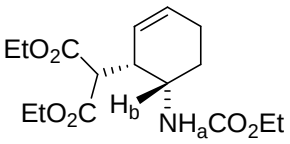

101'

Not Observed

COSY of Diester 101

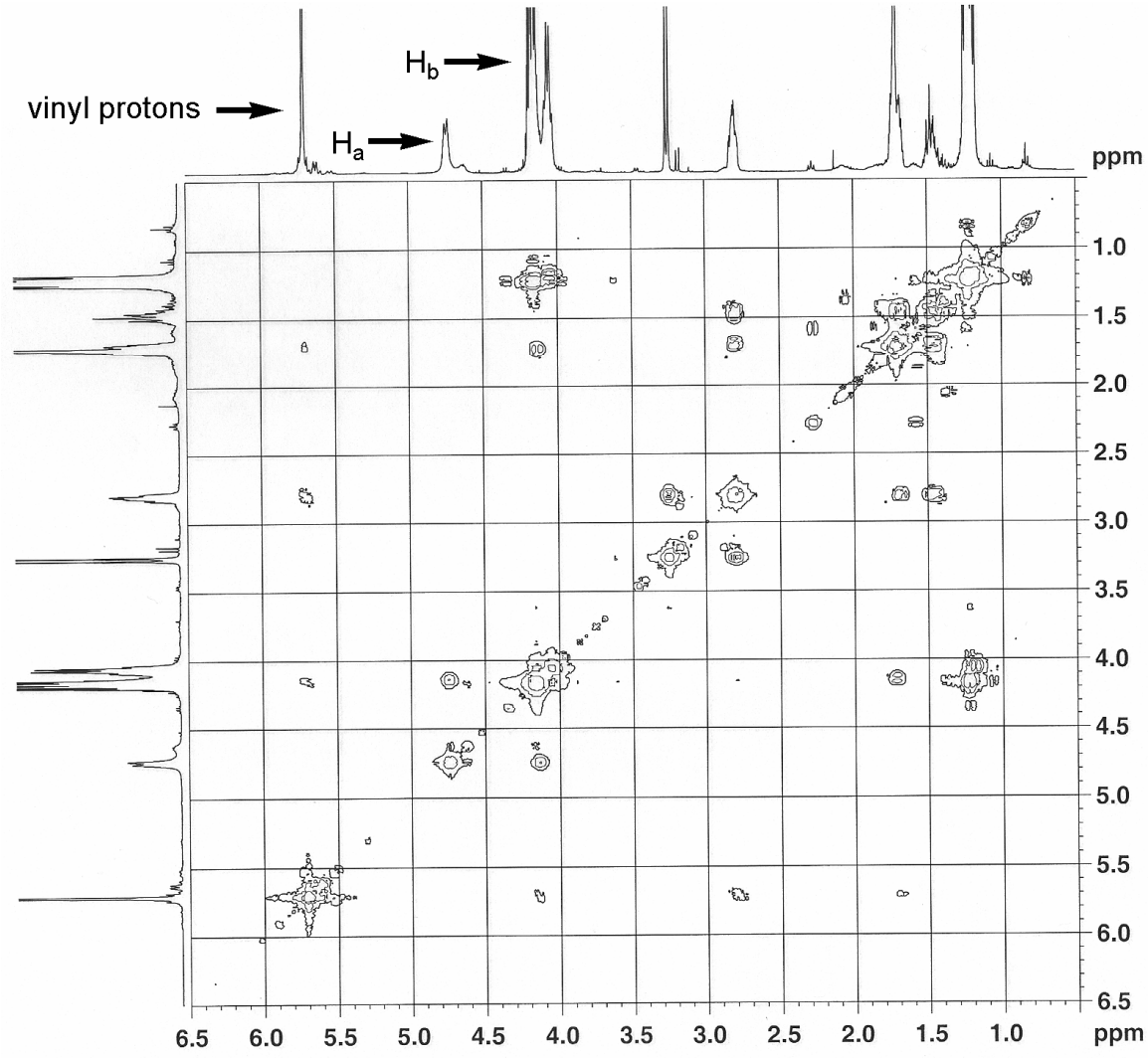

Diesters 102 and 103

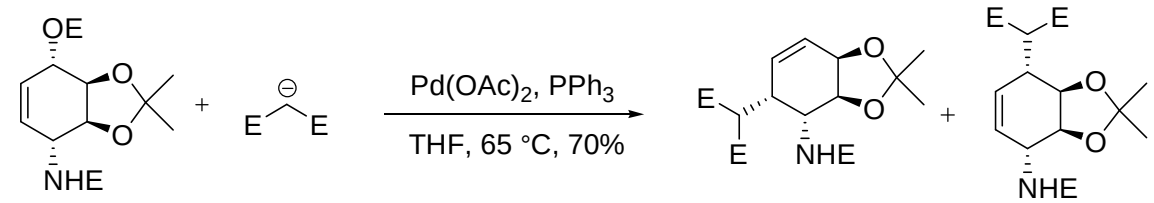

87 **100** **102** **103**

E = CO_2Et

102:103 = 4.8:1.0

Sodium hydride (37.9 mg of 60% dispersion in oil, 0.948 mmol, 3.00 equiv.) was washed with 3 × 3 mL of hexane and 3 × 3 mL of anhydrous THF. To a suspension of the oil-free sodium hydride in 2 mL THF was added 0.152 mL (1.01 mmol, 3.20 equiv.) of diethyl malonate and stirred for 10 minutes. The diethyl malonate anion **100** was then added to a solution of 104 mg (0.316 mmol, 1.00 equiv.) of allyl carbonate **87** dissolved in 2 mL anhydrous THF. This was followed by addition of 41.4 mg (0.158 mmol, 0.500 equiv.) triphenyl phosphine and 7.09 mg (0.0316 mmol, 0.100 equiv.) of palladium acetate. The reaction mixture was allowed to stir at 65 °C for 24 h. The solution was filtered through celite and the filtrate was extracted with 5 × 25 mL Et_2O and washed with 25 mL H_2O. The combined organic layers were dried over $MgSO_4$, concentrated in vacuo to give crude as brown oil. Flash column chromatography on silica gel (20% EtOAc/80% hexane, R_f = 0.29) gave 88 mg (70%) of diesters **102** and **103** (**102**:**103** = 4.8:1.0) as light yellow oil; The ratio of regioisomers was determined from the ^{1}H NMR. The major regioisomer was established to be **102** based on COSY (400 MHz, $CDCl_3$). Diesters **102** and **103** : IR (CCl_4) 3439 (w), 2984 (m), 2936 (w), 2913 (w), 1737 (s) 1506 (s), 1373 (m), 1220 (s) cm^{-1}; Diester **102**: ^{1}H NMR (400 MHz, $CDCl_3$) 5.82-5.72 (m, 2H), 4.77 (br s, 1H), 4.52 (s, 1H), 4.28 (s, 1H), 4.24-4.13 (m, 5H), 4.06 (q, *J* = 7 Hz, 2H), 3.45 (s, 2H),

1.39 (s, 3H), 1.34 (s, 3H), 1.27-1.19 (m, 9H); Diesters **102** and **103**: FAB mass spectrum *m/z* (relative intensity) 532 ($(M+Cs)^+$, 75), 342 (32), 179 (22), 133 (100); HRMS (FAB) calcd for $(M+Li)^+$ 406.2053, found 406.2056.

^{1}H NMR spectrum of diesters **102** and **103** indicated predominantly one regioisomer. The ratio of two regioisomers was determined from the integration of methyl groups of isopropylidene moiety. Diester **102** was established as the major regioisomer by COSY (400 MHz, $CDCl_3$). H_a proton (NH_a proton identified using HSQC spectroscopy) is coupled only to H_b proton. However, H_b proton is not coupled to vinyl proton (which is the case only for regioisomer **102**). Therefore, the predominant regioisomer was determined to be diester **102**.

COSY of diesters 102 and 103

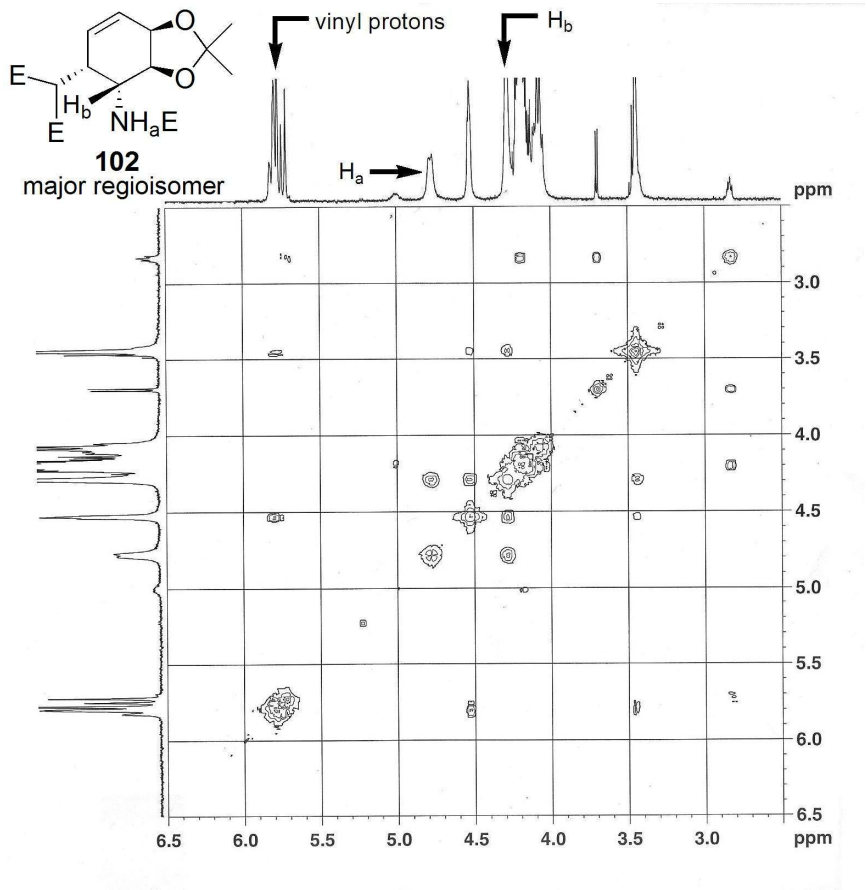

Carbamate 104

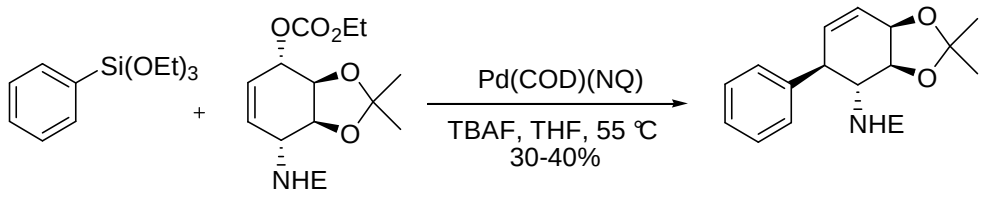

6 **87** **104**

Carbamate (E = CO_2Me): To 97.0 mg (0.404 mmol, 2.00 equiv.) of aryl siloxane **6** and 66.5 mg (0.202 mmol, 1.00 equiv.) of carbonate-carbamate **87** dissolved in 4.00 mL anhydrous THF was added 0.404 mL (0.404 mmol, 2.00 equiv.) TBAF under argon. This was followed by addition of 37.6 mg (0.101 mmol, 0.500 equiv.) Pd(COD)(NQ). The reaction mixture was heated at 55 °C for 24 h. The reaction was then quenched by addition of 25.0 mL H_2O. The product was extracted with 3 × 25 ml CH_2Cl_2 and washed with H_2O. The combined organic extracts were dried over $MgSO_4$, filtered and concentrated *in vacuo* to give a brown oil. Flash column chromatography on silica gel (20% EtOAc/80% hexane, R_f = 0.15) gave 24 mg (38%) of carbamate **104** as pale yellow solid, mp 148-150 °C; IR (CCl_4) 3469 (w), 3448 (w), 2987 (w), 1730 (s), 1507 (s), 1246(s), 1221 (s) cm^{-1}; ^{1}H NMR (400 MHz, $(CD_3)_2CO$) δ 7.30-7.27 (m, 2H), 7.22-7.18 (m, 3H), 6.22 (br d, *J* = 8 Hz, 1H), 5.99-5.95 (m, 1H), 5.87 (d, *J* = 10 Hz, 1H), 4.68 (t, *J* = 5 Hz, 1H), 4.26 (m, 1H), 3.69 (q, *J* = 10 Hz, 1H), 3.51 (br d, *J* = 10 Hz, 1H), 3.38 (s, 3H), 1.45 (s, 3H), 1.33 (s, 3H); ^{13}C NMR (100 MHz, $(CD_3)_2CO$) δ 157.3, 142.7, 136.8, 129.3, 129.1, 127.5, 124.8, 109.8, 77.9, 73.3, 56.7, 51.6, 47.4, 28.7, 26.5; HRMS (ESI) calcd for $C_{17}H_{22}O_4N$ $(M+H)^+$ 304.1549, found 304.1563.

Carbamate (E = CO_2Et): light yellow solid. mp 109-112 °C. IR (CCl_4) 3469 (w), 3452 (w), 3032 (w), 2987 (m), 2929 (w), 2876 (w), 1726 (s), 1548 (s), 1511 (s), 1381 (m),

1246 (s), 1221(s) cm^{-1}; ^1H NMR (400 MHz, $(CD_3)_2CO$) δ 7.30-7.26 (m, 2H), 7.22-7.18 (m, 3H), 6.23 (br d, *J* = 8 Hz, 1H), 5.99-5.96 (m, 1H), 5.87 (d, *J* = 12 Hz, 1H), 4.68 (t, *J* = 4 Hz, 1H), 4.28 (dd, *J* = 4 Hz, *J* = 8 Hz, 1H), 3.81 (q, *J* = 4 Hz, 2H), 3.69 (dd, *J* = 8 Hz, *J* = 12 Hz, 1H), 3.53 (br d, *J* = 8 Hz, 1H), 1.45 (s, 3H), 1.33 (s, 3H), 1.01 (t, *J* = 8 Hz, 3H); ^{13}C NMR (100 MHz, $(CD_3)_2CO$) δ 156.9, 142.8, 136.8, 129.3, 129.1, 127.5, 124.9, 109.8, 77.9, 73.4, 60.3, 56.7, 47.5, 28.7, 26.5, 15.0; HRMS (ESI) calcd for $C_{18}H_{24}O_4N$ $(M+H)^+$ 318.1705, found 318.1674. The regiochemistry of carbamate **104** was established using ^1H-^1H COSY (400 MHz, $(CD_3)_2CO$) in a manner similar to carbamate **49** (page 64, Figure 3.2)

COSY of carbamate 104

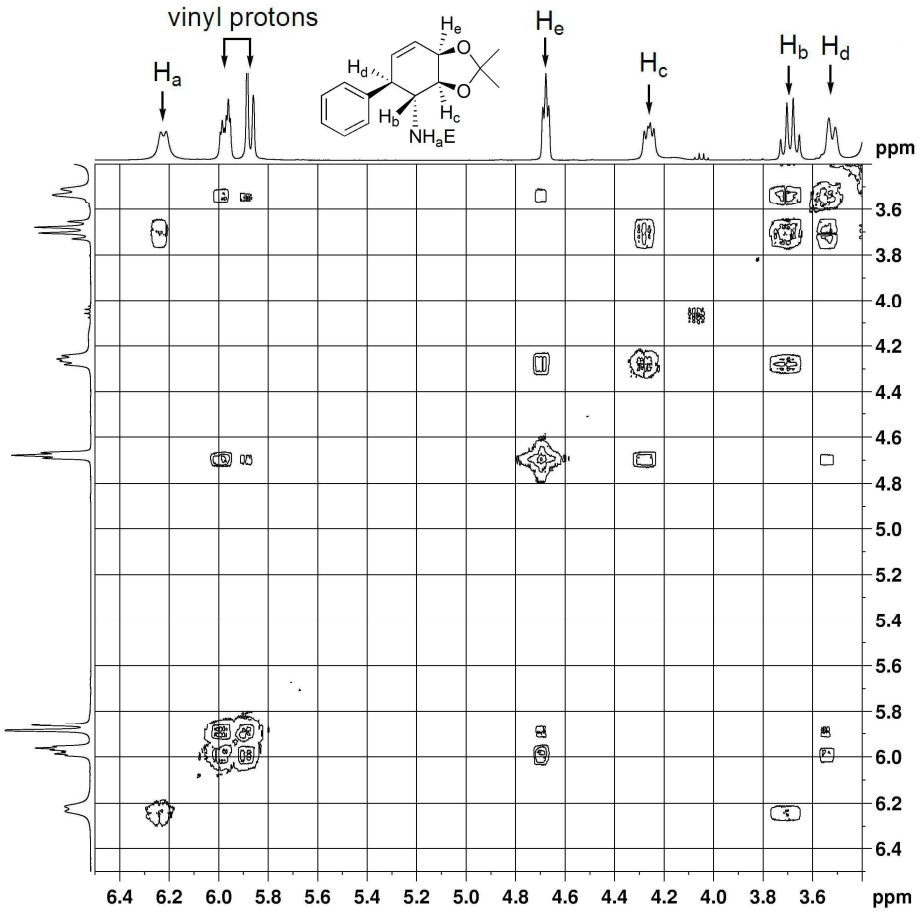

Carbamate 49 (Hudlicky's Intermediate)

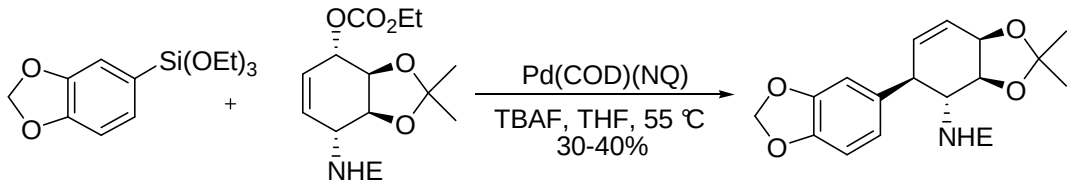

72 **87** **49**

Carbamate (E = CO_2Me): To 462 mg (1.63 mmol, 2.00 equiv.) of aryl siloxane **72** and 256 mg (0.813 mmol, 1.00 equiv.) of carbonate-carbamate **87** dissolved in 15.0 mL anhydrous THF was added 1.63 mL (1.63 mmol, 2.00 equiv.) TBAF under argon. This was followed by addition of 152 mg (0.407 mmol, 0.500 equiv.) Pd(COD)(NQ). The reaction mixture was heated at 55 °C for 24 h. The reaction was then quenched by addition of 30.0 mL H_2O. The product was extracted with 3 × 50 ml CH_2Cl_2 and washed with H_2O. The combined organic extracts were dried over $MgSO_4$, filtered and concentrated *in vacuo* to give brown oil. Flash column chromatography on silica gel (30% EtOAc/70% hexane, R_f = 0.17) gave 98 mg (35%) of carbamate **49** as pale yellow solid, mp 177-179 °C ((lit.[80] 190-191 °C); IR (CCl_4) 3467 (w), 3442 (w), 3042 (w), 2995 (w), 2881 (w), 1730 (s), 1504 (s), 1486 (s), 1250 (s) cm^{-1}; ^{1}H NMR (500 MHz, $(CD_3)_2CO$) δ 6.75 (d, *J* = 8 Hz, 1H), 6.68-6.65 (m, 2H), 6.18 (br d, *J* = 8 Hz, 1H), 5.97-5.93 (m, 3H), 5.85 (d, *J* = 10 Hz, 1H), 4.66 (t, *J* = 5 Hz, 1H), 4.25-4.22 (m, 1H), 3.62 (q, *J* = 10 Hz, 1H), 3.46 (br d, *J* = 10 Hz, 1H), 3.42 (s, 3H), 1.45 (s, 3H), 1.33 (s, 3H); ^{13}C NMR (125 MHz, $(CD_3)_2CO$) δ 157.4, 148.6, 147.4, 136.9, 136.6, 124.8, 122.5, 109.9, 109.4, 108.8, 101.9, 77.9, 73.3, 56.9, 51.6, 47.1, 28.7, 26.6; HRMS (ESI) calcd for $C_{18}H_{22}O_6N$ $(M+H)^+$ 348.1447, found 348.1440. ^{1}H and ^{13}C NMR spectra in $CDCl_3$ are

identical with that reported by Hudlicky.[80] The regiochemistry of carbamate **49** was established using ^{1}H-^{1}H COSY (500 MHz, $(CD_3)_2CO$), provided on page 64, Figure 3.2.

Carbamate (E = CO_2Et): light yellow solid. mp 151-153 °C; IR (CCl_4) 3467 (w), 3446 (w), 3042 (w), 2995 (w), 2935 (w), 2874 (w), 1726 (s), 1547 (s), 1511 (s), 1486 (s), 1250 (s) cm^{-1}; ^{1}H NMR (500 MHz, $(CD_3)_2CO$) δ 6.75 (d, *J* = 8 Hz, 1H), 6.68-6.65 (m, 2H), 6.11 (br d, *J* = 8 Hz, 1H), 5.97-5.94 (m, 3H), 5.86 (d, *J* = 10 Hz, 1H), 4.66 (t, *J* = 5 Hz, 1H), 4.25-4.22 (m, 1H), 3.86 (q, *J* = 5 Hz, 2H), 3.62 (q, *J* = 10 Hz, 1H), 3.46 (br d, *J* = 10 Hz, 1H), 1.45 (s, 3H), 1.33 (s, 3H), 1.05 (t, *J* = 5 Hz, 3H); ^{13}C NMR (125 MHz, $(CD_3)_2CO$) δ 157.0, 148.7, 147.4, 136.8, 136.7, 124.9, 122.6, 109.9, 109.5, 108.8, 102.0, 77.9, 73.4, 60.5, 57.0, 47.3, 28.8, 26.6, 15.0; HRMS (ESI) calcd for $C_{19}H_{24}O_6N$ $(M+H)^+$ 362.1604, found 362.1563.

CHAPTER 4
MECHANISTIC STUDIES ON PALLADIUM-CATALYZED ALLYLIC-ARYLATION

INTRODUCTION

The DeShong group has developed palladium-catalyzed arylation of allylic esters *via* coupling of aryl siloxanes (see Chapter 1).[29-34] This methodology has been shown to be both highly regio- and stereoselective and has been successfully applied to the synthesis of a (±)-7-deoxypancratistatin analogue **69** (Scheme 4.1) (see Chapter 2). However, repeated attempts to effect coupling between carbonate **87** and siloxane **72** for the synthesis of 7-deoxypancratistatin (**24**) were unsuccessful and no trace of the desired adduct **49** was detected.

Scheme 4.1

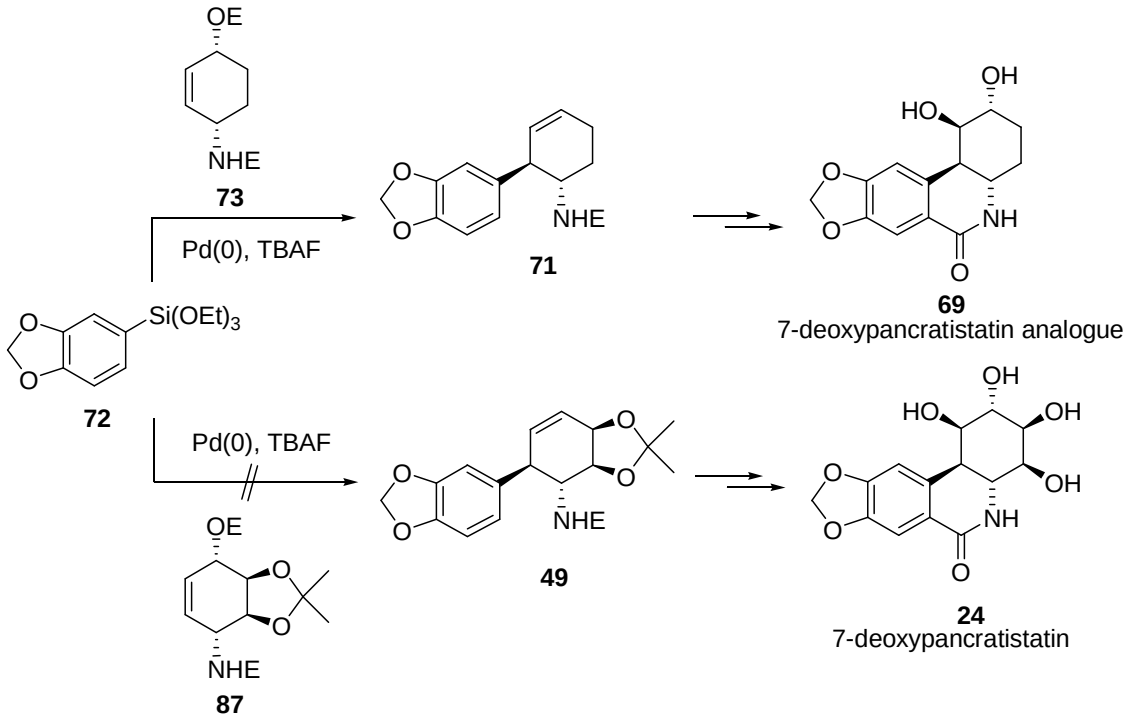

It was hypothesized initially that failure of allyl carbonate **87** to undergo arylation was the result of the steric bulk of the isopropylidene group that blocked the β-face of the alkene and prevented formation of the requisite π-allyl intermediate **99** (Scheme 4.2). However, the successful coupling of allylic carbonate **87** with malonate anion **100** demonstrated that formation of π-allyl intermediate **99** had been produced since it underwent Tsuji-Trost coupling. This result led us to infer that either transmetalation or the subsequent reductive elimination step, latter steps in the mechanism, must be responsible for failure of the coupling reaction between aryl siloxane **72** and allyl carbonate **87** (Scheme 4.3). Since both transmetalation and reductive elimination involve transfer of an aryl group during the catalytic cycle, we anticipated that altering substituents on the aryl ring would affect the relative rates of these processes. Accordingly, we chose to investigate the role of substituents on aryl siloxane in controlling the rate of the coupling reaction *via* Hammett analysis.

Scheme 4.2

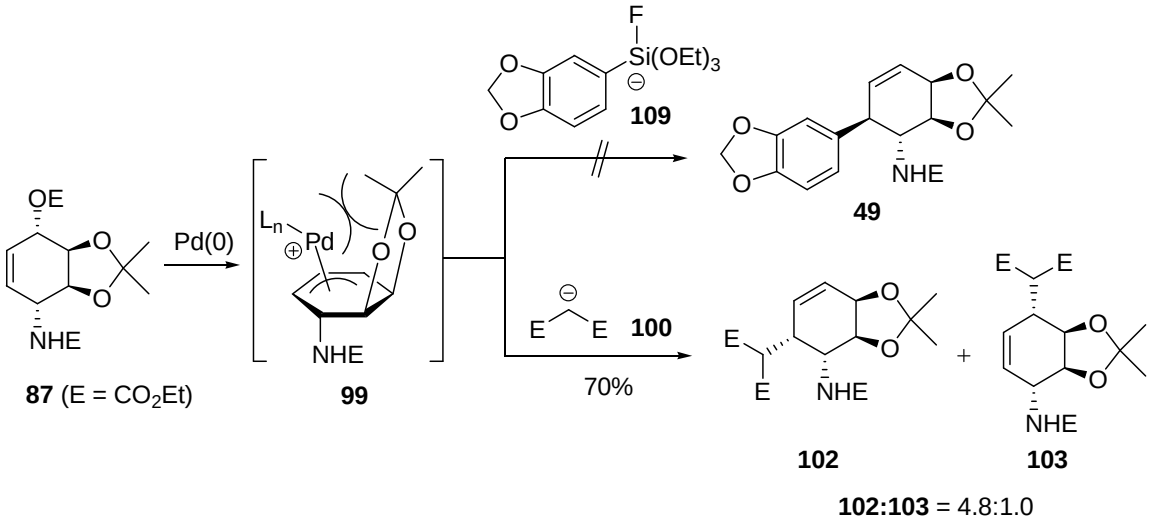

Scheme 4.3

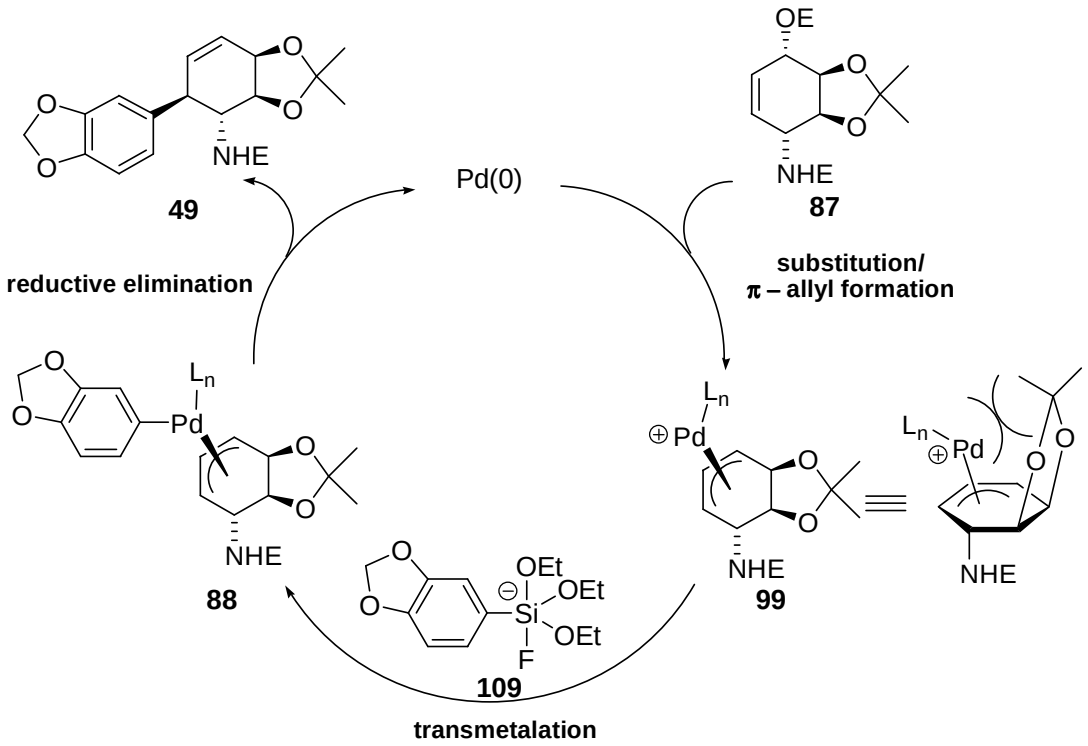

Transmetalation

Transmetalation of organometallic compounds with transition metal complexes is one of the key steps in carbon-carbon bond formation. However, mechanistic details of the transmetalation process are not well understood for most of these catalytic processes. Among many useful coupling variants, the Stille reaction is the most extensively studied system with regard to the mechanism of transmetalation. One of the earliest studies is that of palladium-catalyzed coupling of benzoyl chloride with benzyltin reagents by Stille.[115,116] Subsequently, Farina reported a kinetic analysis of the effect of palladium ligands on the Stille reaction[117] and Hartwig investigated the mechanism of transmetalation of tin amides and tin thiolates.[118] More recently, Amatore and Jutand have studied the mechanism of Stille reaction in the presence of $AsPh_3$ ligated palladium

catalyst, and confirmed Farina's proposal that $AsPh_3$ increased the efficiency of the Stille reaction compared to PPh_3.[119] An extensive kinetic study of the transmetalation reaction in Stille coupling has been carried out recently by Espinet, who has proposed an associative transmetalation model for the key step and also investigated the nature of the transition state (Figure 4.1).[120-123] Studies on internal-coordination driven transmetalation are also known in literature.[124-126] Transmetalation studies on palladium-catalyzed cross couplings of alkynyl stannanes with aryl iodides and that with metal-halides have been reported by Crociani[127] and Lo Sterzo[128], respectively. Additionally, Wendt[129] and Clarke[130] have reported studies on transmetalation of organostannanes and organozincs, respectively, with platinum complexes. More recently, theoretical calculations on transmetalation of Stille reaction have appeared.[131-135]

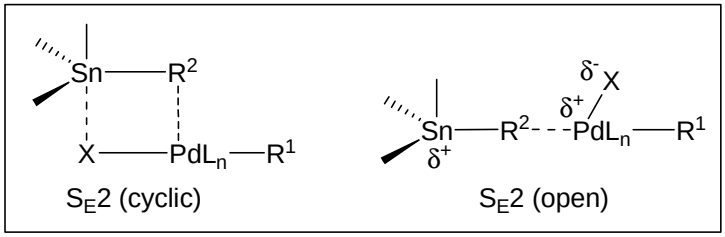

Figure 4.1: Espinet's model for transmetalation in Stille reaction

Transmetalation in the Suzuki-Miyaura and Hiyama protocols have been studied less extensively. Transmetalation processes for cross-coupling of organoboron compounds in alkaline solution have been studied by Miyaura.[136] Three possible pathways for transmetalation process have been proposed (Scheme 4.4). In Path A, the addition of sodium hydroxide generates tetravalent boronate anion **110** which enhances nucleophilicity of organic group and thus accelerates transmetalation. Alternatively, ligand exchange between R-Pd-X and a base R″O generates oxo palladium(II) complex

111 *in situ* (Path B). The high bascity of the Pd-OR species as well as the high oxophilicity of boron results in enhanced reactivity of the oxo palladium complex. On the other hand, reaction of allyl acetate can proceed under neutral conditions since oxidative addition directly yields π-allylpalladium acetate complex **111** (Path C). These three pathways are highly dependent on the combination of bases and organoboron reagents, as well as organic electrophiles.

Scheme 4.4

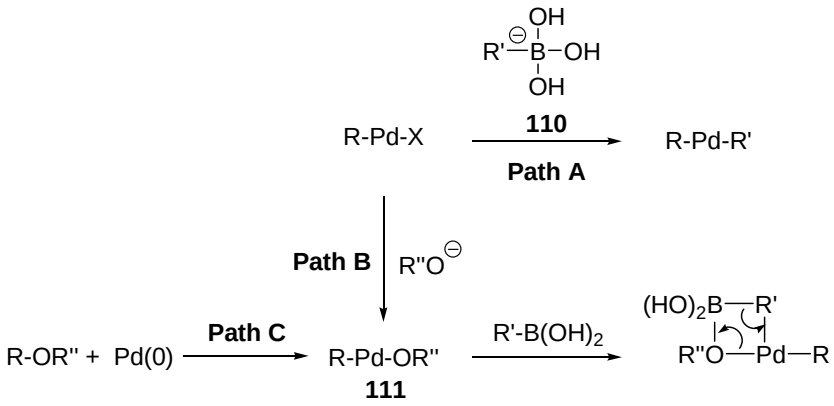

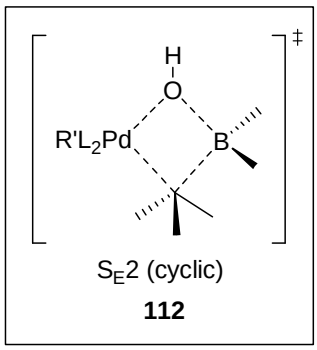

Figure 4.2: Transmetalation of alkyl boranes

Woerpel and Soderquist studied transmetalation of primary alkyl borane derivatives to palladium and proposed a hydroxo bridged S_E2 (cyclic) transition state **112** (Figure 4.2).[137,138] More recently, theoretical studies on mechanism of Suzuki-Miyaura

reaction catalyzed by diphosphine palladium complexes have been reported. According to these studies arylboronic acid is activated by an external base, which attacks the palladium center as an boronate anion.[139-144]

The use of organosilanes rather than boranes as cross-coupling partners has been less studied and mechanistic knowledge for Hiyma coupling is scarce. Because the Si-C bond is less polarized than the corresponding B-C bond, Hiyama introduced use of a nucleophilic fluoride source to polarize Si-C bond *via* formation of a reactive pentacoordinate silicate and enhance transmetalation.[145-148] Hiyama showed that the stereochemistry of transmetalation can be influenced by the reaction temperature and the solvent used.[145,147] For example, the cross-coupling reaction of aryl triflates **113** with chiral alkylsilanes **114** (Scheme 4.5) in THF at low temperatures proceeded with retention of configuration, whereas reaction at higher temperatures or in polar solvents (HMPA) resulted in inversion of configuration. Retention of configuration is attributed to fluorine-bridged S_E2 (cyclic) transition state **115** in the transmetalation (Scheme 4.6). At higher temperature or in polar solvents, a fluorine-silicon bridge is cleaved resulting in S_E2 (open) transition state **116** and thus inversion of configuration. Stereochemistry in cross-coupling of allyltrifluorosilanes with aryl triflates was shown also to be influenced by temperature and fluoride source.[148]

Scheme 4.5

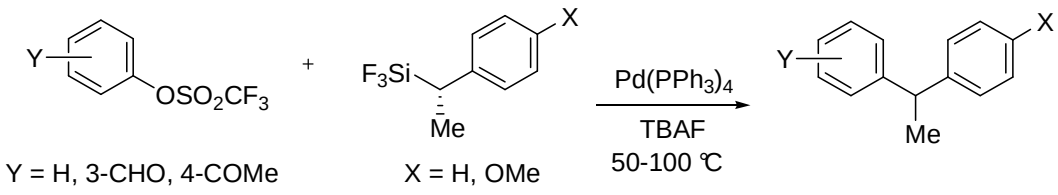

Scheme 4.6

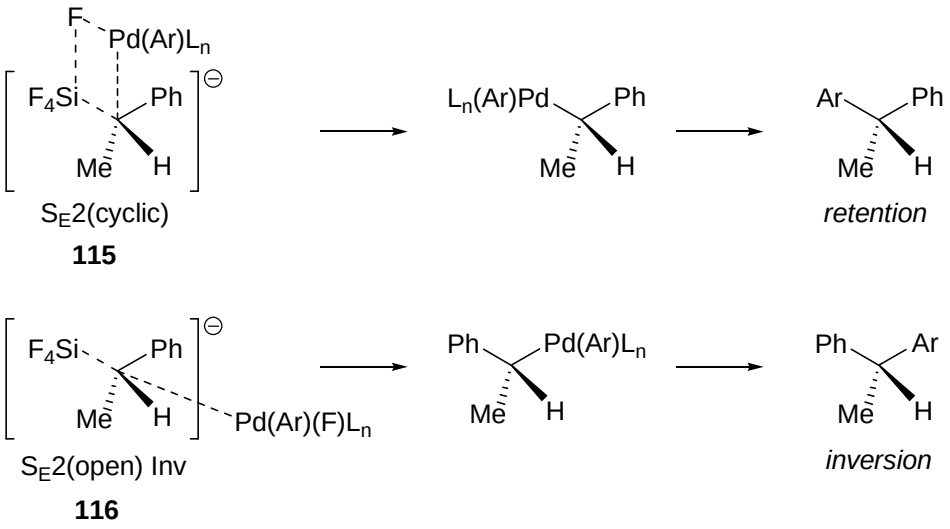

Recently, Sakaki reported a theoretical study of the transmetalation between palldium(II)-vinyl complex and vinyl silane.[149] The study indicated a very large activation barrier for transmetalation process in the absence of fluoride anion. In the presence of fluoride anion, transmetalation is accelerated by the formation of a very strong Si-F bond and the stabilization of the transition state by hypervalent Si center induced by the fluoride anion.

Denmark has also performed mechanistic studies on organosilanes *via* kinetic analysis under both fluoride-mediated and fluoride-free conditions.[150,151] In an effort to study transmetalation process, stable transmetalation intermediates in Stille, Suzuki and Hiyama cross-coupling have also been isolated.[152-155]

Hammett Analysis

Hiyama Coupling

Mechanistic studies of transmetalation of an aryl group in metal-catalyzed couplings of organosilanes using Hammett analysis have been reported previously (Scheme 4.7). For example, Hatanaka and Hiyama have shown that electron-donating groups (EDG) enhance the rate of transmetalation of diarylfluorosilicates with an aryl-palladium complex (Figure 4.3).[156] The negative slope is indicative of the electrophilic character of the transmetalation. The presence of EDG on diarylfluorosilicate **117** increases the nucleophilicity of the aryl-silicon bonds, which aids in electrophilic attack of arylpalladium(II) complex **118** *via* a Si-Pd binulclear intermediate **119** formed by a fluoride bridge (Scheme 4.8).

Scheme 4.7

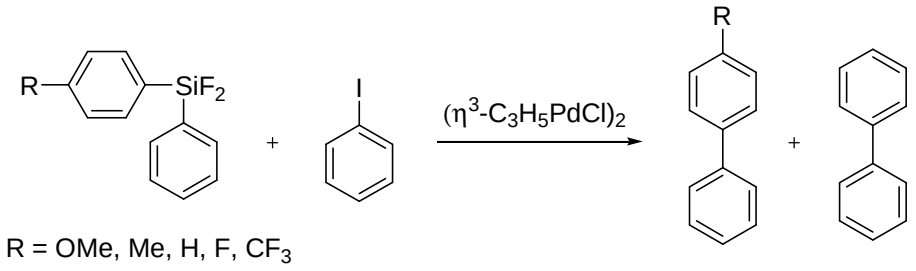

Scheme 4.8

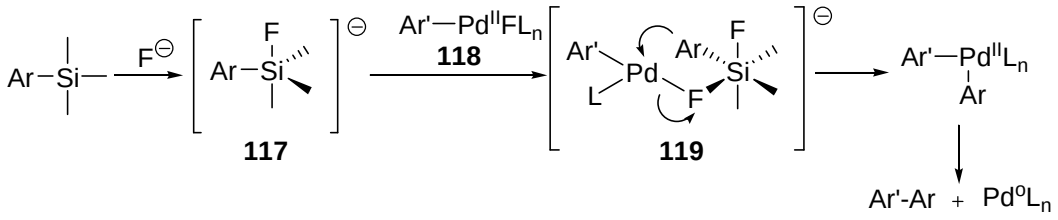

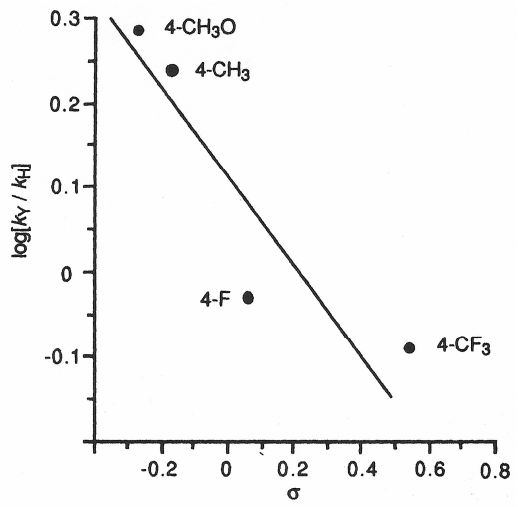

Figure 4.3: Hammett analysis of the reaction of diaryl(difluoro)silanes with iodobenzene. Taken from ref 156.

Suzuki Coupling

The reactivity of various arylboronic acid for the coupling of (*E*)-bromostilbene in the presence of $Pd(OAc)_2/PPh_3$ was evaluated by competitive experiments (Scheme 4.9).[157] Arylbornic acids containing an electron-donating group (EDG) in the para position were found to be more reactive (ρ = -0.71) (Figure 4.4). EDG increases nucleophilicity of the aryl group, promoting transfer of aryl group to the electron deficient palladium. This result is analogous to the results from the $Pd(OAc)_2/PPh_3$ catalyzed cross-coupling reaction of arylboronic acid with vinyl bromide, generated *in situ* from 1,2-dibromoethane (ρ = -1.26).[158] On the other hand, nickel-catalyzed Suzuki coupling of an arylboronic acid and an aryl tosylate gave the opposite result: electron-withdrawing groups (EWG) on the aryl boronic acid facilitated transmetalation and gave a slope of ρ = 0.81.[159]

Scheme 4.9

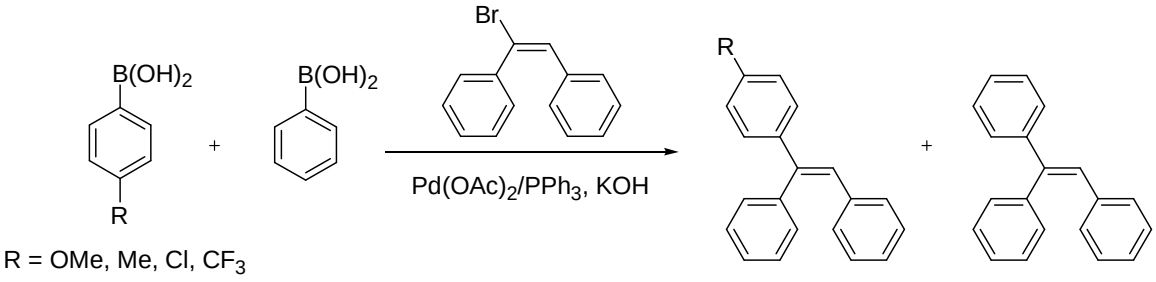

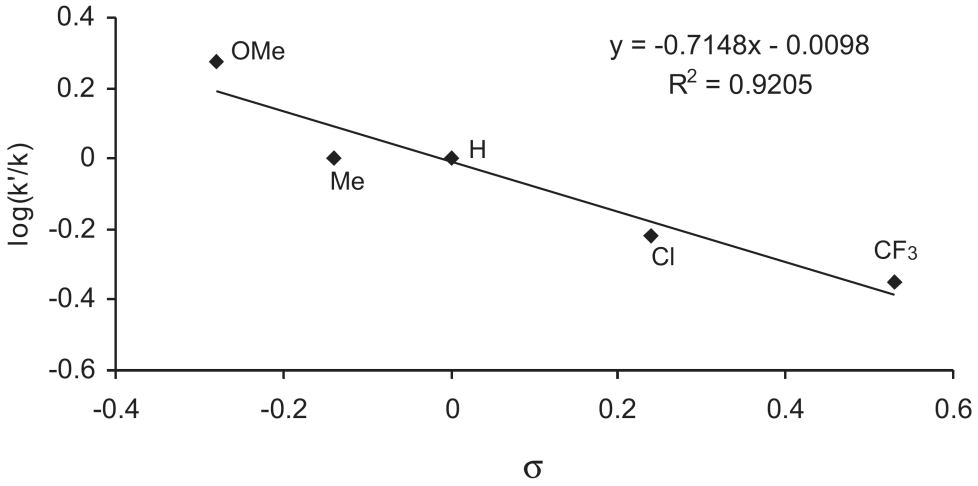

Figure 4.4: Hammett analysis of the reaction of arylboronic acid with *E*-bromostilbene. Taken from ref 157.

Additionally, Hammett analysis has also been employed to study the mechanism of the reaction of aryl bromides and arylboronic acid catalyzed by palladacycles (Figure 4.5). It was found that aryl bromides bearing EWG accelerated the rate of reaction and gave correlation values of $\rho = 0.48$, $\rho = 0.66$, and $\rho = 0.99$ for palladacycles **VI**[160], **VII**[160] and **VIII**[161] respectively. Transmetalation processes have also been studied for the cross-coupling of phenyl boronates with propargylic carbonates ($\rho = 0.73$)[162], γ-selective cross-coupling of potassium allyltrifluoroborates with aryl bromides ($\rho = -1.1$)[163], and 1,4-addition of arylboronic acids to enones ($\rho = -0.54$).[164]

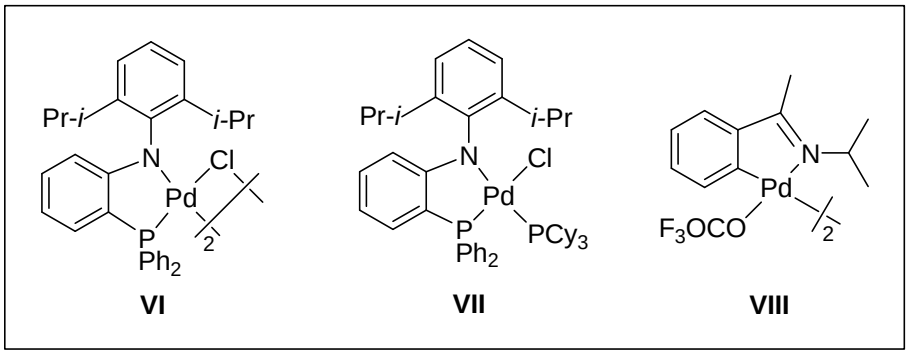

Figure 4.5: Palladacycles used in Hammett analysis of arylboronic acid with aryl bromides

Stille Coupling

Farina studied the electronic influence of aryl stannane on the transmetalation step by competitive experiment of vinyl triflate with various para-substituted aryl stannanes (Scheme 4.10).[165] In the absence of lithium chloride, EDG on the aryl stannane accelerated transmetalation (ρ = -0.89), indicating development of positive charge in the transition state (Figure 4.6). However, in the presence of LiCl, the linear relationship could not be obtained (Figure 4.7). This indicated two mechanistically different pathways for the transmetalation process in the presence of salt. Farina's results are in contrast to that by Stille employing acid chlorides and benzylic stannanes (ρ = 1.2).[116]

Scheme 4.10

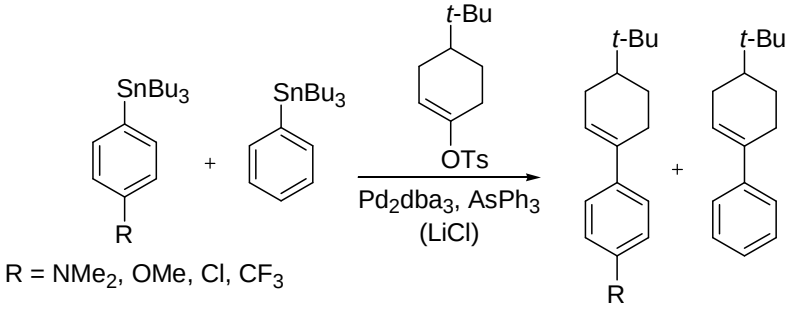

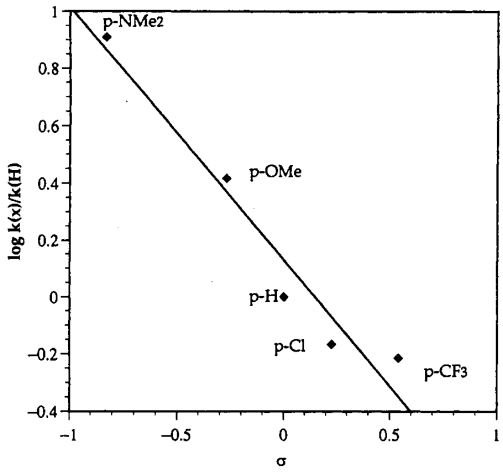

Figure 4.6: Hammett analysis of Stille coupling reaction in absence of LiCl. Taken from ref 165.

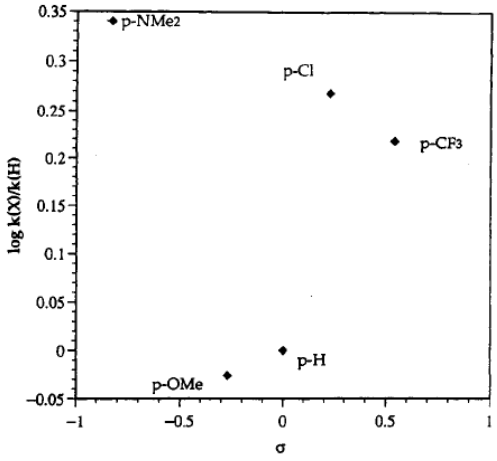

Figure 4.7: Hammett analysis of Stille coupling reaction in presence of LiCl. Taken from ref 165.

In summary (Table 4.1), Hammett studies of cross-coupling reactions have indicated that transmetalation is a complex process in which the rates of coupling are strongly influenced by substituents on the ring as well as the catalyst and/or ligand. In light of the failure of our *aryl-allyl coupling* reaction in the 7-deoxypancratistatin (**24**) synthesis (Scheme 4.1), we chose to investigate the mechanism of the siloxane-based coupling reaction in detail.

The goal of this project was to perform a Hammett study of the coupling reaction utilizing palladium-catalyzed siloxane derivatives. The study reported below is the first mechanistic investigation of an *allyl-aryl coupling* process involving silicon-based reagents.

	Organometallic Partner	Electrophilic Partner	Catalyst	ρ
1.	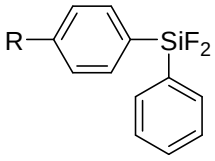	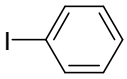	$(\eta^3\text{-}C_3H_5PdCl)_2$	-1.5
2.	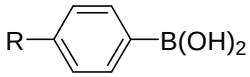	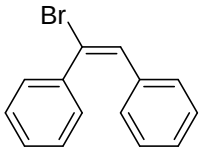	$Pd(OAc)_2/PPh_3$	-0.71
3.	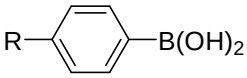	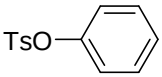	$NiCl_2(PCy_3)_2$	0.81
4.	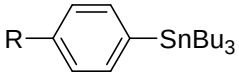	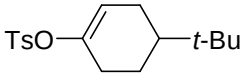	Pd_2dba_3, $AsPh_3$	-0.89

Table 4.1: Summary of Hammett studies

RESULTS AND DISCUSSION

Hammett Analysis

The proposed mechanism for the allyl-aryl coupling reaction is summarized in Scheme 4.11. The relative rates for each individual step of the coupling will be discussed below. Cyclohexenyl carbonate (**120**) was chosen as the coupling partner for the siloxane study because it was known to undergo facile allyl-aryl coupling with siloxane derivatives under established protocols. There is significant literature precedent for the *rapid and reversible* formation of π-allyl palladium complexes from allylic derivatives with both phosphine and dibenzylideneacetone (dba) ligands.[166,167] (The reversibility of

the reaction is diminished with carbonates since the carbonate anion decomposes to carbon dioxide and alkoxide under the typical coupling conditions).[166]

Scheme 4.11

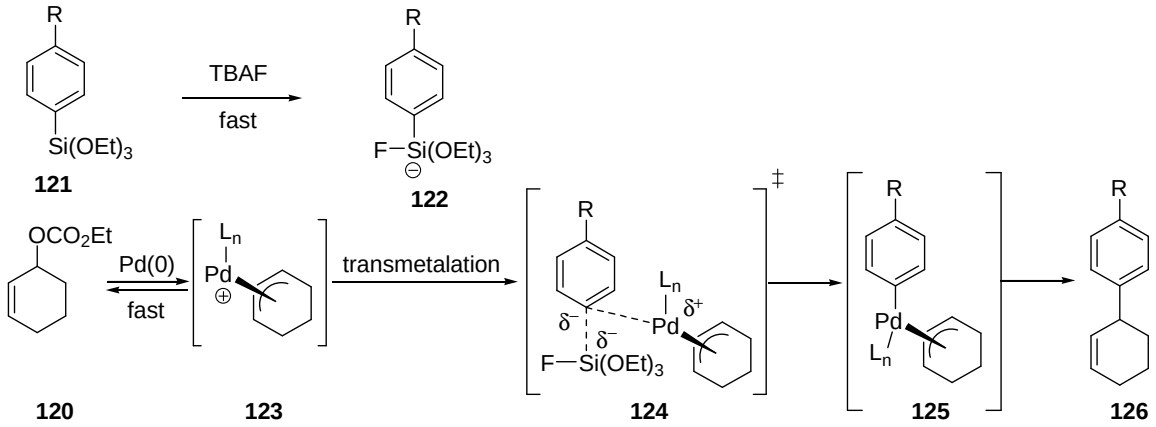

However, it was important to conclusively demonstrate that this step was not rate-determining in this coupling system, and that result can be inferred from the subsequent Hammett analysis reported below. If formation of the π-allyl intermediate **123** were rate-determining, then a correlation of rates with Hammett parameters on the siloxane moiety would not be observed because the siloxane would not appear in the rate equation for formation of the π-allyl complex. Accordingly, the Hammett correlation observed (*vide infra*) is consistent with the formation of the π-allyl palladium complex being a fast process.

Formation of the hypercoordinate silicate **122** from the reaction of fluoride anion (TBAF) with the siloxane derivative **121** is not rate-determining either. This was demonstrated by ^{19}F NMR spectroscopy of the reaction of TBAF and phenylsiloxane derivatives **121**. In the key experiment, a hypercoordinate silicate species (**121**, R = H)

was generated *in situ* by reaction with fluoride source (TBAF) (Scheme 4.12 and Figure 4.8). The formation of hypercoordinate silicates was observed using ^{19}F NMR where the fluorine signal of TBAF (δ -114)[168] disappeared rapidly (10 min) *at room temperature* on addition of phenylsiloxane to give two new fluorine signals: a sharp singlet at δ -121, and a broad resonance centered at ca. δ -127, respectively, as shown in Figure 4.8. The signals at δ -121 and δ -127, respectively, are consistent with chemical shifts of hypercoordinate fluorosilicate species such as **122** and **127**, respectively reported by this and other groups.[169-177] Upon cooling (-29 °C), the ^{19}F signal at δ -121 sharpened, showing silicon satellites (J_{Si-F} = 207 Hz). Additonally, ^{29}Si NMR also indicated coupling of 207 Hz at δ -129 confirming the formation of hypervalent silicate species (see Experimental Section, Figure 4.15).

Scheme 4.12

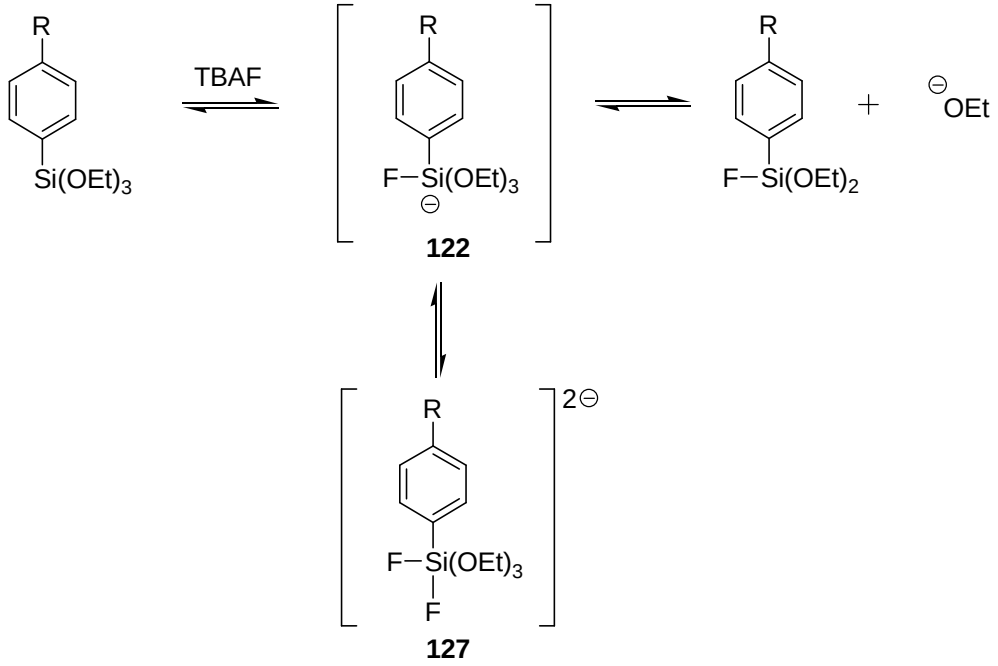

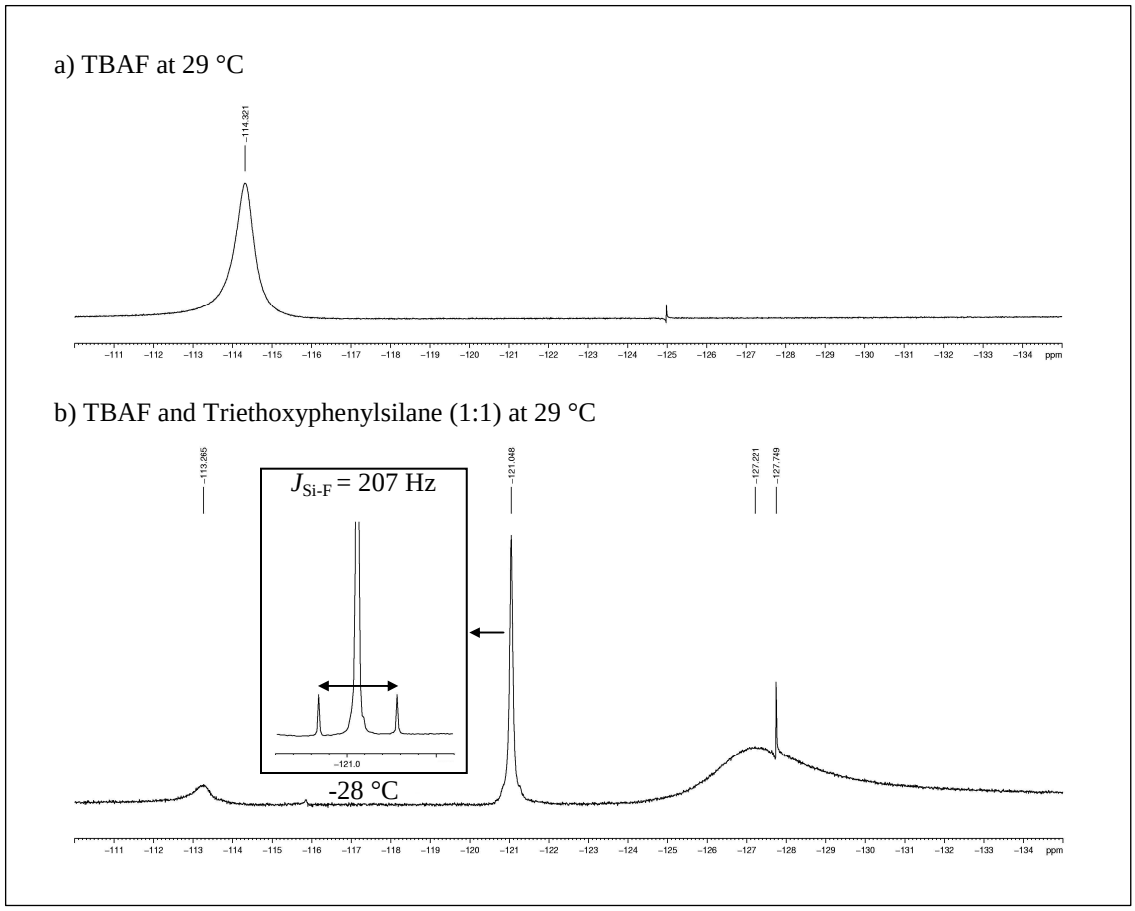

Figure 4.8: ^{19}F NMR spectra of silicate formation (a) TBAF in THF at 29 °C (b) ^{19}F NMR spectrum of silicate complexes resulting from 1:1 mixture of TBAF and Triethoxyphenylsilane at 29 °C. Insert is ^{19}F signal at δ -121 after cooling to -28 °C.

The broad signals in the ^{19}F NMR spectrum are consistent with formation of hypercoordinate complex(es) that undergo dynamic processes including ligand exchange and pseudorotation. The equilibrium between the various silicates is dependent on stoichiometry of fluoride:siloxane and other electronic factors. The ^{19}F NMR spectra are also temperature dependent, indicating a dynamic process (see Experimental Section). Preliminary studies of silicate formation indicated that the electronic effects of the groups attached to the aryl ring had an effect on the relative quantities of each component, but additional studies have to be undertaken to determine the relative importance of each silicate to the overall coupling reaction. Nonetheless, the conclusion drawn from this

study is that *at room temperature, the siloxane reacted with fluoride ion to provide hypercoordinate silicates rapidly, much more rapidly than coupling occurred.*

Analogously, when TBAF (2 equiv.) was added to a mixture of phenylsiloxane (1 equiv.) and its *p*-methoxy congener (1 equiv.), the signal for TBAF rapidly disappeared and was replaced by a series of resonances indicative of hypercoordinate silicate formation. This experiment conclusively demonstrated that formation of the silicate from the reaction of fluoride ion and the siloxane derivatives was fast and could not be the rate-determining step in the coupling reaction.

We had proposed initially that either transmetalation of silicate **122** to π-allyl palladium complex **123** or subsequent reductive elimination was the rate-determining step in the coupling reaction (Scheme 4.11). If this assumption were correct, then the rate of the allyl-aryl coupling should be influenced by the electronic characteristics of the substituent present on the aryl ring of siloxane **121**, and substituents in the para-position would stabilize (or destabilize) transition state **124** resulting in a rate enhancement (or diminution). Competition experiments between phenyltriethoxysilane **6** and para-substituted aryl siloxanes **121** (R = OMe, Me, Cl, CO_2Et) were performed and the results are summarized in Figure 4.9. The relative rate of transmetalation was enhanced by electron-withdrawing groups (EWG). Electron-withdrawing groups are better at stabilizing the developing negative charge on the *ipso*-carbon in transition state **124** through inductive effects.

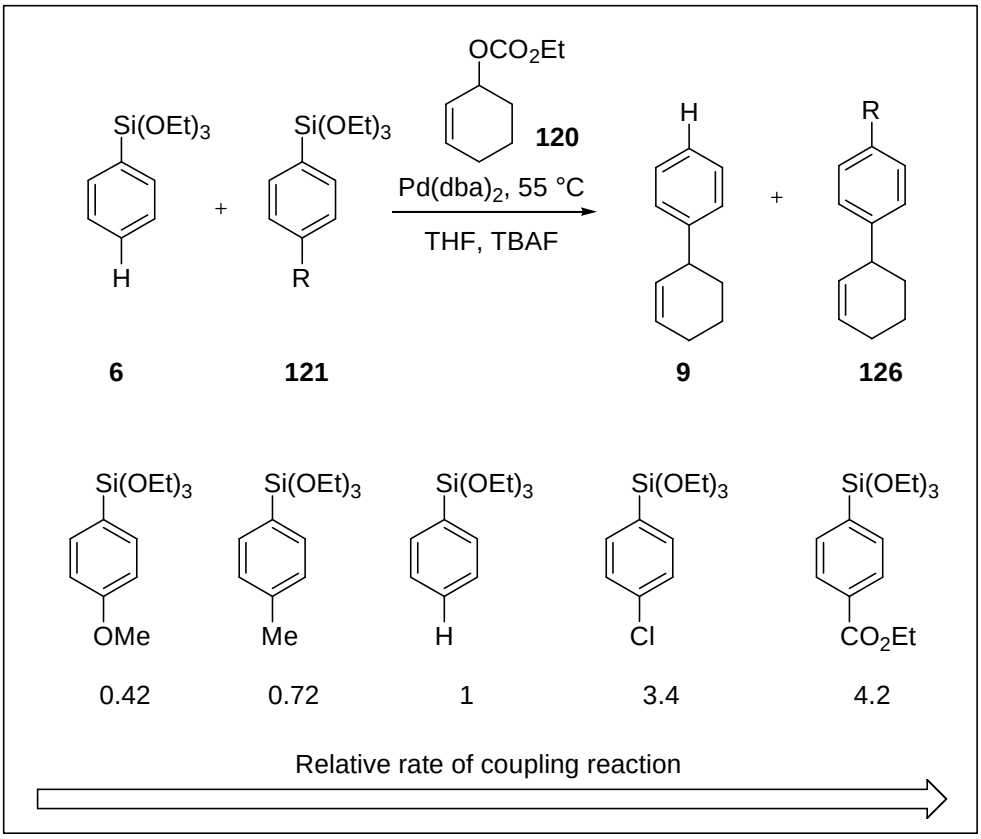

Figure 4.9: Summary of relative rates of coupling reactions with siloxane derivatives

More importantly, the excellent correlation observed in the Hammett analysis is consistent with the proposal that the rate-determining step is either the transmetalation or reductive elimination reaction. As was noted above, if π-allyl formation were the slow step, then no difference in the relative rates would have been observed since the substituents on the aryl ring would not be able to manifest their influence in the rate determining step of the coupling reaction.

Having established the nature of the substituent effect for the siloxane coupling protocol, the magnitude of the stabilization that occurred in the transition state for the coupling was determined from the Hammett correlation. Hammett plots were obtained by plotting log (k/k_0) against substituent parameters σ_p, σ^-, and σ^+.[178] The plot of log (k/k_0)

against σ_p gave the best linear correlation to the experimental data (Figure 4.10) with slope $\rho = 1.4$. The linear regression with σ_p value indicated that an inductive effect was chiefly responsible for stabilization of the transition state.

The positive slope ($\rho = 1.4$) of the line indicated that coupling was sensitive to the electronic effects of substituents and that a significant amoung of negative charge was to be found on the aromatic ring in the transition state **124** (Scheme 4.11). Contrast the magnitude of the ρ value (+1.4) with the values obtained in studies of borates and stannanes, respectively (described above) where $|\rho| = 0.7\text{-}1.1$ (Table 4.1). The positive slope of $\rho = 1.4$ is in sharp contrast with the studies reported by Hiyama ($\rho = -1.5$)[156], Monteiro ($\rho = -0.71$)[157] and Farina ($\rho = -0.89$)[165] using silicon, boron and stannane derivatives, respectively, in the presence of palladium catalyst, where EWG retarded the rates of coupling reaction (Table 4.1).

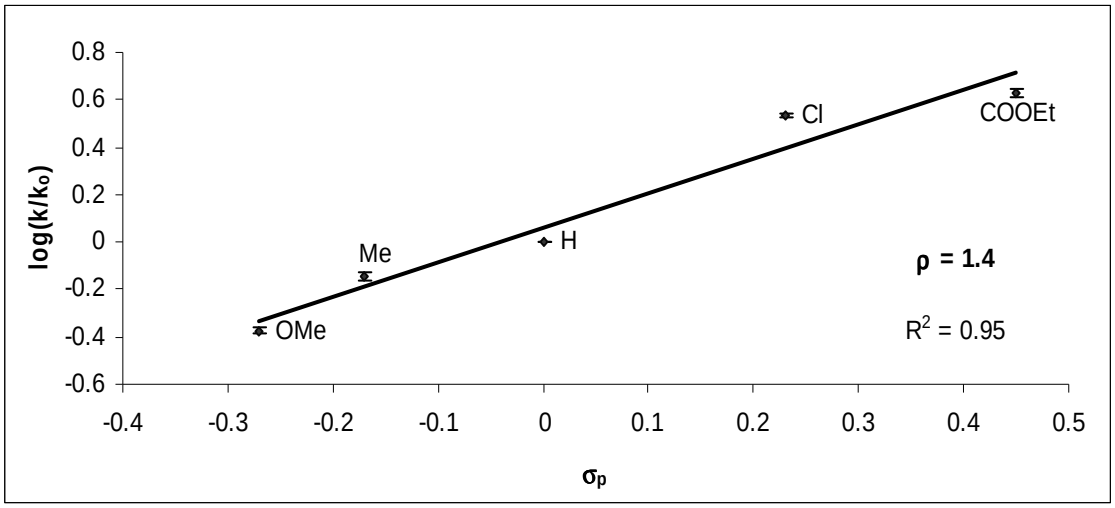

Figure 4.10: Hammett analysis of allyl-aryl coupling reaction

It is noteworthy to reiterate the significance of the Hammett correlation: the observed substituent effects are consistent with formation of the π-allyl complex being a fast and reversible reaction as was noted above and either the transmetalation or the

reductive elimination is rate-determining (Scheme 4.11). If formation of π-allyl complex were rate-determining, then the Hammett plot should have had a slope of zero because the aryl siloxane was not involved in that step of the mechanistic cycle.

It is worth emphasizing that the term "rate-determining step" in the discussion above is not precise. Rate-determining and product-determining have been used interchangably, although this is not valid in a strict interpretation. We know that formation of π-allyl intermediate **123** is fast and reversible step (Scheme 4.13). Assuming transmetalation and reductive elimination is irreversible, if reductive elimination is slow, the product-determining step is transmetalation since it is the first irreversible step. This may not be the rate-determining step, but it is the step that leads to selective formation of one coupling product over the alternative. On the other hand, if transmetalation is slower than reductive elimination, transmetalation is still product-determining as well as rate-determining. In this study, relative rates of irreversible steps were measured and not the absolute rates. Nonetheless, regardless of which step is slow (rate-determining), transmetalation is the product determining step.

Scheme 4.13

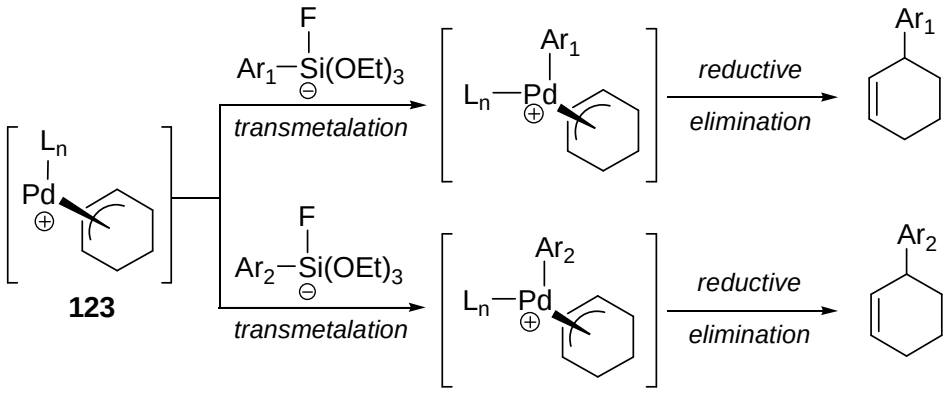

From the data provided it is not possible to unambiguously determine which of these two steps is rate-determining. For this coupling reaction, however, we propose that the rate-determining step is transmetalation, rather than reductive elimination, based on several lines of circumstantial evidence.

First, since no coupled product **49** was obtained in the 7-deoxypancratistatin (**24**) synthesis, it is reasonable to assume that the transmetalation had not occurred to give palladium complex **88** (Scheme 4.3). Although the rationale for this conclusion is complex, the analysis is important for the mechanistic study in question. Formation of π-allyl complex **99** (Scheme 4.3) was fast and reversible; thus the experimentally observed rearrangement of the cyclohexenyl carbonate was observed as a byproduct in this coupling (see Chapter 3). If the rate-determining step was transmetalation, then a slow transmetalation reaction would provide greater opportunity for rearrangement and decomposition of the cyclohexenyl starting material without leading to coupled product. If, on the other hand, reductive elimination were the rate-determining step, *coupled product, even if only trace amounts, would have been obtained since it is unlikely that transmetalation was reversible.* Reductive elimination must result in formation of coupled product or reduced arene (*via* beta-hydride elimination followed by reductive elimination). No trace of either coupled product or reduced arene was observed under these conditions.

A second piece of evidence supporting the conclusion that transmetalation was rate-determining was derived from the study of Kurosawa on the reductive elimination of diorganopalladium complexes.[179,180] Kurosawa was able to prepare allyl-aryl palladium complexes (utilizing an alternative methodology) and measured the rate of reductive

elimination at 0 °C. If extrapolated to 55 °C, as in our coupling protocol, the rates of reductive elimination would be much faster than the rate of coupling observed, thus suggesting that transmetalation, and not reductive elimination, is rate-determining step for the allyl-aryl coupling reaction reported in our study. Admittedly, the evidence is circumstantial, since the Kurosawa system involved different ligands on the metal center than our coupling protocol.

Even more significant is that Kurosawa demonstrated that electron-deficient alkenes *promoted*, not retarded, the reductive elimination in his system. This observation is particularly germane to our coupling system in which the electron-deficient dba (dibenzylideneacetone) is a ligand on the catalyst that functions for this coupling. Assuming that the silicate system behaves analogously to the Kurosawa analog, we would anticipate that the reductive elimination step would be facilitated by the presence of electron-deficient ligand as was observed by Kurosawa.[179-181]

As has been noted by Denmark in his mechanistic studies of analogous silanol-based aryl-aryl coupling reactions, there is no unambiguous evidence for the intermediacy of a diorganopalladium (II) complex that undergoes reductive elimination to produce the product (Scheme 4.11).[151] In the allyl-aryl system described herein, it is possible that π-allyl complex **123** reacted with the activated silicate **122** *via* a substitution reaction to yield the product directly. Nonetheless, one would observe that this step would be rate-determining.

Further support for our hypothesis that the rate-determining step in the coupling reaction is transmetalation, and not reductive elimination comes from Hartwig's lab. Hartwig has reported several mechanistic studies of palladium-catalyzed coupling

reactions in which reductive elimination is the rate determining step.[182-186] In each of these studies, however, an isolable palladium (II) complex was prepared and then decomposed thermally *via* reductive elimination to provide product. Hammett analyses of these systems have shown significant substituent effects, but the results are not as straightforward as is observed in our system. For C-S bond formation, the substituent effect was *qualitatively* similar to those observed in our study, namely faster rates with electron-withdrawing substituents, but there was no correlation with Hammett sigma values. They were able to correlate the rates of reductive elimination only with a mixed Hammett value that included both inductive and resonance contributions.[184] Analogous situations were observed for C-N and C-C coupling reactions, respectively.[185,186]

Role of Ligands

The studies summarized above have established that Hammett analysis is an excellent method for gathering mechanistic information regarding the transition state (**124**) for the transmetalation step of the mechanism (Scheme 4.11). *Furthermore, this Hammett methodology can be employed for investigating the roles of catalyst-ligand combinations in the coupling reaction*. Typically, the development of an "optimized" catalyst system for a coupling reaction involves the empirical development of conditions and reagents using various ligand-metal ratios and is based on yield or turnover of product. The actual role that the ligand (L_n in **124**, Scheme 4.11) plays in transmetalation cannot be assessed except in a qualitative sense: the reaction yield was high or low. Adding ligand or substituting a new metal may change the yield of the reaction, but does not provide precise mechanistic information about the rate-determining step in the

catalytic process. However, once the relative rates for various substituents had been measured *under standardized conditions,* we were able to extend our Hammett study to include various catalyst-ligand combinations. In particular, we were interested in determining whether the rate of transmetalation could be enhanced by changing ligands on the palladium. Ligands with different electronic and steric properties[187] might be able to stabilize the transition state **124** (Scheme 4.11) differently and hence affect the rate of transmetalation. By measuring the relative rates between two aryl siloxanes, it should be possible to investigate the role that electronic factors play in the coupling reaction.

As shown in the Table 4.2, entry 1, the best catalyst for the coupling of siloxanes and cyclohexenyl carbonate (**120**) is $Pd(dba)_2$. Changing the catalyst to either $Pd_2(dba)_3$ or $Pd_2(dba)_3 \cdot CHCl_3$ resulted in a considerable decrease in the yield of coupled product. Why the yield is diminished is less clear since all three of these Pd-complexes are thought to behave comparably as Pd(0) sources. On the other hand, the relative rates of *p*-anisoylsiloxane/phenylsiloxane (**121**:**6**) with all three catalyst systems, it was observed that the ratio of 0.42 ± 0.02 was maintained. The result clearly demonstrated that the rate-determining step in the coupling reaction was identical with all three catalysts systems and that another step in the mechanism must be responsible for the diminished yields of product. The effect of various added ligands on the coupling reaction was evaluated and the results are summarized in the Table 4.2.

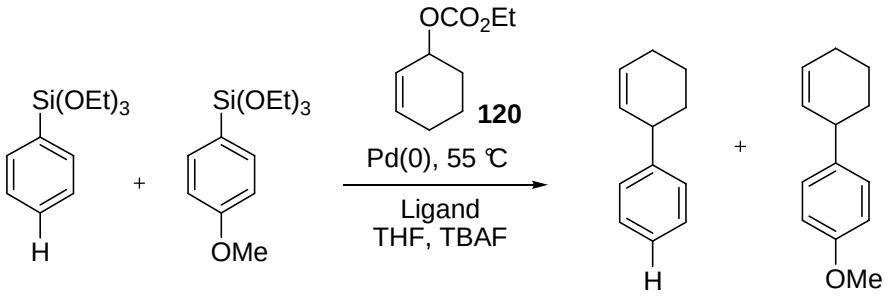

6 **121** **9** **126**

Entry	Pd (0) Source (10 mol %)	Ligand (20 mol %)	Relative Rate	Yield (%)[a]
1	**$Pd(dba)_2$**	**-**	**0.42**	**80**
2	$Pd_2(dba)_3$	-	0.42	63
3	$Pd_2(dba)_3{\cdot}CHCl_3$	-	0.40	61
4	$Pd(dba)_2$	$AsPh_3$	0.39	53
5	$Pd(dba)_2$	$PPh_2(C_6F_5)$	0.42	32
6	$Pd(dba)_2$	PCy_3	0.42	55
7	$Pd(dba)_2$	P(*o*-tolyl)$_3$	0.43	48
8	$Pd(dba)_2$	PPh_3	0.25	<20[b]
9	$Pd(dba)_2$	I	0.33	<20[b]
10	$Pd(dba)_2$	II	-	NA
11	$Pd(dba)_2$	III	-	NA
12	$Pd(dba)_2$	P(2-Fu)$_3$	-	NA
13	$Pd(dba)_2$	-	0.45	79[c]
14	$Pd(dba)_2$	-	0.39	64[d]
15	$Pd(OAc)_2$	PCy_3	0.39	<20[b]
16	$Pd(OAc)_2$	$AsPh_3$	0.44	<20[b]
17	$Pd(OAc)_2$	PPh_3	-	NA
18	$Pd(OAc)_2$	P(2-Fu)$_3$	-	NA
19	Pd_2(dba-4,4'-OMe)$_3$	-	0.39	55
20	Pd(dba-4,4'-CF_3)$_2{\cdot}H_2O$	-	0.41	51

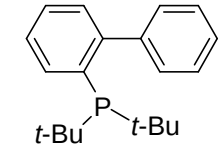

128

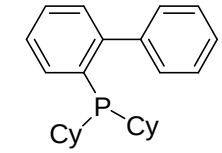

129

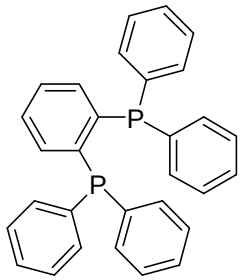

130

[a] Yield determined by gas chromatography using a standard. [b] Yield determined by column chromatography. [c] DMF was used as a solvent. [d] Dioxane was used as a solvent. Note: relative rates and yields in entry 1 are averages of three runs, entries 2-9, 15-16 and 19-20 are averages of two runs. P(2-Fu)$_3$ is tri-2-furylphosphine (TFP).

Table 4.2: Role of ligands in the allyl-aryl coupling reaction

Strongly electron-donating ligands (PCy_3 and P(*o*-tolyl)$_3$, entries 6 and 7) with cone angles significantly greater than triphenylphosphine, gave higher yields of coupled products than triphenylphosphine, respectively, but did not alter the relative rate of arylated products. The larger cone angle of these phosphines would be expected to provide a π-allyl complex with a low coordination number due to steric bulk, thus facilitating transfer of aryl group from the fluoride-activated siloxane. More electron-withdrawing ligands (entries 5 and 12) significantly reduced the yields of coupled product also, but had no effect on the relative rates. $AsPh_3$ (entry 4) gave a better yield of coupled products when compared with PPh_3 (entry 8). Since, the As-Pd bond is longer than the P-Pd bond; the As-Pd complex might be experiencing less steric hindrance from phenyl groups. With stannane derivatives, Farina had also shown that $AsPh_3$ ligand dissociates more readily from palladium intermediates compared to PPh_3, thus enhancing the rate of transmetalation ($>10^3$) compared to PPh_3.[117] Large deviations from the relative rate ratios were observed for the addition of ligands such as PPh_3 and the Buchwald ligand **128**[188,189] (entries 8 and 9). Unfortunately, the yields of coupling products in these systems were so low that it is inappropriate to draw meaningful conclusions about the coupling reactions.

The study of ligand effects on allyl-aryl coupling reaction revealed that Pd(dba)$_2$ in absence of any phosphine ligands is the best catalytic system (Table 4.2, entry 1). It is known that electronic and steric properties of phosphine ligands can be tuned to achieve desired catalytic reactivity. We wondered if the same idea can be applied to design metal-olefin catalysts for our allyl-aryl coupling reaction. As seen in the Figure 4.11, the metal-olefin bond is described as a combination of σ-donation from a filled olefin

π-orbital to an empty metal orbital and π-back donation from a filled metal orbital to an empty olefin π* orbital.[190,191] For an electron rich d^{10}-configuration such as Pd^0, π-back donation from palladium center to olefin is important. Stronger π-back donation results in stronger palladium-olefin bond, thus increasing the stability of palladium complex, but reducing the lability of the olefin ligand. Both the electronic and steric nature of olefins plays an important role in determining the binding affinity to palladium. Electron deficient alkenes are bound more tightly to palladium because of increased π-back-donation. Additionally, strained olefins such as norbornene possess high binding affinity to palladium because of relief of ring strain upon carbon rehybridization and reduction of steric hindrance.[190]

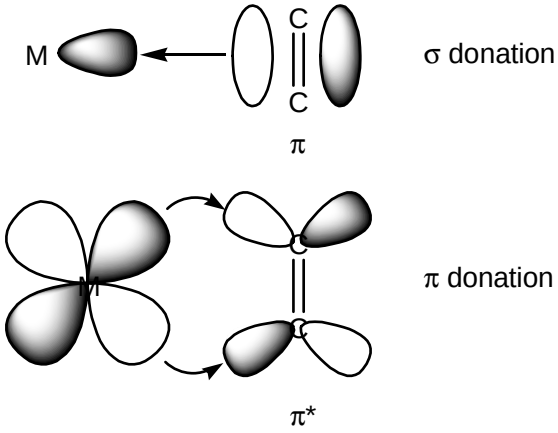

Figure 4.11: Donor-Acceptor model for transition-metal-olefin complexes. Redrawn from ref 190.

The catalytic activity as well as stability of metal-olefin complex can be tuned by adjusting the electronics and sterics of the olefin ligand. It is believed that for most transmetalations an open coordination site is required.[190] We envisioned that an olefin ligand lacking an electron withdrawing group that can readily dissociate from palladium would facilitate transmetalation of the aryl group from silicon to palladium. However, such olefins may also reduce the stability of palladium complex. For example, palladium

complexes such as Pd(norbornene)$_3$, Pd(COD)$_2$ and Pd(ethene)$_3$ are stable only at extremely low temperatures.[192,193]

First, effect of electronic nature of dba (dibenzylideneacetone) ligands (Figure 4.12) on the relative rate of allyl-aryl coupling reaction was studied (Table 4.2, entries 19 and 20). It was anticipated that electron donating groups (OMe) on the dba ligand will destabilize π-back donation compared to more electron withdrawing groups (H, CF_3). This would promote dissocation of dba from the palladium and faciliate transmetaltion. Accordingly, [Pd_2(dba-4,4'-OMe)$_3$] and [Pd(dba-4,4'-CF_3)$_2$·H_2O] catalysts were prepared according to Fairlamb's procedure[194] and a competition experiment of allyl carbonate **120** was performed. The change of electronic character of the dba ligands, respectively, did not change the relative rate; however the yield of coupled product decreased (entries 19 and 20, Table 4.2). In contrast to our coupling results, the Suzuki coupling of aryl chlorides with arylboronic acids performed by Fairlamb showed that electron donating groups on Pd(dba)$_2$ increased the rate of the cross-coupling reaction, relatively to unsubstituted dba (**131**, R = H).[194] Very recently, Fairlamb has reported palladium(0) complexes containing thienyl analogues (**132**, **133**) of dibenzylideneacetone (dba) and evaluated their reactivity in oxidation addition reaction with iodobenzene.[195]

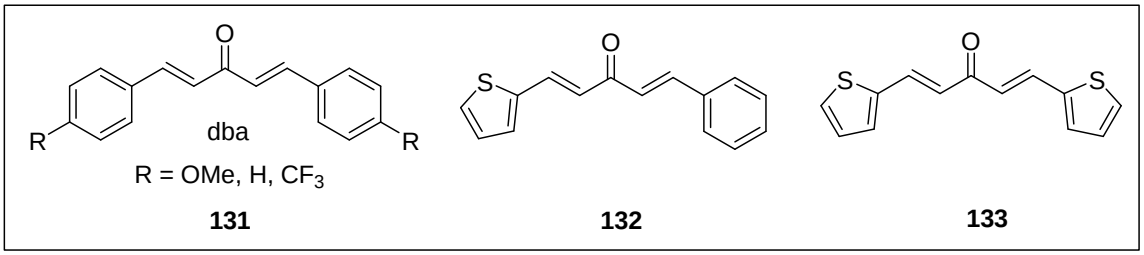

Figure 4.12: Various alkenyl ligands

$Pd_2(dba)_3$ serve as an important precursor for the synthesis of zerovalent palladium complexes bearing additional ligands such as phosphines, nitrogen, sulfur as well as olefins.[112-114,196-208] The stability of these complexes is governed by subtle interplay between electron-donating and electron-withdawing properties of the ligand. Our intial attempts involved preparation of mixed olefin complexes according to the procedure reported by Itoh and co-workers.[112] Itoh prepared mixed olefin complexes of Pd(0) by a ligand substitution of $Pd_2dba_3{\cdot}CHCl_3$. By an appropriate combination of electron-donating and electron-withdrawing olefin ligands it was possible to isolate three-coordinate mixed olefin complexes (**IV**, **IX**, **X**, Figure 4.13). Catalysts **IV**, **IX** and **X**were prepared and used in the aryl-allyl coupling reaction (Table 4.3, entries 1-3).

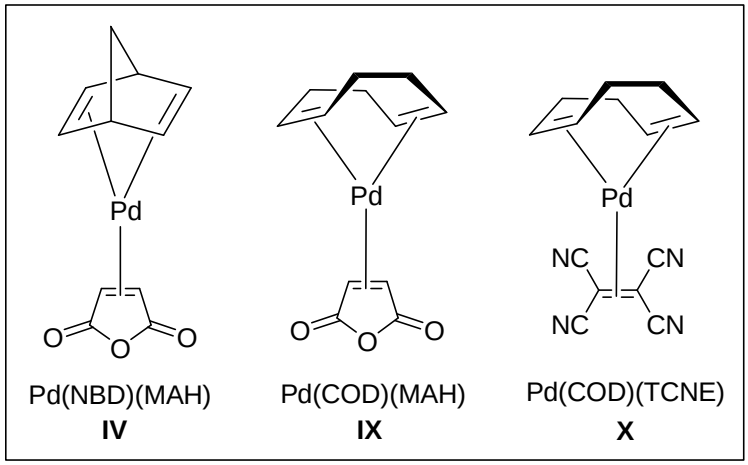

Figure 4.13: Pd(NBD)(MAH), Pd(COD)(MAH) and Pd(COD)(TCNE) complexes

As seen in Table 4.3, replacing olefin MAH (maleic anhydride) with TCNE (tetracyanoethylene), but retaining COD (cyclooctadiene) as diene, reduced the yield of coupled product dramatically (entries 2 and 3). On other hand, by subsituting COD (cyclooctadiene) with NBD (norbornadiene) but retaining MAH improved yield (entries 2 and 4). Interestingly, the catalytic activity of Pd(NBD)(MAH) **IV** and Pd(COD)(MAH)

IX does not correlate to the strain energy of NBD and COD. One would anticpate NBD having larger strain energy compared to COD to bind tighter to the palladium due to the relief of strain and thus be less labile. However, higher yields with Pd(NBD)(MAH) **IV** compared to Pd(COD)(MAH) **IX** suggested NBD to be more labile olefin. This result is constistent with that of Orchad and Weiss who showed despite higher strain energy, NBD bings less strongly to metal (copper or silver) compared to COD and pointed to significance of steric factors.[209,210]

It is important to note that both Pd(NBD)(MAH) **IV** and Pd(COD)(MAH) **IX** catalyzed allyl-aryl coupling reaction even at ambient temperature, which is not the case with $Pd(dba)_2$. This suggests that these catalysts are far more reactive than $Pd(dba)_2$. However they produce lower yields compared to $Pd(dba)_2$ (Table 4.3, entry 1). This can be attributed to instability of these complexes in solution compared to $Pd(dba)_2$. During coupling reaction precipitation of palladium black is observed within 2-3 hrs when using Pd(NBD)(MAH) **IV** and Pd(COD)(MAH) **XI**, but this is not the case with $Pd(dba)_2$. While the preparation of Pd(NBD)(MAH) **IV** was easy, the preparation of Pd(COD)(MAH) **XI** and Pd(COD)(TCNE) **X** was tedious and required careful handling due to their instability (precipitation of palladium black) when exposed to air and ambient temperature. This was also the case with catalysts Pd(cyclopentene)$(MAH)_2$ and Pd(norbornene)MAH_2 which could not be isolated due to extensive decomposition to palladium black.

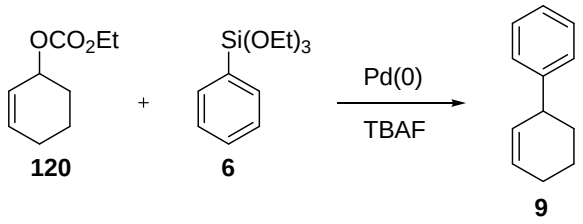

Entry	**Pd(0) (25 mol%)**	**TBAF equiv.**	**Siloxane equiv.**	**Yield (%)**
1	$Pd(dba)_2$	2.0	2.0	70
2	Pd(COD)(MAH)	2.0	2.0	38
3	Pd(COD)(TCNE)	2.0	2.0	17
4	**Pd(NBD)(MAH)[a]**	**2.0**	**2.0**	**54**
5	**Pd(COD)(NQ)**	**2.0**	**2.0**	**48**
6	Pd(COD)(DQ)	2.0	2.0	23
7	Pd(COD)(NQ)	2.0	2.0	41[b]
8	Pd(COD)(NQ)	8.0	8.0	45
9	Pd(COD)(BQ)	2.0	2.0	20
10	$Pd(NBE)_2(BQ)_2$	2.0	2.0	21

All reactions were performed at 55 °C for 24 h. [a] 12 mol% of catalyst used.
[b] Reaction in entry 6 was performed in DMF.

Table 4.3: Optimization of Pd(0)-olefin catalyzed allyl-aryl coupling reaction

The instability of mixed olefin complexes prepared by Itoh limited their application in the allyl-aryl coupling reaction. We next chose to examine Pd(0)-triolefin complexes containing quinones prepared from $Pd_2dba_3{\cdot}CHCl_3$ (Figure 4.14).[113,114] These catalysts are stable at ambient temperature and therefore easy to prepare. When employed in the allyl-aryl coupling reaction, Pd(COD)NQ **V** gave superior yields in comparison to palladium complexes formed using Pd(COD)BQ **XI** and Pd(COD)DQ **XII**, indicating a strong electronic influence on the catalyst's performance. It is interesting to note that subtle changes such as inclusion of aromatic ring (NQ = naphthoquinone) in the catalyst dramatically improve the yield compared to BQ (benzoquinone) and DQ (duroquinone).

Optimization of reaction conditions using Pd(COD)(NQ) **V** showed no improvements in yield. Dinuclear Pd(0) complex possessing BQ as a bridging ligand and NBE (norbornene) as a monodentate ligand was also prepared[114], however, this catalyst **XIII** resulted in poor yield (Table 3, entry 10).

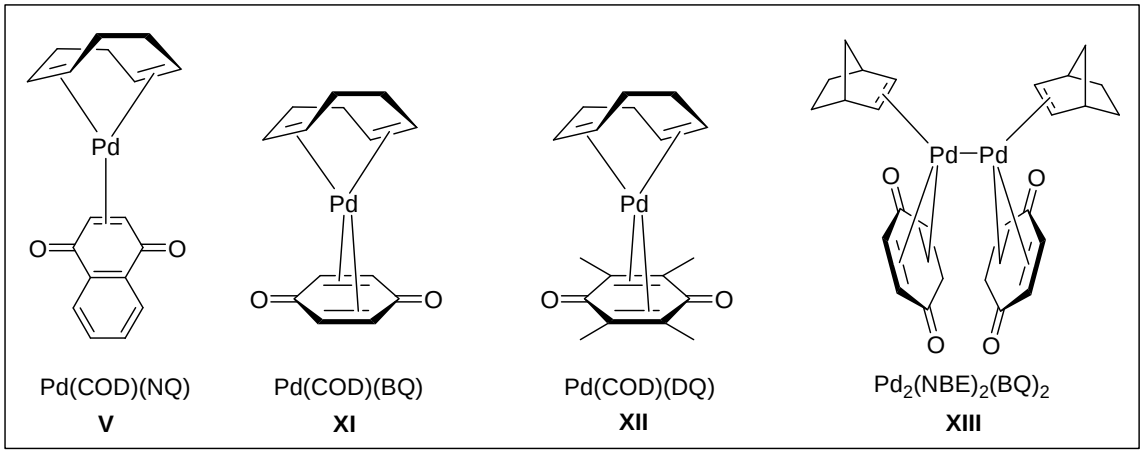

Figure 4.14: Pd(COD)(NQ), Pd(COD)(BQ), Pd(COD)(DQ), $Pd_2(NBE)_2(BQ)_2$ complexes

From the results summarized in Table 4.3, Pd(NBD)(MAH) **IV** and Pd(COD)(NQ) **V** were identified as appropriate cataysts for allyl-aryl coupling reaction using cyclohexenyl carbonate as substrate **120**. Next, these catalysts were applied in the coupling of more complex carbonate **87** with aryl siloxane **6** and siloxane **72**. (Scheme 4.14). It was observed that even stoichiometric amounts of Pd(NBD)(MAH) **IV** gave worse yields (11-13%) compared to Pd(COD)(NQ) **V** for the coupling reaction (Scheme 4.13). Thus, Pd(COD)(NQ) **V** is the best catalyst as of now for the reaction shown in the Scheme 4.14.

Scheme 4.14

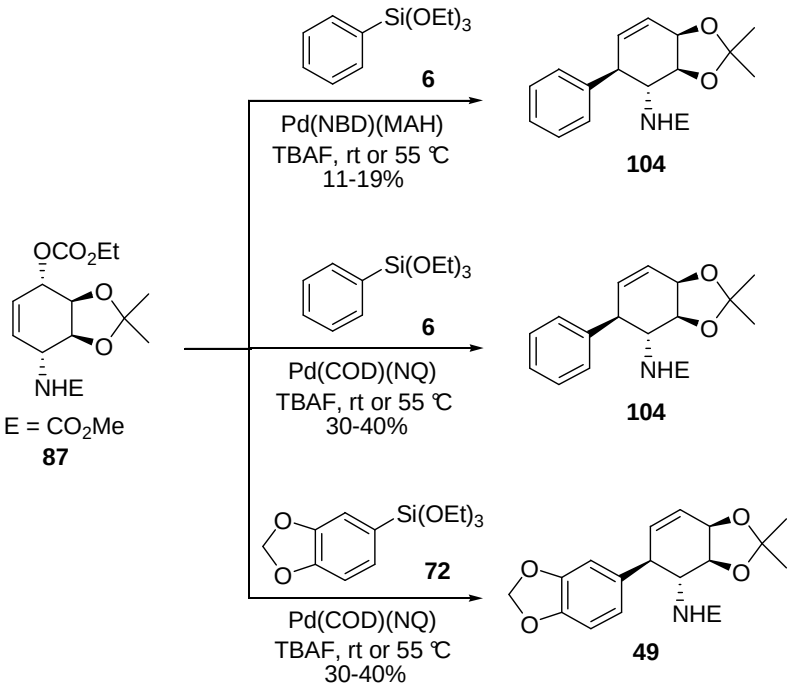

Though $Pd(dba)_2$ works well (70% yield, Table 4.3) with the simple allyl-aryl coupling reaction it does not function in the coupling of complex allyl carbonate **87** with aryl siloxane **72**. This might be because electron withdrawing dba disssociates less readily from the palladium compared to COD, hindering transfer of aryl group to the palladium center. However, Pd(COD)(NQ) results in lower yields compared to $Pd(dba)_2$ in case of cyclohexenyl carbonate (Table 4.3) presumably because of its decompostion to palladium black.

The coupling product **49** is the desired compound for the synthesis of natural product 7-deoxypancratistatin (**24**) (see Chapter 3). The moderate yield of the coupling reaction is one of the drawbacks of this reaction. Future goals would aim at application of different kinds olefin-based catalysts in palladium-catalyzed allylic arylation to optimize the key reaction.

CONCLUSION

Mechanistic studies on coupling reaction of allyl carbonate and aryl siloxane has offered several useful insights;

1. On the basis of Hammett analaysis of allyl-aryl coupling of para-substituted siloxane derivatives with cylcohexenyl carbonate, the rate-determining step of the coupling reaction was identified as either transmetalation or reductive elimination. Furthermore, it was observed that the rate of coupling reaction was enhanced by electron-withdrawing substituents, indicating deveopment of negative charge on the aromatic ring in the transition state of the rate-determining step.
2. Competition studies as a function of ligand type revealed that electronic as well as the steric nature of phosphine ligands on the metal site dramatically affect yield of coupled product, but rarely affect the relative rates of the coupling reaction. This idea was used to explore steric and electronic nature of olefin-based palladium catalyst on allyl-aryl coupling reaction.
3. A new family of catalysts for the siloxane coupling process that overcomes the limitations have been developed. These catalyst are more reactive than $Pd(dba)_2$ which is apparent from their ability to catalyze the reaction at ambient temperature.
4. Tri-olefin-based Pd(0) catalyst, Pd(COD)(NQ) has been succesfully applied in the coupling reaction of complex allyl carbonate **87** with aryl siloxane **72** (Scheme 4.14) to produce much needed coupling product **49** (Hudlicky's intermediate) for the synthesis of natural product 7-deoxypancratistatin (**24**).

EXPERIMENTAL DETAILS

General Methods

All reactions were run under an atmosphere of argon unless otherwise noted. Glassware used in the reactions was dried for a minimum of 12 h in an oven at 120 °C. Tetrahydrofuran was distilled from sodium/benzophenone ketyl, while methylene chloride, pyridine, dimethylformamide and dioxane were distilled from calcium hydride. PPh_3, PCy_3, and 2-(dicyclohexylphosphino)biphenyl were recrystallized from hexanes prior to use. P(*o*-tolyl)$_3$ and P(2-Fu)$_3$ were recrystallized from ethanol. $AsPh_3$, $PPh_2(C_6F_5)$ and 2-(di-*t*-butylphosphino)biphenyl were used as received. [Pd_2(dba-4,4'-OMe)$_3$] and [Pd(dba-4,4'-CF_3)$_2$·H_2O] catalysts were prepared using the procedure reported by Fairlamb.[194] Pd(COD)(TCNE)[112], Pd(COD)(MAH)[112], Pd(NBD)(MAH)[112] Pd(COD)(NQ)[113], Pd(COD)(BQ)[113], Pd(COD)(DQ)[113], $Pd_2(NBE)_2(BQ)_2$[114] were prepared as reported in the literature.

^{19}F NMR and ^{29}Si NMR were recorded on a high field 500 MHz NMR spectrometer. ^{19}F and ^{29}Si chemical shifts are referenced to external standard TFA and TMS respectively. Gas chromatography was performed on a Hewlett Packard 5890 GC equipped with a flame ionization detector using a 25m methyl silicon column.

Allyl carbonate 120

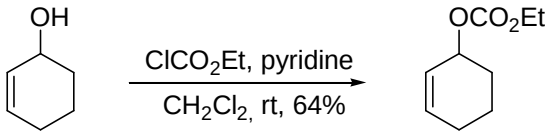

120

To 2.09 g (21.3 mmol, 1.00 equiv.) of commercially available 2-cyclohexen-1-ol in 20.0 mL anhydrous CH_2Cl_2 and 2.57 mL (31.9 mmol, 1.50 equiv.) anhydrous pyridine was added 3.17 mL (31.9 mmol, 1.50 equiv.) of ethyl chloroformate dropwise *via* syringe under argon. The reaction was allowed to stir at room temperature for 7 days. The reaction mixture was extracted with CH_2Cl_2 (3 × 50 mL), washed with H_2O (50 mL), dried over $MgSO_4$ and concentrated *in vacuo*. Flash chromatography on silica gel (5% EtOAc/95% hexane, R_f = 0.51) afforded 2.32 g (64%) of the allyl carbonate **120** as a colorless oil; IR (CCl_4) 3042 (w), 2981 (w), 2947 (m), 2875 (w), 2838 (w), 1737 (s), 1373 (s), 1265 (s), 1017 (s) cm^{-1}; ^1H NMR (400 MHz, $CDCl_3$) δ 5.97-5.93 (m, 1H), 5.77-5.73 (m, 1H), 5.10-5.09 (m, 1H), 4.16 (q, *J* = 7 Hz, 2H), 2.05 (m, 1H), 2.05-1.98 (m, 1H), 1.88-1.80 (m, 3H), 1.62 (m, 1H), 1.28 (t, *J* = 7 Hz, 3H); ^{13}C NMR (100 MHz, $CDCl_3$) δ 154.8, 133.2, 125.0, 71.5, 63.6, 28.2, 24.8, 18.5, 14.2. The spectral data (^1H NMR) were identical to that reported in the literature.[211]

General procedure for competition experiments for allyl-aryl coupling reaction (Table 4.2)

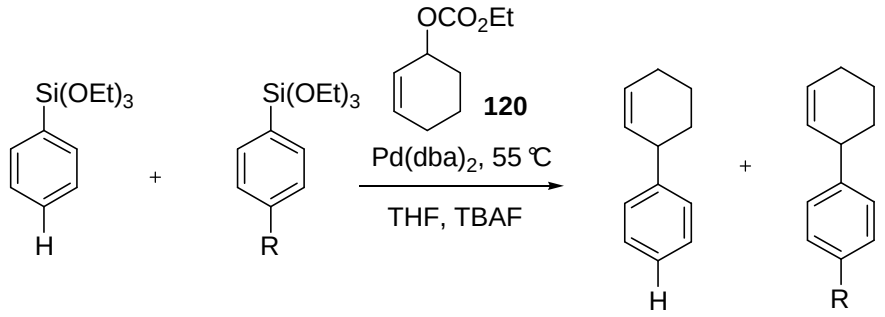

To 121 mg (0.712 mmol, 1.00 equiv.) of allyl carbonate **120**, 342 mg (1.42 mmol, 2.00 equiv.) of aryl siloxane **6** and 383 mg (1.42 mmol, 2.00 equiv.) of *p*-anisoylsiloxane **121** (R = OMe) dissolved in 4.00 mL of anhydrous THF was added 40.9 mg (0.0712 mmol, 0.100 equiv.) of $Pd(dba)_2$ under an atmosphere of argon. This was followed by addition of 2.84 mL (2.84 mmol, 4.00 equiv.) of 1 M TBAF solution in THF and the reaction mixture was stirred at 55 °C for 24 h. The product was extracted with 5 × 20 mL Et_2O and washed with 20 mL H_2O. The combined organic layers were dried over $MgSO_4$ and concentrated *in vacuo* to give coupling products **9** (R = H) and **126** (R = OMe). The crude product was filtered through a short silica plug. The relative quantity of 0.44 for *p*-anisoylsiloxane **121** (R = OMe) was determined from the amount of methoxyphenylcyclohexene **126** (R = OMe) obtained relative to phenylcyclohexene **9** using GC (gas chromatography). The same experimental procedure was used to determine relative rates of different aryl siloxanes **121**. Moreover, effects of different catalysts, ligands and solvents on the relative rate of transmetalation were examined

(Table 4.2), using analogous competition experiments, where yields were determined by GC using standard unless otherwise noted.

Aryl siloxanes 121

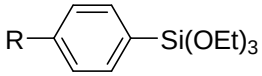

121

R = OMe, Me, Cl, CO_2Et

p-anisoylsiloxane (R = OMe), *p*-tolylsiloxane (R = Me), and *p*-chlorophenylsiloxane (R = Cl) were prepared from commercially available *p*-bromoansiole, *p*-bromotoluene and *p*-chloroiodobenzene respectively according to the procedure previously reported by DeShong and Manoso.[20,212] *p*-Carboethoxyphenylsiloxane (R = CO_2Et) was prepared from ethyl-4-iodobenozate by Masuda's procedure.[213] The ^{1}H NMR spectral data of aryl siloxanes **121** (R = OMe[212], R = Me[212], R = Cl[20], R = CO_2Et[213]) were identical to that reported in the literature.

Alkene (9, 126)

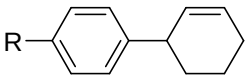

9 R = H

126 R = OMe, Me, Cl, CO_2Et

The spectral data of phenylcyclohexene[214] **9**, methoxyphenylcyclohexene.[32,215] (**126**, R = OMe), methylphenylcyclohexene[32,33] **(126**, R = Me), chlorophenylcyclohexene[32,33] (**126**, R = Cl) and carboethoxyphenylcyclohexene[33] **126** (R = CO_2Et) matched to those previously reported in the DeShong group.

General procedure for allyl-aryl coupling using Tri-olefin-based Pd(0) catalysts (Table 4.3)

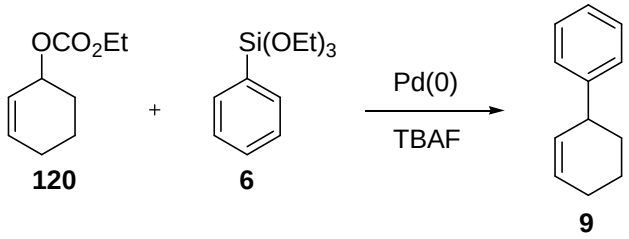

To 76.5 mg (0.450 mmol, 1.00 equiv.) of allyl carbonate **120**, 216 mg (0.900 mmol, 2.00 equiv.) of aryl siloxane **6** in 4.00 mL of anhydrous THF was added 41.9 mg (0.113 mmol, 0.250 equiv.) of Pd(COD)(NQ) under an atmosphere of argon. This was followed by addition of 0.900 mL (0.900 mmol, 2.00 equiv.) of 1 M TBAF solution in THF and the reaction mixture was stirred at 55 °C for 24 h. The product was extracted with 5 × 25 mL Et_2O and washed with 25 mL H_2O. The combined organic layers were dried over $MgSO_4$ and concentrated *in vacuo* to give crude cyclohexene **9**. Purification by column chromatography (100% pentane; R_f = 0.65) rendered 37.0 mg (52%) of cyclohexene **9** as a colorless oil. ^{1}H NMR (400 MHz, $CDCl_3$) δ 7.31-7.27 (m, 2H), 7.22-7.18 (m, 3H), 5.89-5.86 (m, 1H), 5.72-5.69 (m, 1H), 3.41-3.38 (m, 1H), 2.08-1.99 (m, 3H), 1.74-1.71 (m, 1H), 1.61-1.53 (m, 2H); The NMR spectrum was identical to the literature.[214]

Formation of hypercoordinate silicates

Triethoxyphenylsilane (0.18 mmol, 43 mg) was mixed with 1 M TBAF (0.18 mmol, 0.18 mL) in 0.50 mL THF and ^{19}F NMR spectrum was recorded after 10 minutes at 29 °C. ^{19}F spectrum indicated two major resonances at δ -121 and -127 and two minor resonances at δ -113 and -128 (see Figure 1, (b)). After 1 h, TBAF and siloxane mixture was cooled to -28 °C. Upon cooling, the ^{19}F signal at δ -121 sharpened, showing silicon satellites (J_{Si-F} = 207 Hz). ^{19}F NMR spectrum of hypercoordinate silicates is provided in Chapter 4, Figure 4.8. While ^{19}F NMR was obtained at 0.36 mM concentration, ^{19}Si NMR required higher concentration (3 × 0.36 mM) and longer time (18 h). The chemical shift of triplet at δ -129 ppm indicates hypercoordinate silicate anion, J_{Si-F} = 207 Hz.

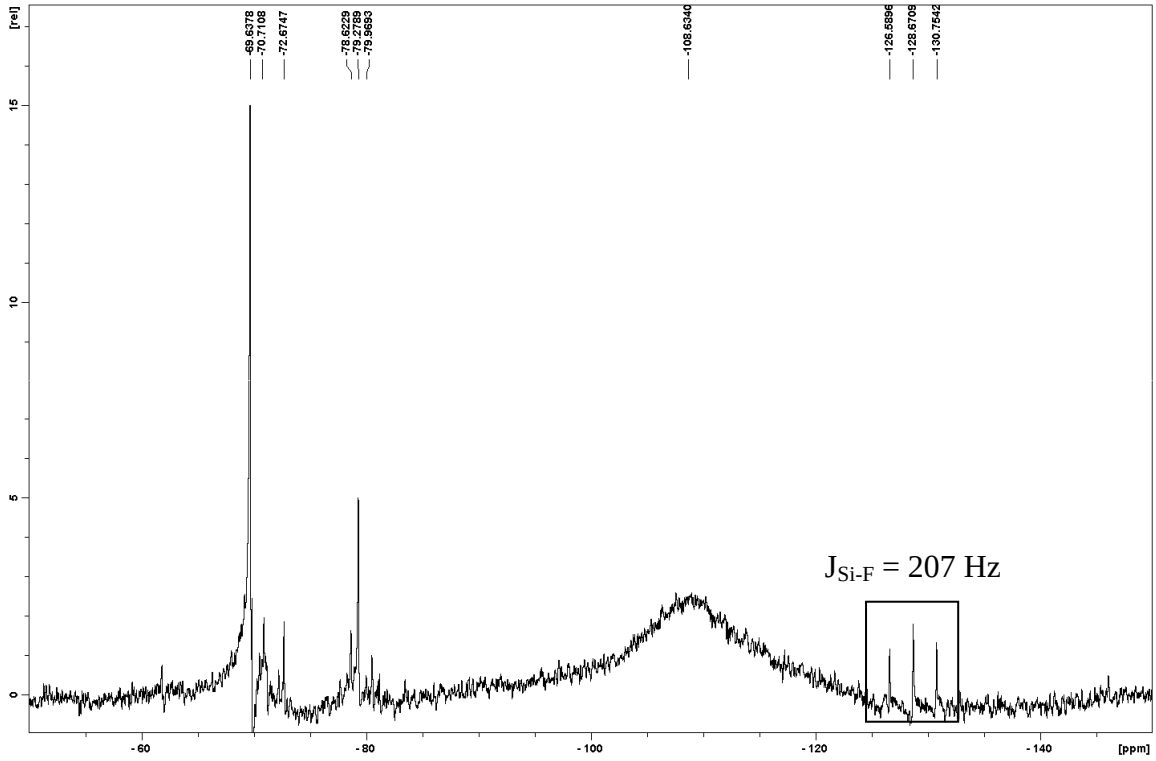

Figure 4.15: ^{29}Si NMR spectrum of silicate formation at -28 °C.

Based on ^{19}F and ^{29}Si NMR, we have tentatively assigned conformationally stable bis-fluorosilicate derivative **135** or **136** as the hypercoordinate arylfluorosilicate which arises from conformationally mobile mono-fluorosilicate **134** (Scheme 4.15). The ^{19}F and ^{29}Si NMR spectra and coupling constant are consistent with that of TBAT, previously characterized by the DeShong group. Additionally, it was observed that bis-fluorosilicate when reacted with allyl carbonate **120**, gave coupled product in 60% yield.

Scheme 4.15

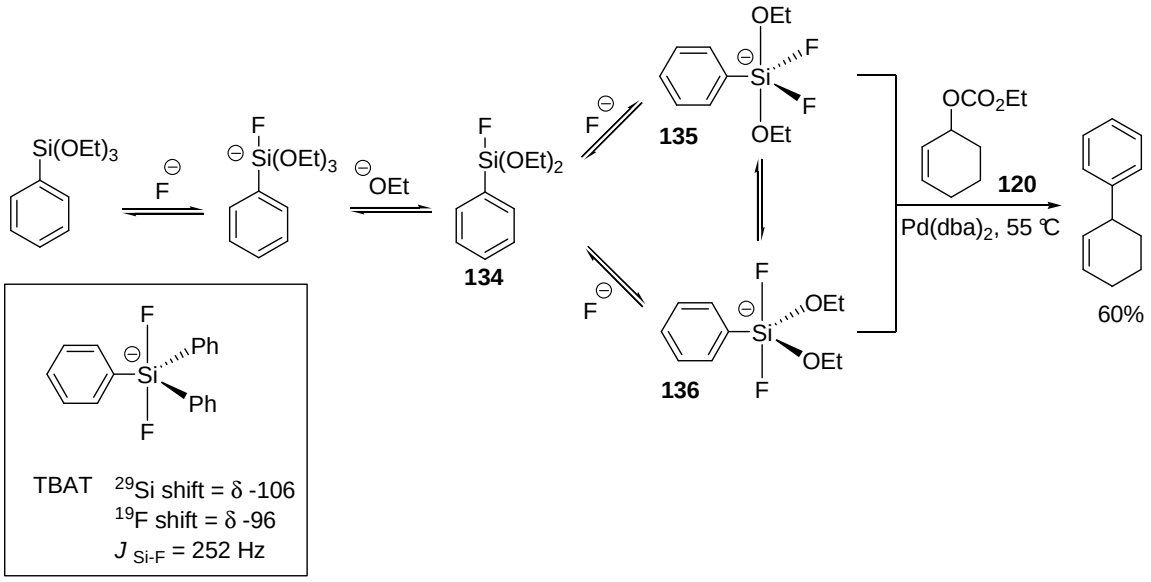

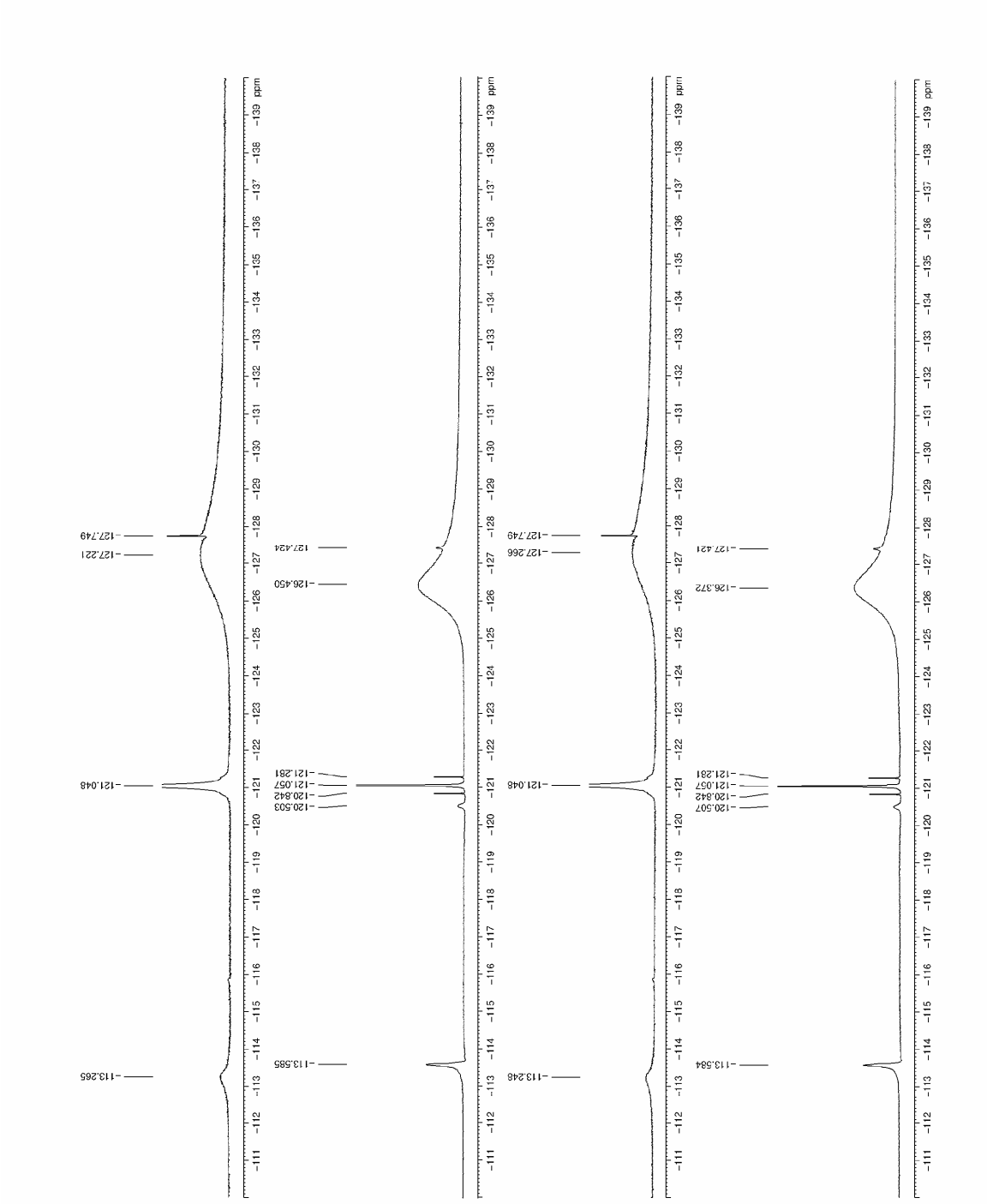

Figure 4.16: Effect of temperature on silicate formation (^{19}F NMR spectrum). Mixture of TBAF and phenyltriethoxysilane (a) 10 min, at rt. (b) 2 h 25 min, at -30 °C. (c) 2 h 40 min, at rt. (d) 4 h 55 min, at -30 °C.

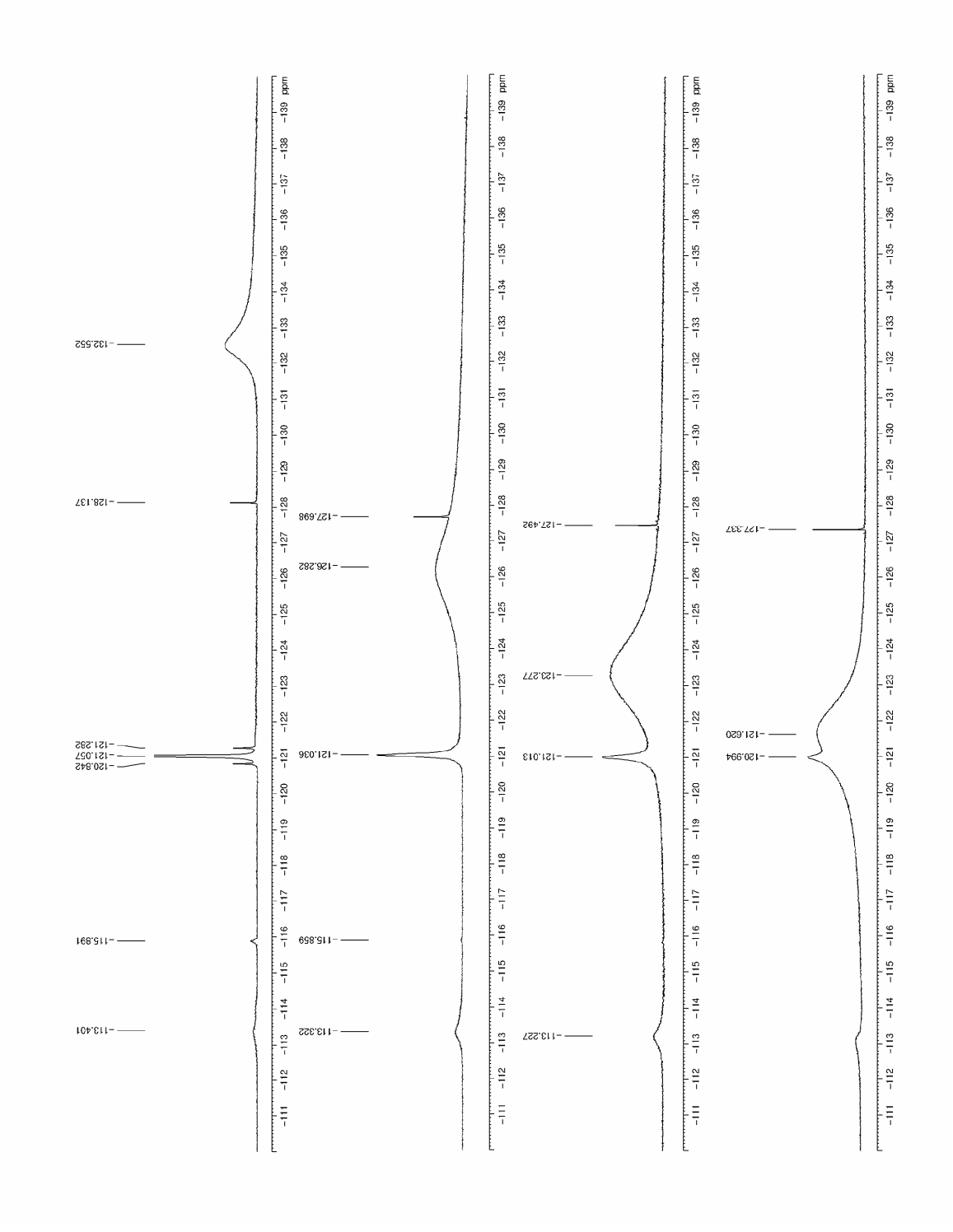

Figure 4.17: Effect of TBAF concentration on silicate formation (^{19}F NMR spectrum) (a) 0.5 equiv. TBAF, 1.0 equiv. siloxane. (b) 1.0 equiv. TBAF, 1.0 equiv. siloxane. (c) 1.5 equiv. TBAF, 1.0 equiv. siloxane. (d) 2.0 equiv. TBAF, 1.0 equiv. siloxane.

REFERENCES

1. Diederich, F.; Stang, P. J., Eds. *Metal-catalyzed cross-Coupling Reactions*. Wiley-VCH: New York, 1998.

2. Tsuji, J., Eds. *Palladium Reagents and Catalysts. Innovations in Organic Synthesis*; John Wiley & Sons: New York, 1995.

3. Stille, J. K. *Pure Appl. Chem.* **1985**, *57*, 1771-1780.

4. Miyaura, N.; Suzuki, A. *Chem Rev*. **1995**, *95*, 2457-2483.

5. Hiyama, T. *J. Org. Chem.* **1988**, *53*, 918-920.

6. Hiyama, T.; E. Shirakawa, E. *Top. Curr. Chem.* **2002**, *219*, 61-85.

7. Hatanaka, Y.; Goda, K.; Okahara, Y. *Tetrahedron* **1994**, *50*, 8301-8316.

8. Hiyama, T.; Hatanaka, Y. *Pure Appl. Chem*. **1994**, *66*, 1471-1478.

9. Horn, K. A. *Chem. Rev.* **1995**, *95*, 1317-1350.

10. Hiyama, T. *J. Organomet. Chem.* **2002**, *653*, 58-61.

11. Denmark, S. E.; Sweis, R. F. *Acc. Chem. Res.* **2002**, *35*, 835-846.

12. Mowery, M. E.; DeShong, P. *J. Org. Chem.* **1999**, *64*, 3266-3270.

13. Mowery, M. E.; DeShong, P. *J. Org. Chem.* **1999**, *64*, 1684-1688.

14. Mowery, M. E.; DeShong, P. *Org. Lett.* **1999**, *1*, 2137-2140.

15. DeShong, P.; Handy, C. J.; Mowery, M. E. *Pure Appl. Chem.* **2000**, *72*, 1655-1658.

16. Seganish, W. M.; DeShong, P. *J. Org. Chem.* **2004**, *69*, 1137-1143.

17. Lee, H. M.; Nolan, S. P. *Org. Lett.* **2000**, *2*, 2053-2055.

18. Wolf, C.; Lerebours, R. *Org. Lett.* **2004**, *6*, 1147-1150.

19. Clarke, M. L. *Adv. Synth. Catal.* **2005**, *347*, 303-307.

20. Manoso, A. S.; DeShong, P. *J. Org. Chem.* **2001**, *66*, 7449-7455.

21. Riggleman, S.; DeShong, P. *J. Org. Chem*. **2003**, *68*, 8106-8109.

22. Denmark, S. E.; Sweis, R. F. *J. Am. Chem. Soc.* **2001**, *123*, 6439-6440.

23. Denmark, S. E.; Ober, M. H. *Adv. Synth. Catal.* **2004**, *346*, 1703-1714.

24. Denmark, S. E.; Smith, R. C.; Chang, W. T.; Muhuhi, J. M. *J. Am. Chem. Soc.* **2009**, *131*, 3104-3118.

25. Denmark, S. E.; Regens, C. S. *Acc. Chem. Res.* **2008**, *41*, 1486-1499.

26. Trost, B. M.; Van Vranken, D. L. *Chem. Rev*. **1996**, *96*, 395-422.

27. Hiyama, T.; Hatanaka, Y.; Mori, A.; Matsuhashi, H.; Asai, S.; Hirabayashi, K. *Bull. Chem. Soc. Jpn*. **1997**, *70*, 1943-1952.

28. Nakao, Y.; Ebata, S.; Chen, J.; Imanaka, H.; Hiyama, T. *Chem. Lett*. **2007**, *36*, 606-607.

29. Brescia, M. R.; DeShong, P. *J. Org. Chem.* **1998**, *63*, 3156-3157.

30. Brescia, M. R.; Shimshock, Y. C.; DeShong, P. *J. Org. Chem.* **1997**, *62*, 1257-1263.

31. Hoke, M. E.; Brescia, M. R.; Bogacyzk, S.; DeShong, P.; King, B. W.; Crimmins, M. T. *J. Org. Chem.* **2002**, *67*, 327-335.

32. Correia, R.; DeShong, P. *J. Org. Chem.* **2001**, *66*, 7159-7165.

33. Correia, R. Ph.D. Dissertation, University of Maryland, College Park, MD, 2003.

34. Bogaczyk, S. Ph.D. Dissertation, University of Maryland, College Park, MD, 2002.

35. Dey, R.; Chattopadhyay, K.; Ranu, B. C. *J. Org. Chem.* **2008**, *73*, 9461-9464.

36. Kabalka, G. W.; Dong, G.; Venkataiah, B.; Chen, C. *J. Org. Chem.* **2005**, *70*, 9207-9210.

37. Legros, J. Y.; Fiaud, J. C. *Tetrahedron Lett*. **1990**, *31*, 7453-7456.

38. Moreno-Mañas, M.; Pajuelo, F.; Pleixats, R. *J. Org. Chem.* **1995**, *60*, 2396-2397.

39. Uozumi, Y.; Danjo, H.; Hayashi, T. *J. Org. Chem.* **1999**, *64*, 3384-3388.

40. Ramnauth, J.; Poulin, O.; Rakhit, S.; Maddaford, S. P. *Org. Lett.* **2001**, *3*, 2013-2015.

41. Bouyssi, D.; Gerusz, V.; Balme, G. *Eur. J. Org. Chem.* **2002**, 2445-2448.

42. Ortar, G. *Tetrahedron Lett*. **2003**, *43*, 4311-4314.

43. Mino, T.; Kajiwara, K.; Shirae, Y.; Sakamoto, M.; Fujita, T. *Synlett* **2008**, 2711-2715.

44. Ohmiya, H.; Makida, Y.; Tananka, T.; Sawamura, M. *J. Am. Chem. Soc.* **2008**, *130*, 17276-17277.

45. Singh, R.; Viciu, M. S.; Kramareva, N.; Navarro, O.; Nolan, S. P. *Org. Lett.* **2005**, *7*, 1829-1832.

46. Nájera, C.; Gil-Moltó, J.; Karlström, S. *Adv. Synth. Catal.* **2004**, *346*, 1798-1811.

47. Alacid, E.; Nájera, C. *Org. Lett.* **2008**, *10*, 5011-5014.

48. Manabe, K.; Nakada, K.; Aoyama, N.; Kobayashi, S. *Adv. Synth. Catal*. **2005**, *347*, 1499-1503.

49. Kayaki, Y.; Koda, T.; Ikariya, T. *Eur. J. Org. Chem.* **2004**, 4989-4993.

50. Tsukamoto, H.; Sato, M.; Kondo, Y. *Chem. Commun*. **2004**, 1200-1201.

51. Kabalka, G. W.; Dong, G.; Venkataiah, B.; *Org. Lett.* **2003**, *5*, 893-895.

52. Kabalka, G. W.; Dadush, E.; Al-Masum, M. *Tetrahedron Lett*. **2006**, *47*, 7459-7461.

53. Kabalka, G. W.; Al-Masum, M. *Org. Lett.* **2006**, *8*, 11-13.

54. Chung, K.-G.; Miyake, Y.; Uemura, S. *J. Chem. Soc.; Perkin Trans. 1*, **2000**, 15-18.

55. Hansen, A. L.; Ebran, J.-P.; Gøgsig, T. M.; Skrydstrup, T. *J. Org. Chem.* **2007**, *72*, 6464-6472.

56. Menard, F.; Chapman, T. M.; Dockendorff, C.; Lautens, Mark. *Org. Lett.* **2006**, *8*, 4569-4572.

57. Stille, J. K.; Hegedus, L. S.; Del Valle, L. *J. Org. Chem.* **1990**, *55*, 3019-3023.

58. Castaño, A. M.; Echavarren, A. M. *Tetrahedron Lett*. **1996**, *37*, 6587-6590.

59. Kurosawa, H.; Kajimaru, H.; Ogoshi, S.; Yoneda, H.; Miki, K.; Kasai, N.; Murai, S.; Ikeda, I. *J. Am. Chem. Soc.* **1992**, *114*, 8417-8424.

60. Crawforth, C. M.; Burling, S.; Fairlamb, I. J. S.; Taylor, R. J. K.; Whitwood, A. C. *Chem. Commun*. **2003**, 2194-2195.

61. Shipe, W. D.; Sorensen, E. J. *Org. Lett.* **2002**, *4*, 2063-2066.

62. Nicolaou, K. C.; Koftis, T. V.; Vyskocil, S.; Petrovic, G.; Tang, W.; Frederick, M. O.; Chen, D. Y.-K.; Li, Y.; Ling, T.; Yamada, Y. M. A. *J. Am. Chem. Soc.* **2006**, *128*, 2859-2872.

63. Pettit, G. R.; Gaddamidi, V.; Cragg, G. M.; Herald, D. L.; Sagawa, Y. *J. Chem. Soc, Chem. Commun.* **1984**, 1693-1694.

64. Ghosal, S.; Singh, S.; Kumar, Y.; Srivastava, R. S. *Phytochemistry* **1989**, *28*, 611-613.

65. Gabrielsen, B.; Monath, T. P.; Huggins, J. W.; Kefauver, D. F.; Pettit, G. R.; Groszek, G.; Hollingshead, M.; Kirsi, J. J.; Shannon, W. M.; Schubert, E. M.; DaRe, J.; Ugarkar, B.; Ussery, M. A.; Phelan, M. J. *J. Nat. Prod.* **1992**, *55*, 1569-1581.

66. Hudlicky, T.; Moser, M.; Banfield, S. C.; Rinner, U.; Chapuis, J.-C.; Pettit, G. R. *Can. J. Chem.* **2006**, *84*, 1313-1337.

67. Pettit, G. R.; Gaddamidi, V.; Herald, D. L.; Singh, S. B.; Cragg, G. M.; Schmidt, J. M.; Boettner, F. E.; Williams, M.; Sagawa, Y. *J. Nat. Prod.* **1986**, *49*, 995-1002.

68. Pettit, G. R.; Pettit III, G. R.; Bachaus, R. A.; Boyd, M. R.; Meerow, A. W. *J. Nat. Prod.* **1993**, *56*, 1682-1687.

69. Pandey, S.; Kekre, J.; Naderi, J.; McNulty, J. *Artif. Cells, Blood Substitutes, Immobilization Biotechnol.* **2005**, *33*, 279-295.

70. Kekre, N.; Griffin, C.; McNulty, J.; Pandey, S. *Cancer Chem Pharmacol.* **2005**, *56*, 29-38.

71. Griffin, C.; McNulty, J.; Hamm, C.; Pandey, S. In *Cell Apoptosis Research Trends*; Zhang, C. V., Ed.; Nova Science Publishers, Inc. 2007, pp 93-109.

72. Andersen, M. H.; Becker, J. C.; Straten, P. *Nat. Rev. Drug Discov*. **2005**, *4*, 399-409.

73. Rinner, U.; Hudlicky, T. *Synlett.* **2005**, *3*, 365-387 and references therein.

74. Chapleur, Y.; Chrétien, F.; Ahmed, U.; Khaldi, M. *Curr. Org. Synth.* **2006**, *3*, 341-378 and references therein.

75. Manpadi, M.; Kornienko, A. *Org. Prep. Proced. Int*. **2008**, *40*, 107-161 and references therein.

76. Kornieno, A.; Evidente, A. *Chem. Rev.* **2008,** *108*, 1982-2014 and references therein.

77. Danishefsky, S.; Lee, J. Y. *J. Am. Chem. Soc*. **1989**, *111*, 4829-4837.

78. Tian, X.; Hudlicky, T.; Königsberger, K. *J. Am. Chem. Soc*. **1995**, *117*, 3643-3644.

79. Trost, B. M.; Pulley, S. R. *J. Am. Chem. Soc*. **1995**, *117*, 10143-10144.

80. Hudlicky, T.; Tian, X.; Königsberger, K.; Maurya, R.; Rouden, J.; Boreas, F. *J. Am. Chem. Soc*. **1996**, *118*, 10752-10765.

81. Doyle, T. J.; Hendrix, M.; VanDerveer, D.; Javanmard, S.; Haseltine, J. *Tetrahedron* **1997**, *53*, 11153-11170.

82. Magnus, P.; Sebhat, I. K. *Tetrahedron* **1998**, *54*, 15509-15524.

83. Rigby, J. H.; Maharoof, U. S. M.; Mateo, M. E. *J. Am. Chem. Soc*. **2000**, *122*, 6624-6628.

84. Pettit, G. R.; Melody, N.; Herald, D. L. *J. Org. Chem*. **2001**, *66*, 2583-2587.

85. Ko, H.; Kim, E.; Park, J. E.; Kim, D.; Kim, S. *J. Org. Chem*. **2004**, *69*, 112-121.

86. Li, M.; Wu, A.; Zhou, P. *Tetrahedron Lett*. **2006**, *47*, 3707-3710.

87. Tian, X.; Maurya, R.; Königsberger, K.; Hudlicky, T. *Synlett*. **1995**, *11*, 1125-1126.

88. Chida, N.; Jitsuoka, M.; Yamamoto, Y.; Ohtsuka, M.; Ogawa, S. *Heterocycles*, **1996**, *43*, 1385-1389.

89. Keck, G. E.; McHardy, S. F.; Murry, J. A. *J. Org. Chem*. **1999**, *64*, 4465-4476.

90. Keck, G. E.; Wager, T. T.; McHardy, S. F. *J. Org. Chem.* **1998**, *63*, 9164-9165.

91. Aceña, J. L.; Arjona, O.; León, M. L.; Plumet, J. *Org. Lett.* **2000**, *2*, 3683-3686.

92. Håkansson, A. E.; Palmelund, A.; Holm, H.; Madsen, R. *Chem. Eur. J.* **2006**, *12*, 3243-3253.

93. Padwa, A.; Zhang, H. *J. Org. Chem.* **2007**, *72*, 2570-2582.

94. Lopes, R. S. C.; Lopes, C. C.; Heathcock, C. H. *Tetrahedron Lett*. **1992**, *33*, 6775-6778.

95. Friestad, G. K.; Branchaud, B. P. *Tetrahedron Lett*. **1997**, *38*, 5933-5936.

96. Grubb, L. M.; Dowdy, A. L.; Blanchette, H. S.; Friestad, G. K.; Branchaud, B. P. *Tetrahedron Lett*. **1999**, *40*, 2691-2694.

97. Ibn Ahmed, S.; Chrétien, F.; Chapleur, Y.; Hajjaj, N. *Heterocycl. Commun*. **1997**, *3*, 135-138.

98. Hudlicky, T.; Rinner, U.; Gonzalez, D.; Akgün, H.; Schilling, S.; Siengalewicz, P.; Martinot, T. A.; Pettit, G. R. *J. Org. Chem*. **2002**, *67*, 8726-8743.

99. Chida, N.; Ohtsuka, M.; Ogawa, S. *Tetrahedron Lett*. **1991**, *32*, 4525-4528.

100. Banwell, M. G.; Cowden, C. J.; Gable, R. W. *J. Chem. Soc. Perkin Trans. 1* **1994**, 3515-3518.

101. Pandey, G.; Balakrishnan, M.; Swaroop, P. S. *Eur. J. Org. Chem*. **2008**, 5839-5847.

102. Pandey, G.; Murugan, A.; Balakrishnan, M. *Chem. Commun*. **2002**, 624-625.

103. Jenkins, N. E.; Ware, R. W.; Atkinson, R. N.; King, S. B. *Synth.Commun*. **2000**, *30*, 947-953.

104. Tranmer, G. K.; Tam, W. *Org. Lett*. **2002**, *4*, 4101-4104.

105. Jonasson, C.; Kritikos, M.; Bäckvall, J.-E.; Szabó, K. *Chem. Eur. J.* **2000**, *6*, 432-436 and references therein.

106. Chern, M.-S.; Li, W.-R. *Tetrahedron Lett.* **2004**, *45*, 8323-8326.

107. Castillo, P.; Rodriguez-Ubis, J. C.; Rodriguez, F. *Synthesis* **1986**, 839-840.

108. Kelly, T. R. *J. Org. Chem*. **1972**, *37*, 3393-3397.

109. Paulsen, H.; Stubbe, M. *Liebigs Ann. Chem*. **1983**, 535-556.

110. Shukla, K. H.; Boehmler, D. J.; Bogacyzk, S.; Duvall, B. R.; Peterson, W. A.; McElroy, W. T.; DeShong, P. Org. Lett. 2006, 8, 4183-4186.

111. Yang, N.-C.; Chen, M.-J.; Chen, P. *J. Am. Chem. Soc*. **1984**, *106*, 7310-7315.

112. Itoh, K.; Ueda, F.; Hirai, K.; Ishii, Y. *Chem. Lett*. **1977**, 877-880.

113. Hiramatsu, M.; Shiozaki, K.; Fujinami, T.; Sakai, S. *J. Organomet. Chem.* **1983**, *246*, 203-211.

114. Yamamoto, Y.; Ohno, T.; Itoh, K. *Organometallics* **2003**, *22*, 2267-2272.

115. Labadie, J. W.; Stille, J. K. *J. Am. Chem. Soc*. **1983**, *105*, 669-670.

116. Labadie, J. W.; Stille, J. K. *J. Am. Chem. Soc*. **1983**, *105*, 6129-6137.

117. Farina, V.; Krishnan, B. *J. Am. Chem. Soc*. **1991**, *113*, 9585-9595.

118. Louie, J.; Hartwig, J. F. *J. Am. Chem. Soc.* **1995**, *117*, 11598-11599.

119. Amatore, C.; Bahsoun, A. A.; Jutand, A.; Meyer, G.; Ntepe, A. N.; Ricard, L. *J. Am. Chem. Soc.* **2003**, *125*, 4212-4222.

120. Casado, A. L.; Espinet, P. *J. Am. Chem. Soc*. **1998**, *120*, 8978-8985.

121. Casado, A. L.; Espinet, P.; Gallego, A. M. *J. Am. Chem. Soc*. **2000**, *122*, 11771-11782.

122. Espinet, P.; Echavarren, A. M. *Angew. Chem. Int. Ed.* **2004**, *43*, 4704-4734.

123. Casares, J. A.; Espinet, P.; Salas, G. *Chem. Eur. J.* **2002**, *8*, 4843-4853.

124. Itami, K.; Kamei, T.; Yoshida, J. *J. Am. Chem. Soc.* **2001**, *123*, 8773-8779.

125. Crisp, G. T.; Gebauer, M. G. *Tetrahedron Lett*. **1995**, *36*, 3389-3392.

126. Kakusawa, N.; Yamaguchi, K.; Kurita, J. *J. Organomet. Chem.* **2005**, *690*, 2956-2966.

127. Crociani, B.; Antonaroli, S.; Canovese, L.; Uguagliati, P.; Visentin, F. *Eur. J. Inorg. Chem.* **2004**, 732-742.

128. Antonella, R.; Lo Sterzo, C. *J. Organomet. Chem.* **2002**, *653*, 177-194.

129. Nilsson, P.; Puxty, G.; Wendt, O. F. *Organometallics* **2006**, *25*, 1285-1292.

130. Clarke, M. L.; Heydt, M. *Organometallics* **2005**, *24*, 6475-6478.

131. Álvarez, R.; Faza, O. N.; de Lera, Á. R.; Cárdenas, D. J. *Adv. Synth. Catal.* **2007**, *349*, 887-906.

132. Álvarez, R.; Perez, M.; Faza, O. N.; de Lera, Á. R. *Organometallics* **2008**, *27*, 3378-3389.

133. Ariafard, A.; Lin, Z.; Fairlamb, I. J. S. *Organometallics* **2006**, *25*, 5788-5794.

134. Napolitano, E.; Farina, V.; Persico, M. *Organometallics* **2003**, *22*, 4030-4037.

135. Nova, A.; Ujaque, G.; Maseras, F.; Lledós, A.; Espinet, P. *J. Am. Chem. Soc*. **2006**, *128*, 14571-14578.

136. Miyaura, N. *J. Organomet. Chem*. **2002**, *653*, 54-57.

137. Ridgway, B. H.; Woerpel, K. A. *J. Org. Chem*. **1998**, *63*, 458-460.

138. Matos, K.; Soderquist, J. A. *J. Org. Chem.* **1998**, *63*, 461-470.

139. Braga, A. A. C.; Morgon, N. H.; Ujaque, G.; Lledós, A.; Maseras, F. *J. Organomet. Chem.* **2006**, *691*, 4459-4466.

140. Sicre, C.; Braga, A. A. C.; Maseras, F.; Cid, M. M. *Tetrahedron* **2008**, *64*, 7437-7443.

141. Braga, A. A. C.; Ujaque, G.; Maseras, F. *Organometallics* **2006**, *25*, 3647-3658.

142. Braga, A. A. C.; Morgon, N. H.; Ujaque, G.; Maseras, F. *J. Am. Chem. Soc*. **2005**, *127*, 9298-9307.

143. Goossen, L. J.; Koley, D.; Hermann, H. L.; Thiel, W. *Organometallics* **2006**, *25*, 54-67.

144. Sumimoto, M.; Iwane, N.; Takahama, T.; Sakaki, S. *J. Am. Chem. Soc*. **2004**, *126*, 10457-10471.

145. Hatanaka, Y.; Hiyama, T. *J. Org. Chem.* **1988**, *53*, 918-920.

146. Hatanaka, Y.; Hiyama, T. *J. Am. Chem. Soc.* **1990**, *112*, 793-794.

147. Hatanaka, Y.; Hiyama, T. *Synlett* **1991**, 845-853.

148. Hiyama, T.; Hatanaka, Y. *Pure Appl. Chem.* **1994**, *66*, 1471-1478.

149. Sugiyama, A.; Ohnishi, Y.; Nakaoka, M.; Nakao, Y.; Sato, H.; Sakaki, S.; Nakao, Y.; Hiyama, T. *J. Am. Chem. Soc.* **2008**, *130*, 12975-12985.

150. Denmark, S. E.; Sweis, R. F.; Wehrli, D. *J. Am. Chem. Soc*. **2004**, *126*, 4865-4875.

151. Denmark, S. E.; Sweis, R. F. *J. Am. Chem. Soc*. **2004**, *126*, 4876-4882.

152. Mateo, C.; Ferna´ndez-Rivas, C.; Ca´rdenas, D. J.; Echavarren, A. M. *Organometallics* **1998**, *17*, 3661-3669.

153. Cotter, W. D.; Barbour, L.; McNamara, K. L.; Hechter, R.; Lachicotte, R. J. *J. Am. Chem. Soc.* **1998**, *120*, 11016-11017.

154. Suzaki, Y.; Yagyu, T.; Osakada, K. *J. Organomet. Chem.* **2007**, *692*, 326-342.

155. Pantcheva, I.; Osakada, K. *Organometallics* **2006**, *25*, 1735-1741.

156. Hatanaka, Y.; Goda, K.; Okahara, Y.; Hiyama, T. *Tetrahedron* **1994**, *50*, 8301-8316.

157. Nunes, C. M.; Monteiro, A. L. *J. Braz. Chem. Soc*. **2007**, *18*, 1443-1447.

158. Lando, V. R.; Monteiro, A. L. *Org. Lett.* **2003**, *5*, 2891-2894.

159. Zim, D.; Lando, V. R.; Dupont, J.; Monteiro, A. L. *Org. Lett.* **2001**, *3*, 3049-3051.

160. Liang, L.-C.; Chien, P.-S.; Huang, M.-H. *Organometallics* **2005**, *24*, 353-357.

161. Weissman, H.; Milstein, D. *Chem. Commun*. **1999**, 1901-1902.

162. Moriya, T.; Miyaura, N.; Suzuki, A. *Synlett* **1994**, 149-151.

163. Yamamoto, Y.; Takada, S.; Miyaura, N. *Organometallics* **2009**, *28*, 152-160.

164. Nishikata, T.; Yamamoto, Y.; Miyaura, N. *Organometallics* **2004**, *23*, 4317-4324.

165. Farina, V.; Krishnan, B.; Marshall, D. R.; Roth, G. P. *J. Org. Chem.* **1993**, *58*, 5434-5444.

166. Amatore, C.; Gamez, S.; Jutand, A.; Meyer, G.; Moreno-Mañas, M.; Morral, L.; Pleixats, R. *Chem. Eur. J.* **2000**, *6*, 3372-3376.

167. Amatore, C.; Jutand, A.; Meyer, G.; Mottier, L. *Chem. Eur. J.* **1999**, *5*, 466-473.

168. Sharma, R. K.; Fry, J. L. *J. Org. Chem.* **1983**, *48*, 2112-2114.

169. Klanberg, F.; Muetterties, E. L. *Inorg. Chem.* **1968**, *7*, 155-160.

170. Marat, R. K.; Janzen, A. F. *Can. J. Chem.* **1977**, *55*, 3845-3849.

171. Damrauer, R.; Danahey, S. E. *Organometallics* **1986**, *5*, 1490-1494.

172. Damrauer, R.; O'Connell, B.; Danahey, S. E.; Simon, R. *Organometallics* **1989**, *8*, 1167-1171.

173. Johnson, S. E.; Day, R. O.; Holmes, R. R. *Inorg. Chem.* **1989**, *28*, 3182-3189.

174. Johnson, S. E.; Payne, J. S.; Day, R. O.; Holmes, J. M.; Holmes, R. R. *Inorg. Chem.* **1989**, *28*, 3190-3198.

175. Tamao, K.; Hayashi, T.; Ito, Y. *Organometallics* **1992**, *11*, 182-191.

176. Handy, C. J.; Lam, Y.; DeShong, P. *J. Org. Chem.* **2000**, *65*, 3542-3543.

177. Kost, D.; Kalikhman, I. In *The Chemistry of Organic Silicon Compounds*; Rappoport, Z., Apeloig, Y., Eds.; John Wiley and Sons Ltd.: Chichester, 1998, Vol. 2, pp 1339-1445.

178. Hansch, C.; Leo, A.; Taft, R. W. *Chem. Rev.* **1991**, *97*, 165-195.

179. Kurosawa, H.; Emoto, M.; Urabe, A.; Miki, K.; Kasai, N. *J. Am. Chem. Soc.* **1985**, *107*, 8253-8254.

180. Kurosawa, H.; Emoto, M.; Ohnishi, H.; Miki, K.; Kasai, N.; Tatsumi, K.; Nakamura, A. *J. Am. Chem. Soc.* **1987**, *109*, 6333-6340.

181. Kurosawa, H.; Kajimaru, H.; Miyoshi, M.; Ohnishi, H.; Ikeda, I. *J. Mol. Catal.* **1992**, *74*, 481-488.

182. Hartwig, J. F. *Inorg. Chem*. **2007**, *46*, 1936-1947.

183. Hartwig, J. F. *Acc. Chem. Res*. **1998**, *31*, 852-860.

184. Mann, G.; Baranano, D.; Hartwig, J. F.; Rheingold, A. L.; Guzei, I. A. *J. Am. Chem. Soc.* **1998**, *120*, 9205-9219.

185. Driver, M. S.; Hartwig, J. F. *J. Am. Chem. Soc.* **1997**, *119*, 8232-8245.

186. Culkin, D. A.; Hartwig, J. F. *Organometallics* **2004**, *23*, 3398-3416.

187. Tolman, C. A. *Chem. Rev*. **1977**, *77*, 313-348.

188. Wolfe, J. P.; Tomori, H.; Sadighi, J. P.; Yin, J.; Buchwald, S. L. *J. Org. Chem.* **2000**, *65*, 1158-1174.

189. Wolfe, J. P.; Singer, R. A.; Yang, B. H.; Buchwald, S. L. *J. Am. Chem. Soc.* **1999**, *121*, 9550-9561.

190. Johnson, J. B.; Rovis. T. *Angew. Chem. Int. Ed*. **2008**, *47*, 840-871.

191. Fairlamb, I. J. S. *Org. Biomol. Chem.* **2008**, *6*, 3645-3656.

192. Schwalbe, M.; Walther, D.; Schreer, H.; Langer, J.; Gorls, H. *J. Organomet. Chem.* **2006**, *691*, 4868-4873.

193. Green, M.; Howard, J. A. K.; Spencer, J. L.; Stone, F. G. A. *J. Chem. Soc., Dalton Trans*. 1**977**, 271-277.

194. Fairlamb, I. J. S.; Kapdi, A. R.; Lee, A. F. *Org. Lett*. **2004**, *6*, 4435-4438.

195. Sehnal, P.; Taghzouti, H.; Fairlamb, I. J. S.; Jutand. A.; Lee, A. F.; Whitwood, A. C. *Organometallics* **2009**, *28*, 824-829.

196. Sprengers, J. W.; Wassenaar, J.; Clement, N. D.; Cavell, K. J.; Elsevier, C. J. *Angew. Chem. Int. Ed*. **2005**, *44*, 2026-2029.

197. Clement, N. D.; Cavell, K. J.; Ooi, L. *Organometallics* **2006**, *25*, 4155-4165.

198. Selvakumar, K.; Zapf, A.; Spannenberg, A.; Beller, M. *Chem. Eur. J*. **2002**, *8*, 3901-3906.

199. Cortés, J.; Moreno-Mañas, M.; Pleixats, R. *Eur. J. Inorg. Chem.* **2000**, 239-243.

200. Moreno-Mañas, M.; Pleixats, R.; Sebastián, R. M.; Vallribera, A. R. *J. Organomet. Chem.* **2004**, *689*, 3669-3684.

201. van Asselt, R.; Elsevier, C. J. *Tetrahedron* **1994**, *50*, 323-334. (PhZn, PhMg)

202. van Asselt, R.; Elsevier, C. J.; Smeets, W. J. J.; Spek, A. L. *Inorg. Chem*. **1994**, *33*, 1521-1531.

203. Klein, R.; Witte, P.; van Belzen, R.; Fraanje, J.; Goubitz, K.; Numan, M.; Schenk, H.; Ernsting, J. M. Elsevier, C. J. *Eur. J. Inorg. Chem.* **1998**, 319-330.

204. Grasa, G. A.; Hillier, A. C.; Nolan, S. P. *Org. Lett.* **2001**, *3*, 1077-1080.

205. Kluwer, A. M.; Elsevier, C. J.; Bühl, M.; Lutz, M.; Spek, A. L. *Angew. Chem. Int. Ed.* **2003**, *42*, 3501-3504.

206. Krause, J.; Haack, K.-J.; Cestaric, G.; Goddard, R.; Porschke, K.-R. *J. Am. Chem. Soc.* **1999**, *121*, 9807-9823.

207. Grundl, M. A.; Kennedy-Smith, J. J.; Trauner, D. *Organometallics* **2005**, *24*, 2831-2833.

208. Scrivanti, A.; Beghetto, V.; Matteoli, U.; Antonaroli, S.; Marini, A.; Crociani, B. *Tetrahedron* **2005**, *61*, 9752-9758.

209. Rencken, I.; Orchard, S. W.; *Inorg. Chem*. **1986**, *25*, 1972-1976.

210. Muhs, M. A.; Weiss, F. T. *J. Am. Chem. Soc.* **1962**, *84*, 4697-4705.

211. Genet, J. P.; Juge, S.; Achi, S.; Mallart, S.; Ruiz Montes, J.; Levif, G. *Tetrahedron* **1988**, *44*, 5263-5275.

212. Manoso, A. S.; Ahn, C.; Soheili, A.; Handy, C. J.; Correia, R.; Seganish, W. M.; DeShong, P. *J. Org. Chem.* **2004**, *69*, 8305-8314.

213. Masuda, Y.; Murata, M.; Ishikura, M.; Nagata, M.; Watanbe, S. *Org. Lett.* **2002**, *4*, 1843-1845.

214. Mowery, M. E.; DeShong, P. *J. Org. Chem.* **1999,** *64*, 1684-1688.

215. Tseng, C. C.; Paisley, S. D.; Goering, H. L. *J. Org. Chem.* **1986**, *51*, 2884-2891.